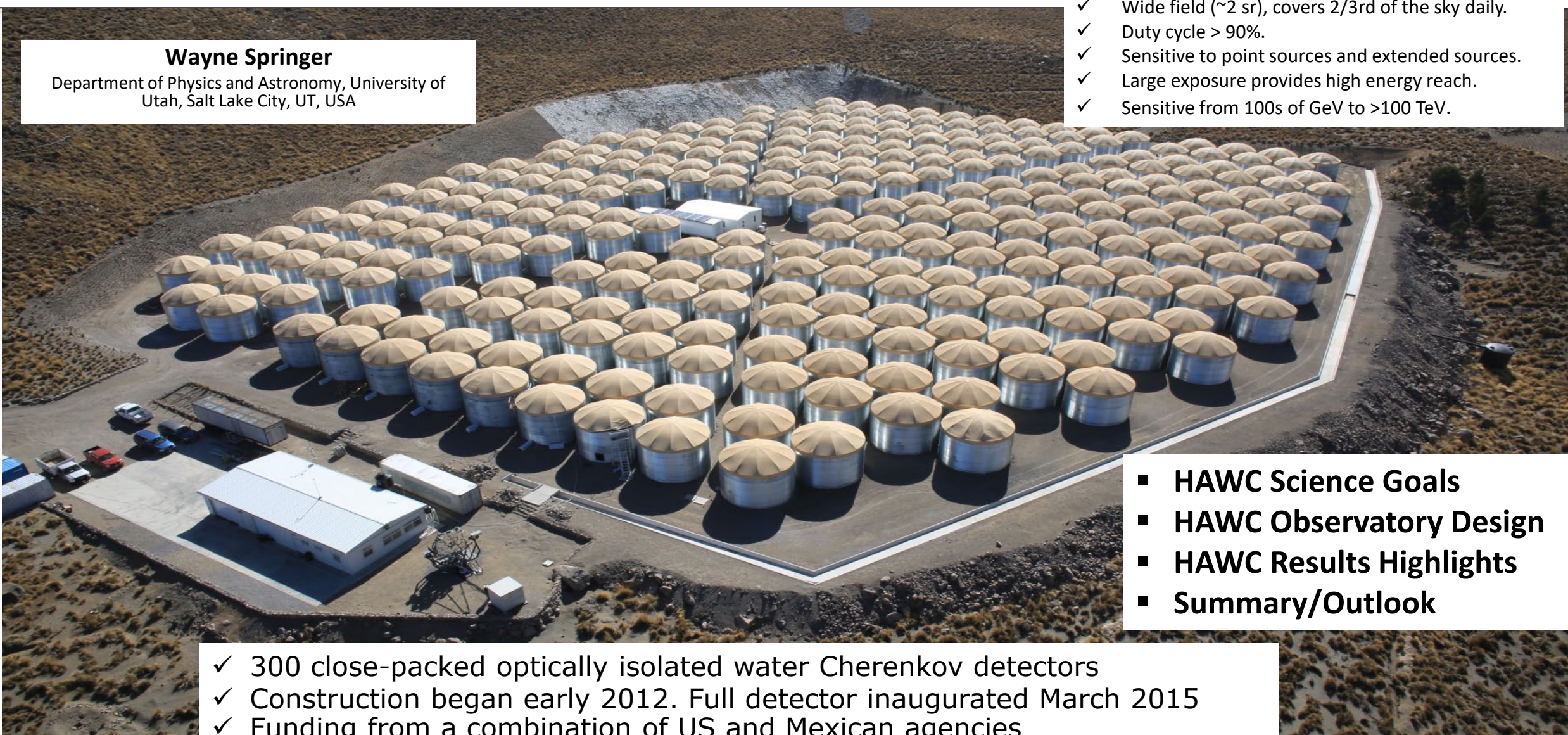


STATUS AND RESULTS OF THE HIGH-ALTITUDE WATER CHERENKOV (HAWC) OBSERVATORY

Wayne Springer

Department of Physics and Astronomy, University of Utah, Salt Lake City, UT, USA

- ✓ Wide field (~2 sr), covers 2/3rd of the sky daily.
- ✓ Duty cycle > 90%.
- ✓ Sensitive to point sources and extended sources.
- ✓ Large exposure provides high energy reach.
- ✓ Sensitive from 100s of GeV to >100 TeV.



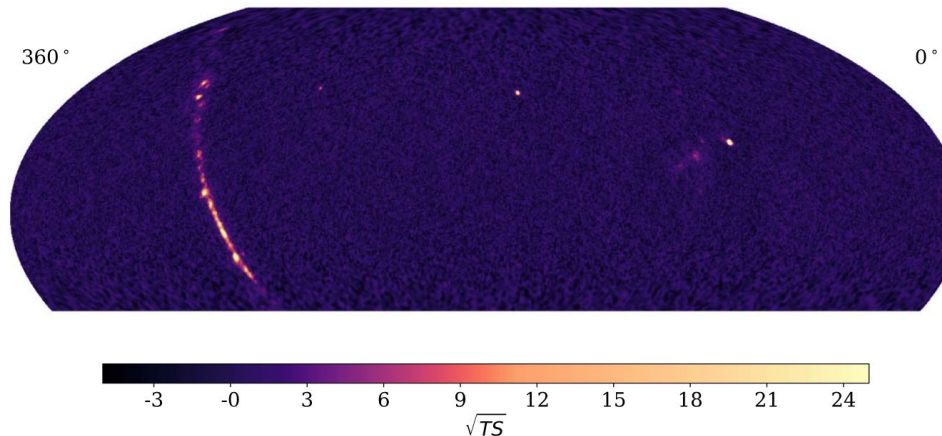
- **HAWC Science Goals**
- **HAWC Observatory Design**
- **HAWC Results Highlights**
- **Summary/Outlook**

- ✓ 300 close-packed optically isolated water Cherenkov detectors
- ✓ Construction began early 2012. Full detector inaugurated March 2015
- ✓ Funding from a combination of US and Mexican agencies
- ✓ High energy extension: Outrigger array, since summer 2018
- ✓ Detector weight (300 tanks water only) 51,600 tons 181 km of cables

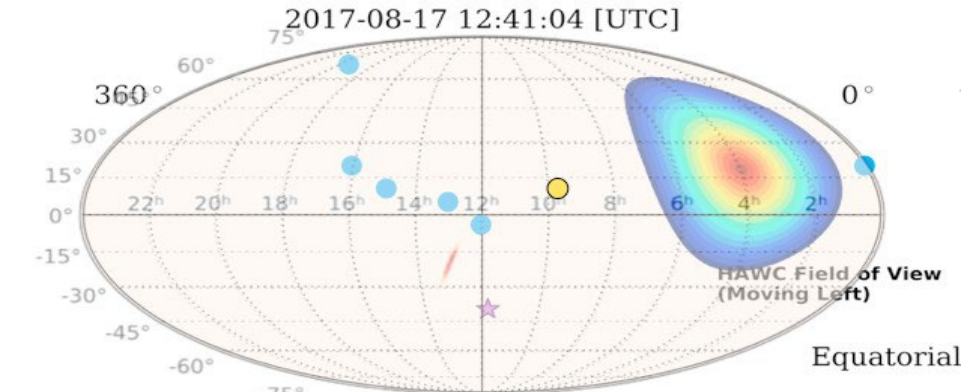
HAWC Observatory – Science Goals (Broadly)

TeV Gamma Ray Sky

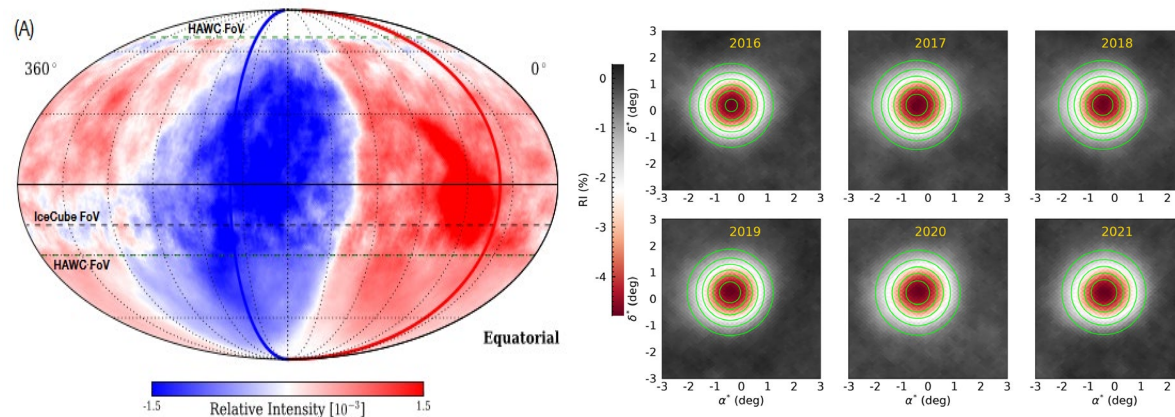
The Third HAWC Catalog



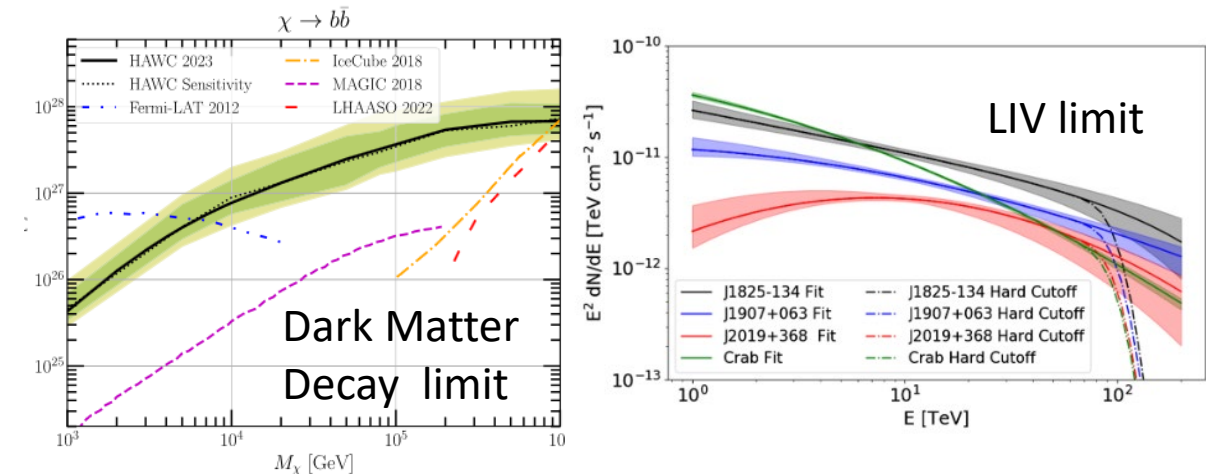
Multi-messenger Astrophysics



Cosmic Ray & Solar Physics Studies



Searches & “Exotica”

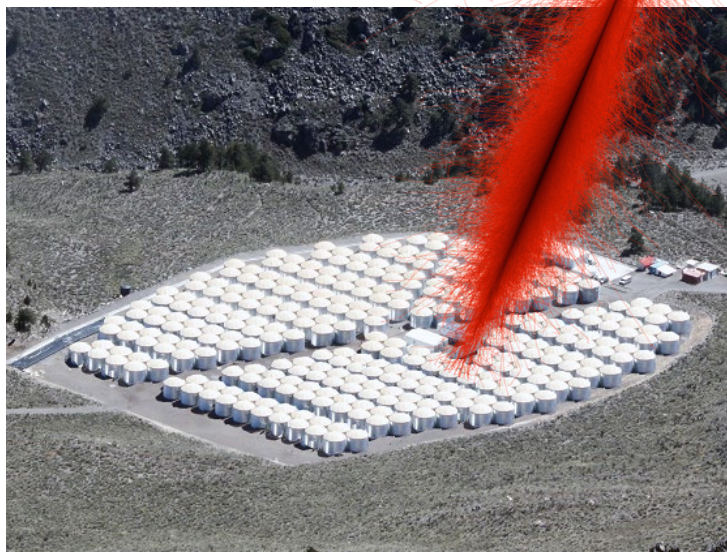


HAWC Observatory - Design Principles

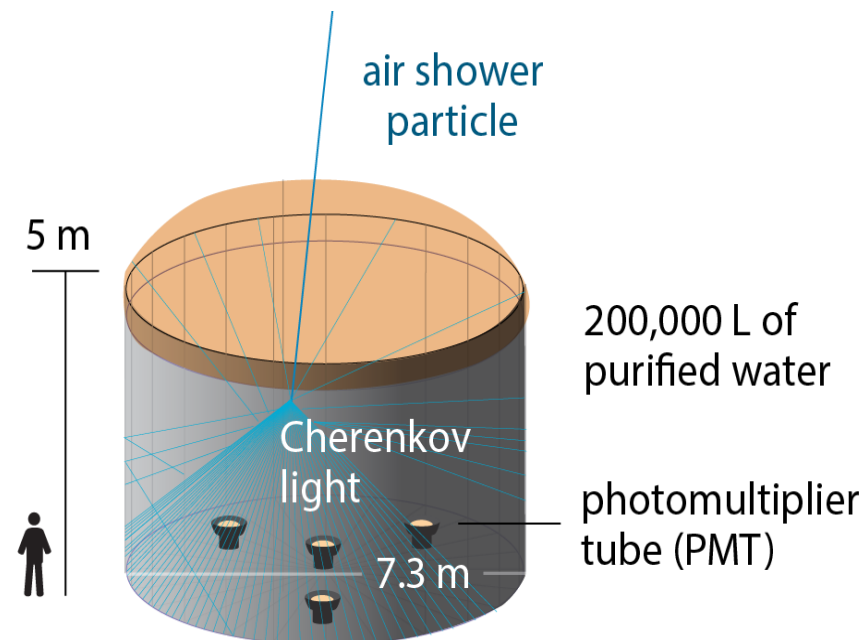
The High-Altitude Water Cherenkov (HAWC) Observatory in México: The Primary Detector
HAWC Collaboration: A.U. Abeysekara et al. 2023, [NIM A1052 \(2023\), 168253](#).

Atmosphere “converts”
particle into an extensive
air shower (EAS).

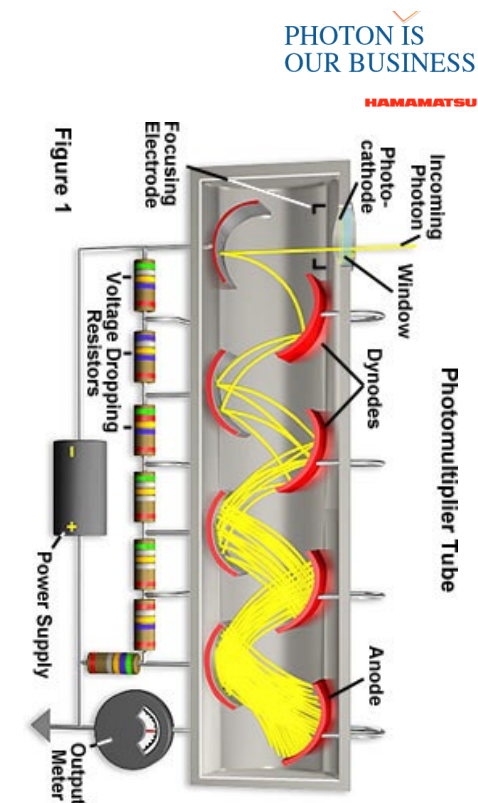
Based upon Milagro Experiment



Water Cerenkov Detector
Samples Extensive Air Shower
particles by measuring their
Cerenkov light emitted in water
tank.



PMT
Converts Cerenkov light into
electrical signal.

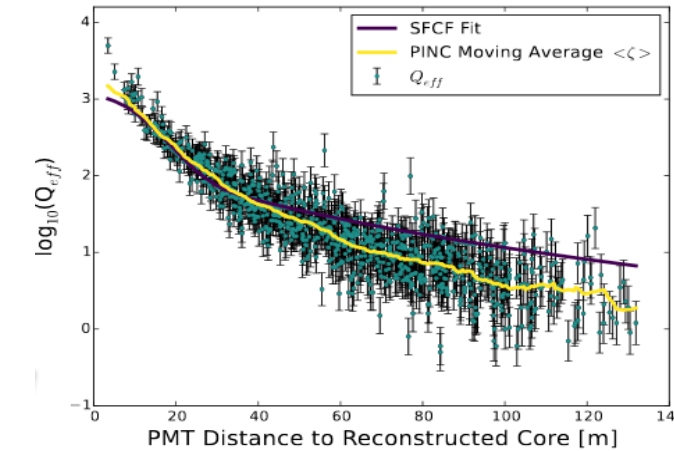
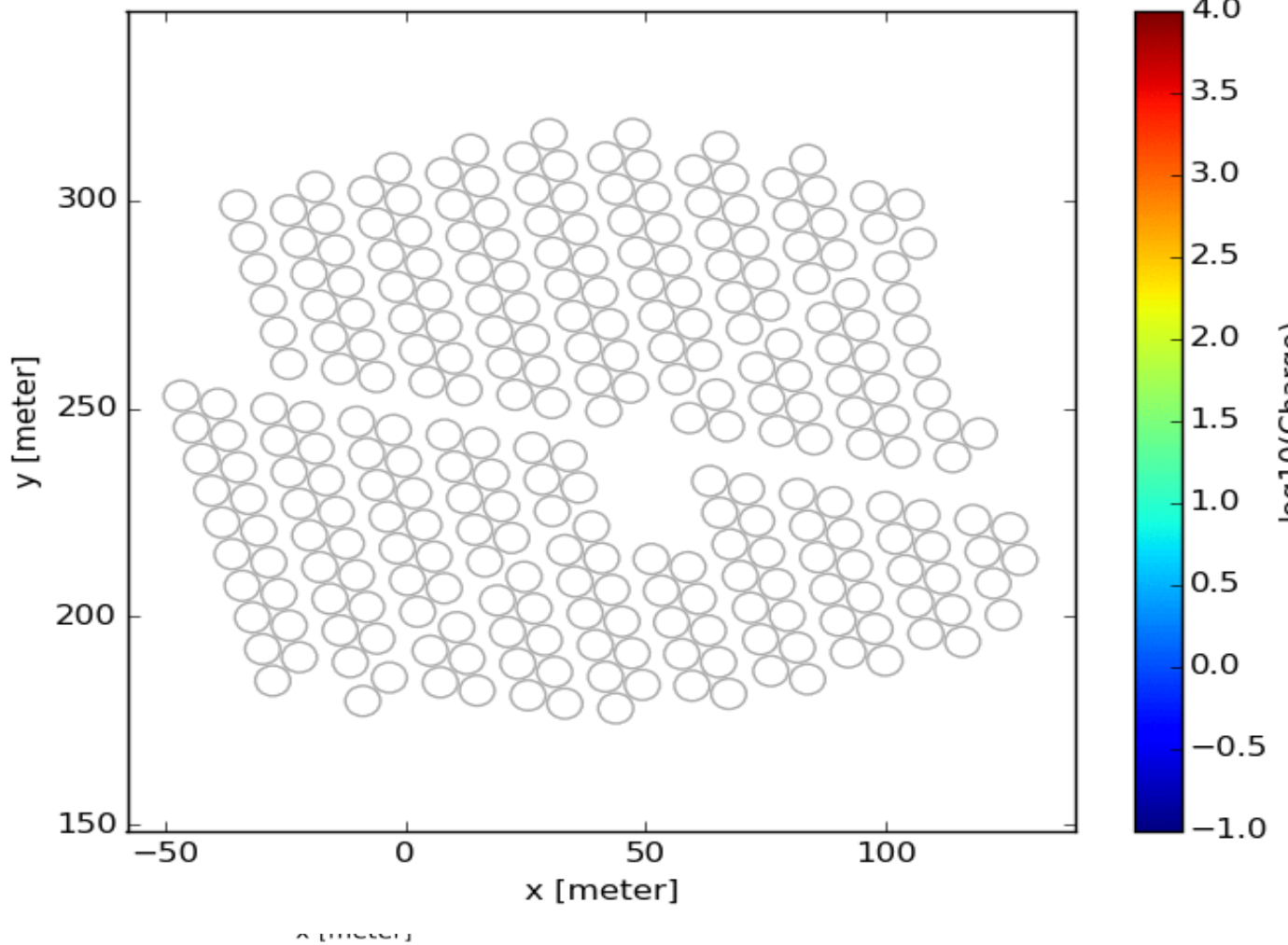


[The HAWC Observatory-Main Detector: NIM A1052 \(2023\) 168253](#)

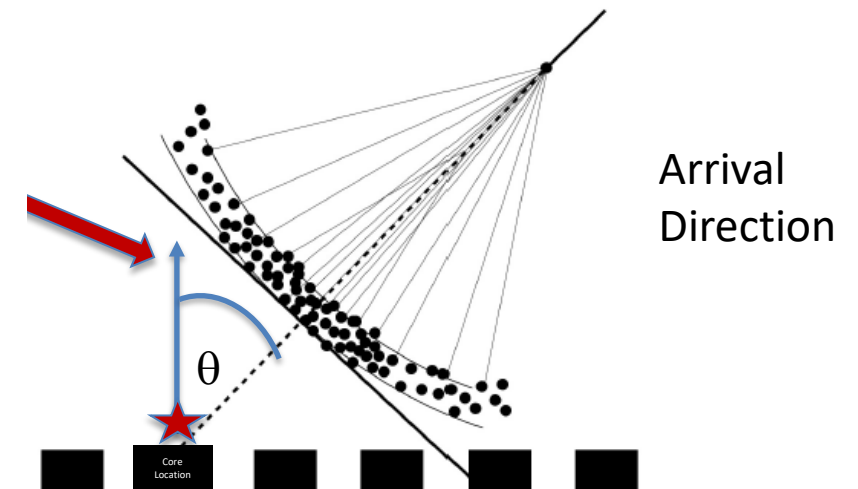


STATUS AND RESULTS OF THE HIGH-ALTITUDE WATER CHERENKOV (HAWC) OBSERVATORY

THE UNIVERSITY OF UTAH
Department of
Physics & Astronomy



Lateral Distribution Function



Energy
Gamma/Hadron

Arrival
Direction

TeV Sky Results- HAWC point source TeV Sky Map 3HWC Catalog

[3hwc: The third HAWC catalog of very-high-energy gamma-ray sources](#)
HAWC Collaboration: A. Albert et al. 2020, [ApJ 905 \(2020\), 76](#).

Wide Field of View
Continuous Operation

360 °

Mrk501
140 Mpc
456 Mly

Mrk 421
130 Mpc
430 Mly

Crab Nebula
2.2 kpc
8.0 kly

0 °

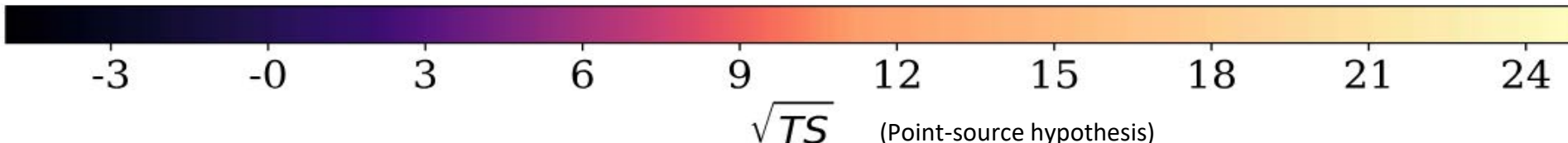
Galactic and extragalactic sources:

- Pulsar wind nebulae, TeV Halos
- Supernova remnants
- Microquasar
- AGN, Blazars
- ???? (GRB, if you are lucky [LHAASO GRB 221009A](#))

- ✓ 1523 day exposure
- ✓ 65 sources detected
- ✓ 8 new sources discovered
- ✓ identified as PWN

Sources of positron excess????

Milky Way Galactic Plane



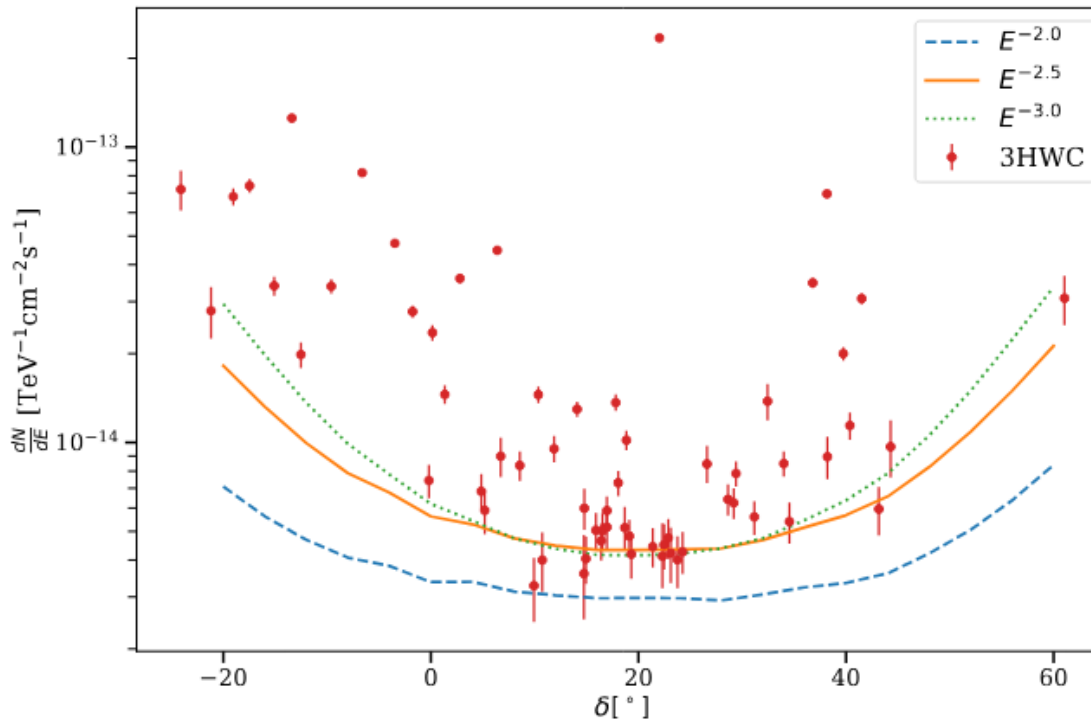
STATUS AND RESULTS OF THE HIGH-ALTITUDE WATER CHERENKOV (HAWC) OBSERVATORY

THE UNIVERSITY OF UTAH
Department of Physics & Astronomy

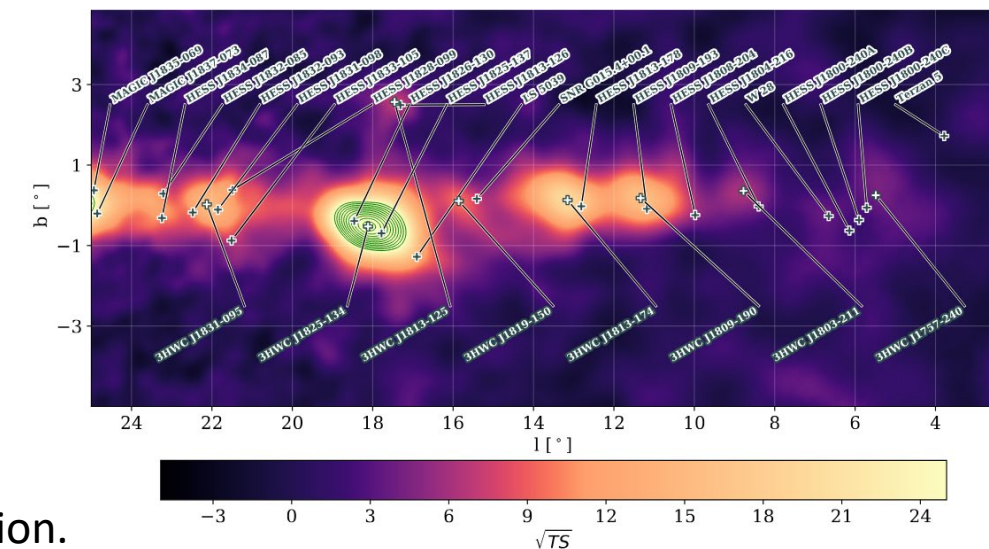
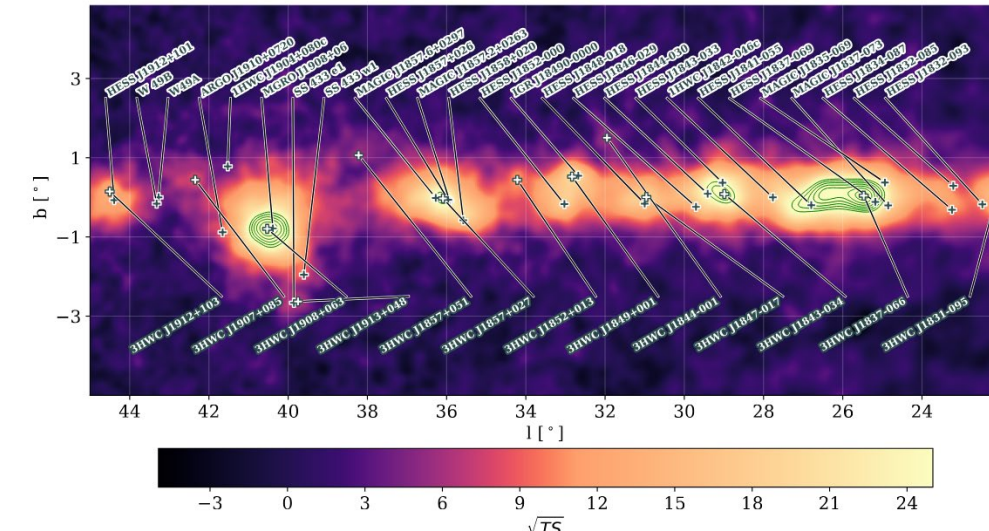
Point Source Map— 1523d livetime

[3hwc: The third HAWC catalog of very-high-energy gamma-ray sources](#)
 HAWC Collaboration: A. Albert et al. 2020, [ApJ 905 \(2020\), 76](#).

- Declination Dependent Sensitivity
- Example Point Source Hypothesis Significance Maps for Inner Galactic Plane Region



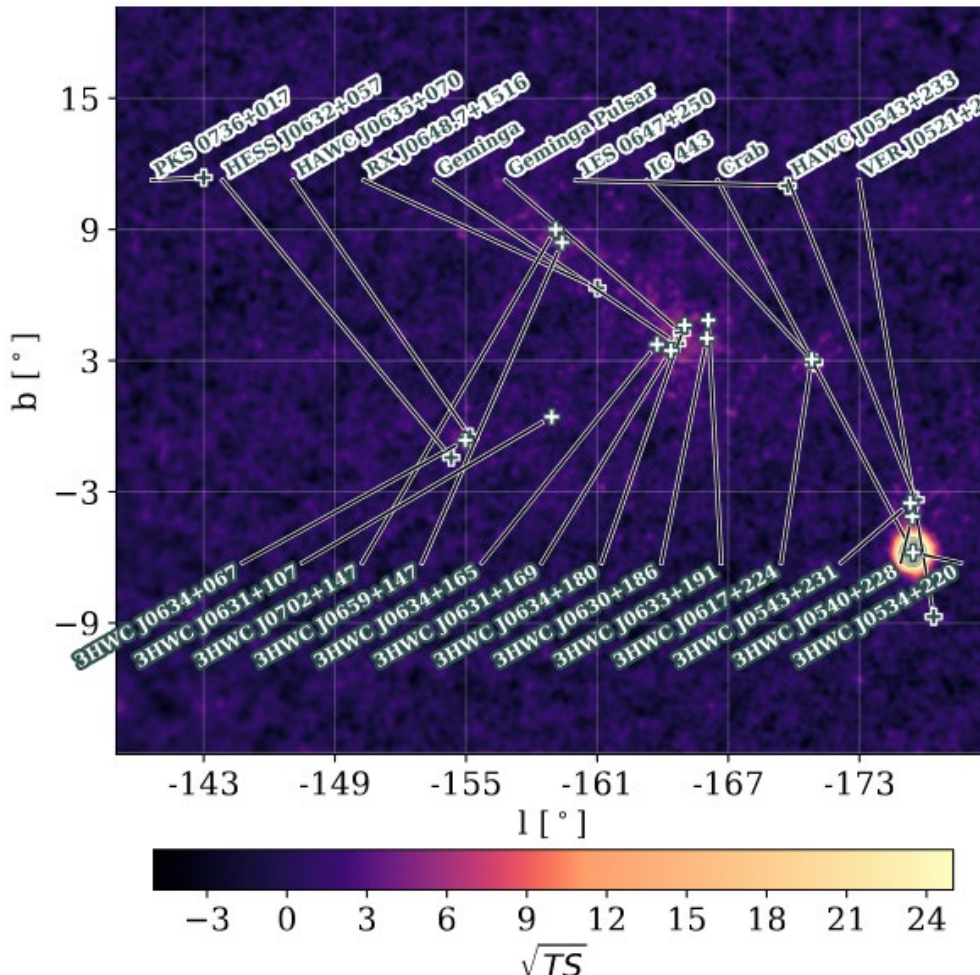
3HWC sensitivity for point source search as a function of declination.



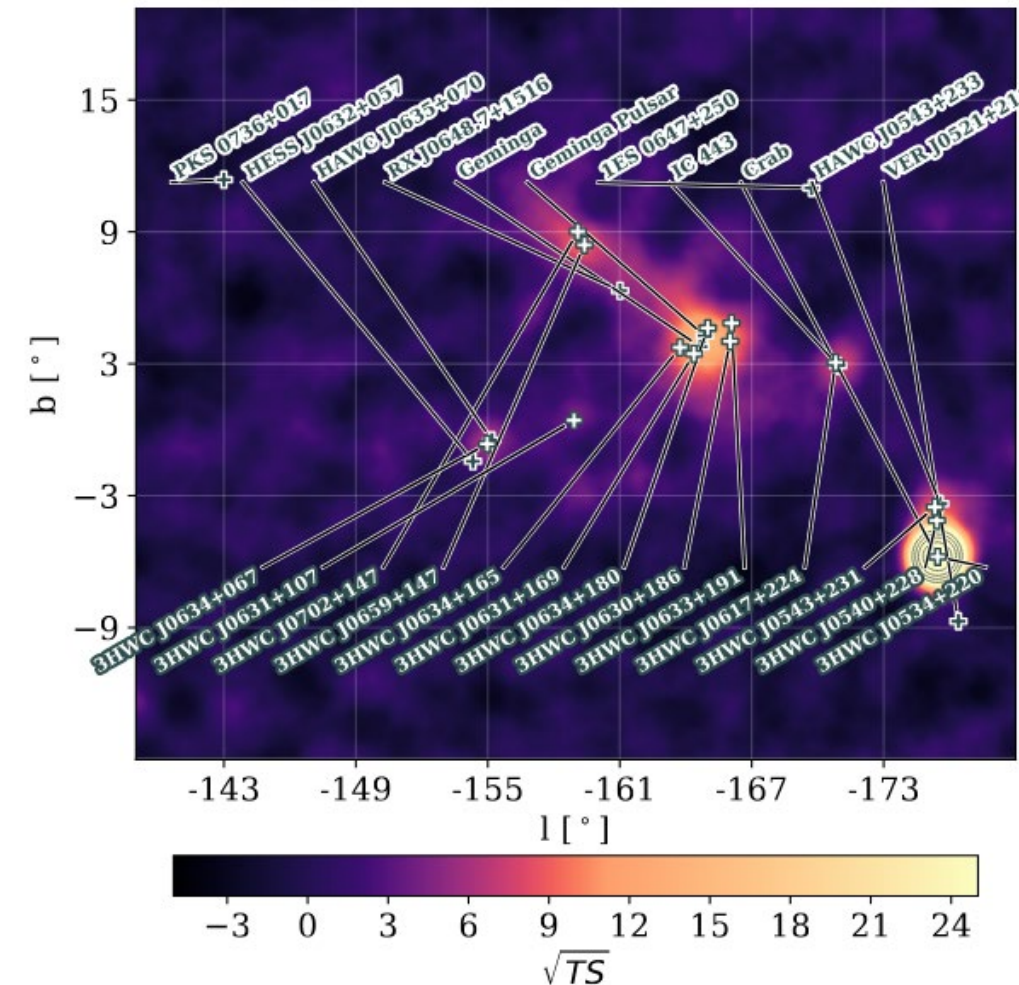
Crab & Geminga Region

[3hwc: The third HAWC catalog of very-high-energy gamma-ray sources](#)
HAWC Collaboration: A. Albert et al. 2020, [ApJ 905 \(2020\), 76](#).

□ Point Source vs 1^0 extended source Hypothesis



Point Source Hypothesis Significance Map

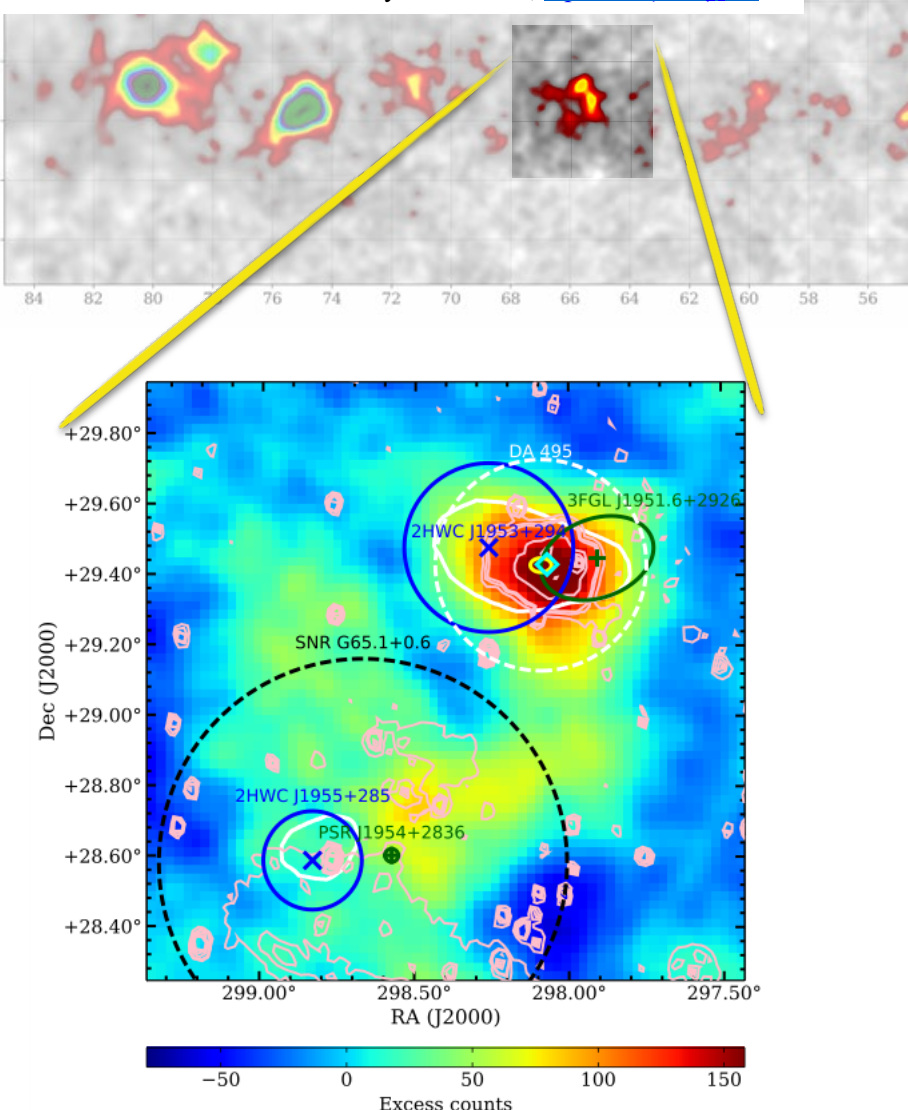


1^0 extended source Hypothesis Significance Map

New Sources: 2HWC J1953+294

The 2HWC HAWC Observatory Gamma-Ray Catalog

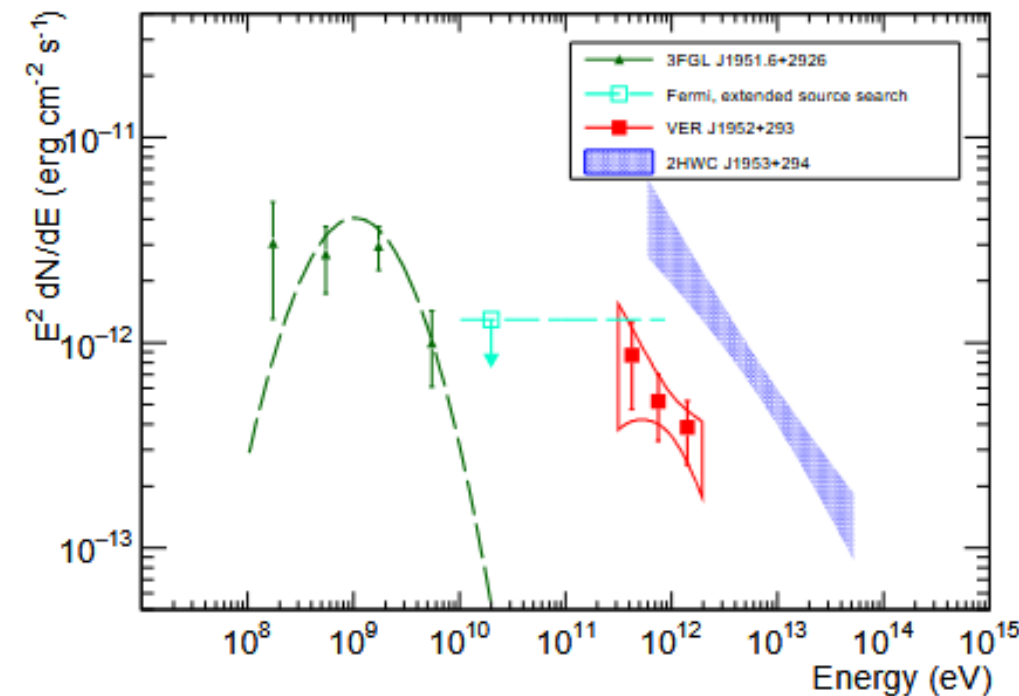
HAWC Collaboration: A.U. Abeysekara et al., [ApJ 843 \(2017\), 40](#).



VERITAS and Fermi-LAT Observations of TeV Gamma-Ray Sources Discovered by HAWC in the 2HWC Catalog

VERITAS Collaboration: Fermi-LAT Collaboration:; HAWC Collaboration: [ApJ 866 \(2018\), 24](#).

- **2HWC J1953+294:** No previously known TeV sources.
- Tentative association 3FGL J1951.6+2926 / PWN DA 495
- Shared privately with Imaging Atmospheric Cherenkov Telescopes
- New observations plus archival data by VERITAS: source confirmed.



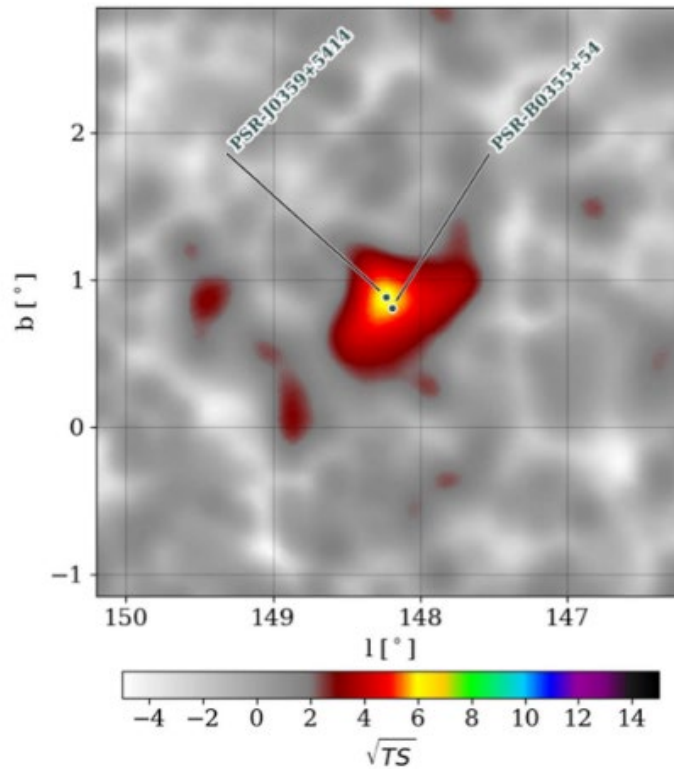


Figure 1. HAWC significance map in Galactic coordinates using 2321 days of live data. The significance is computed with a point-like spatial template and a power-law spectrum with spectral index $\alpha = 2.7$. For comparison, the positions of PSR J0359+5414 and PSR B0355+54 are marked.

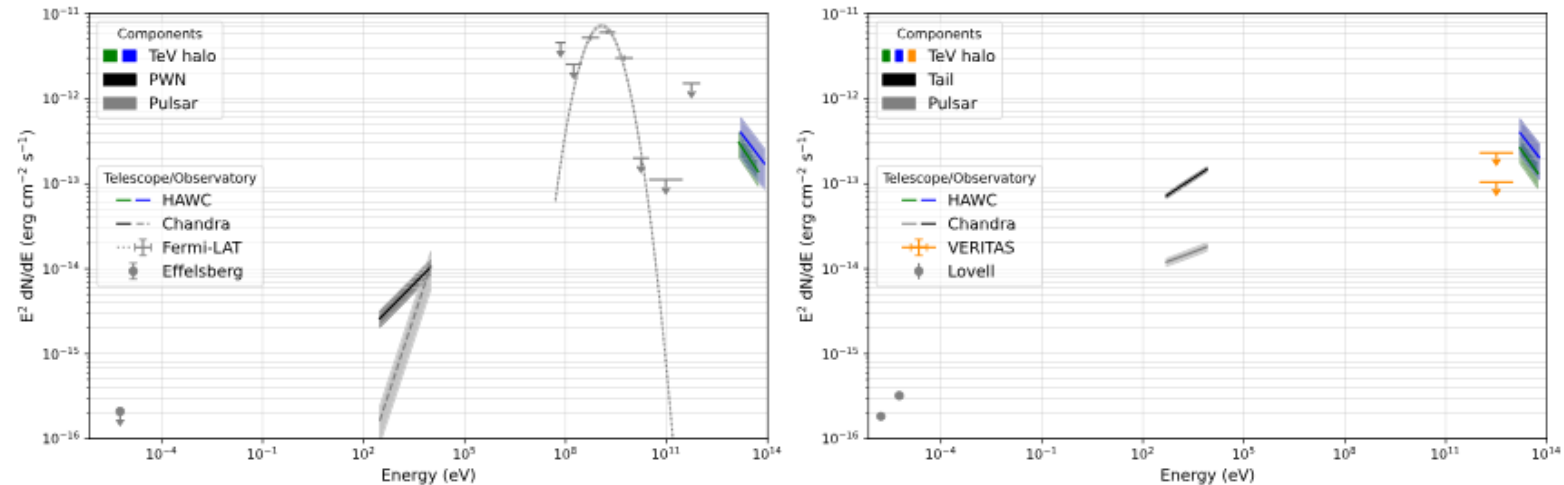
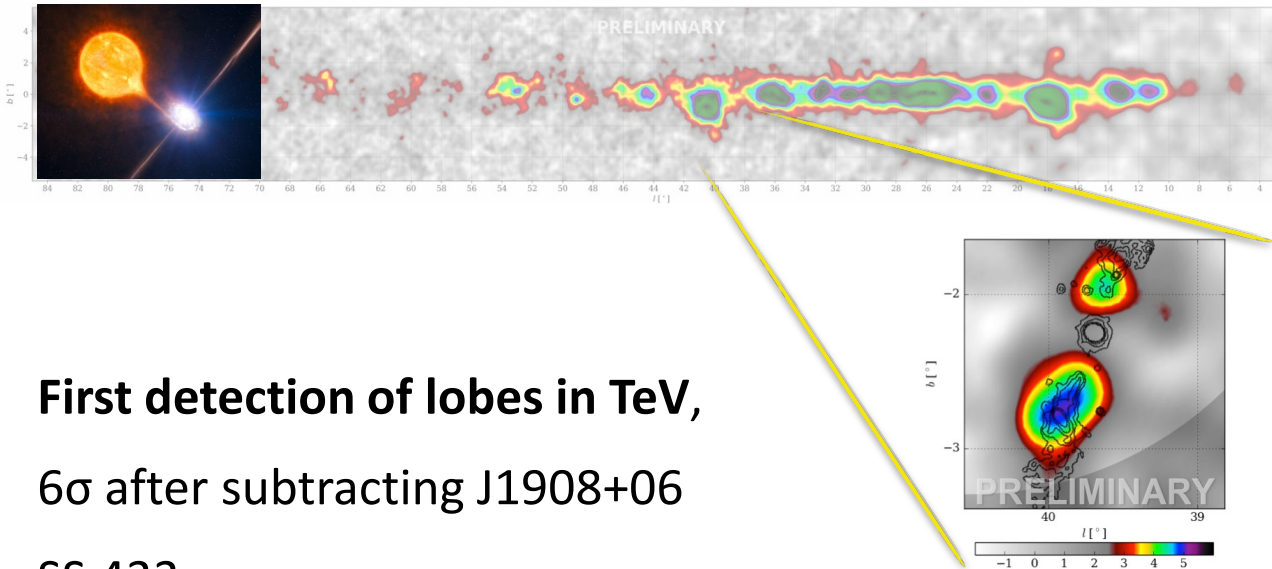


Figure 3. Left panel: spectral energy distribution (SED) of the emission around PSR J0359+5414, including the TeV halo (green and blue bands corresponding to the HAWC observation for a point-like and extended model, respectively, as explained in Section 3), the PWN (black band at 0.3–10 keV; Zyuzin et al. 2018), and the pulsar (in gray color; including the upper limit in radio at 1400 MHz from Grießmeier et al. (2021), the band in X-ray at 0.3–10 keV from Zyuzin et al. (2018), and the data points or limits at 100 MeV–1 TeV from Abdollahi et al. 2020). Right panel: SED of the emission around PSR B0355+54. The green and blue bands indicate the TeV excess emission obtained from fits to the HAWC data with models that center at B0355 with point-like and extended spatial profiles, respectively (see Appendix A). For comparison, the upper limits on VHE gamma-ray emission from the PWN by VERITAS with hard spectral cuts are shown in orange, with the upper and lower bars corresponding to region sizes of $0^{\circ}1$ and $0^{\circ}235$, respectively (Benbow et al. 2021). The black band at 0.5–8 keV indicates the PWN in X-rays (Klingler et al. 2016). The gray band at 0.5–8 keV (Klingler et al. 2016) and the circular data markers at 1400 and 1600 MHz (Lorimer et al. 1995) correspond to the emission from the pulsar. The HAWC bands correspond to statistical uncertainties only.

Microquasar SS-433 – Lobes Detection

[Very high energy particle acceleration powered by the jets of the microquasar SS 433](#)

HAWC Collaboration: A.U. Abeysekara et al., [Nature 562 \(2018\), 82–85](#).



First detection of lobes in TeV,
6 σ after subtracting J1908+06

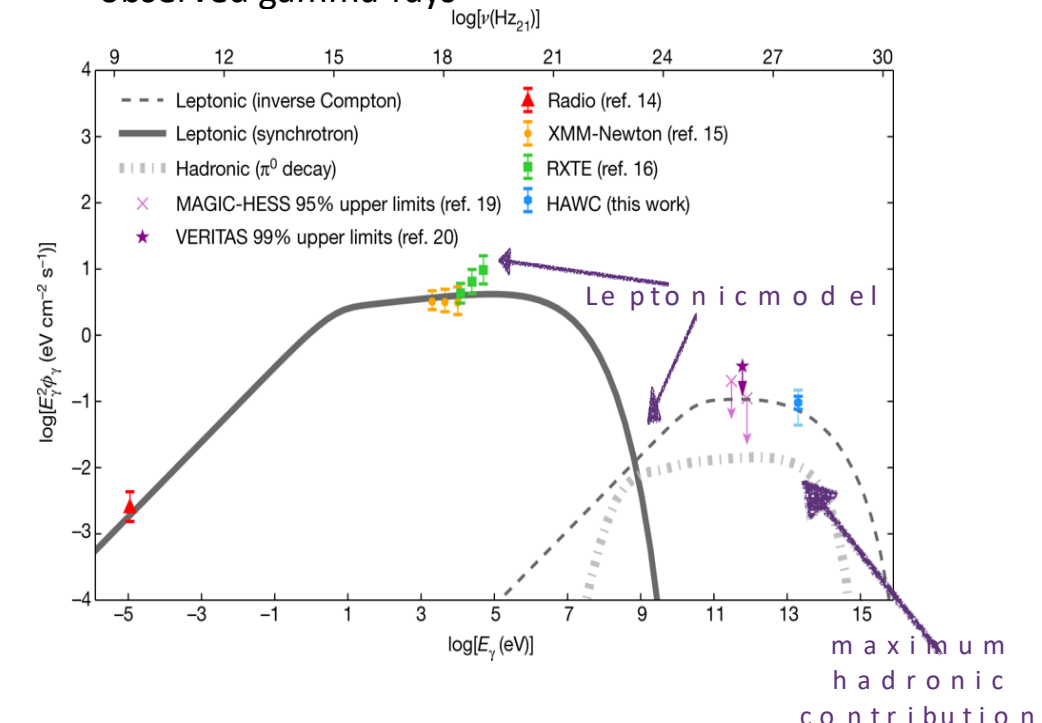
SS 433:

Binary system: supermassive star ($\sim 30 M_{\odot}$),
compact object ($\sim 10 M_{\odot}$)

Powerful jets: $\sim 10^{39}$ erg s $^{-1}$, speed $\sim c/4 - c/3$

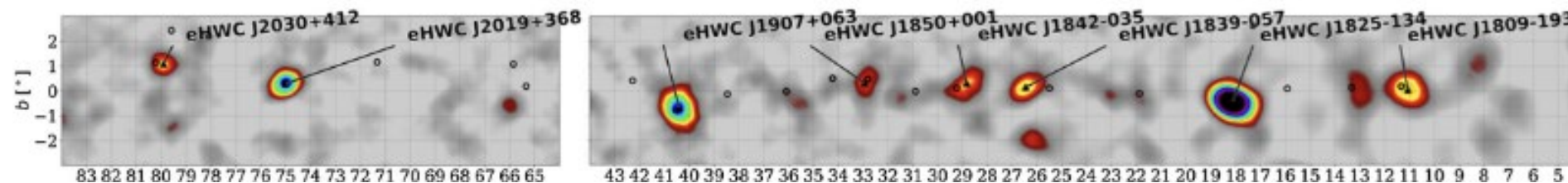
Termination shocks in W50 nebula

- HAWC observation of SS433 is the first direct evidence of particle acceleration to \sim PeV in jets
 - Jets are observed edge-on so the gamma rays are not Doppler boosted to higher energies or higher luminosities
 - Hadronic acceleration disfavored due to extreme energetics required
 - Acceleration does not happen at the black hole because the cooling time of the electrons is too short to make the observed gamma-rays

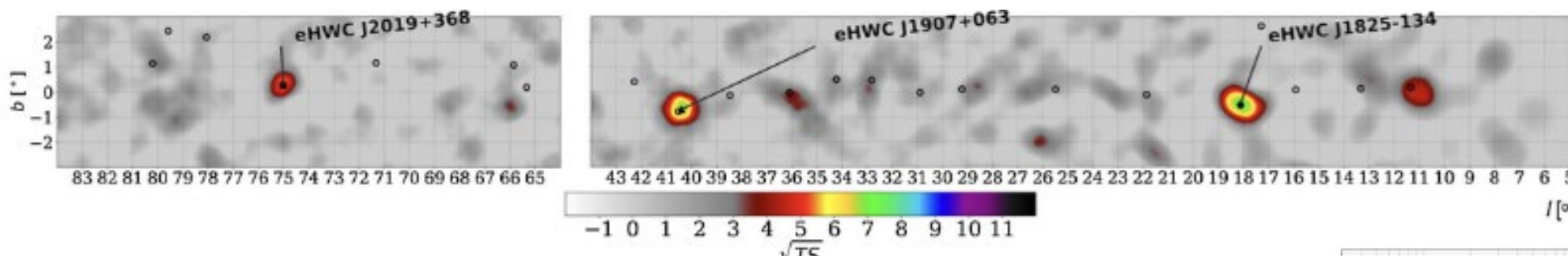


Pushing to Higher Energies: ($E_{\text{reco}} > 56 \text{ TeV},$)

[Multiple Galactic Sources with Emission Above 56 TeV Detected by HAWC](#)
 HAWC Collaboration: A.U. Abeysekara et al., [PRL 124,021102\(2020\)](#).

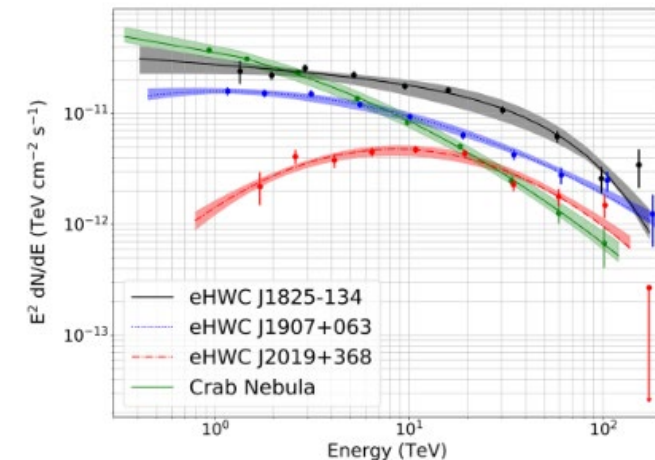


eHWC J2030+412
eHWC J2019+368



eHWC J1907+063
eHWC J1825-134
eHWC J2019+368

- About 30 sources above 50 TeV
- Nine sources $> 56 \text{ TeV}$
- Three sources $> 100 \text{ TeV}$.
- PeVatron candidates?
- Lower limits on Lorentz Invariance Violation in the 10^{30} eV range (linear term)



$E^2 \frac{dN}{dE} (\text{TeV cm}^{-2} \text{s}^{-1})$

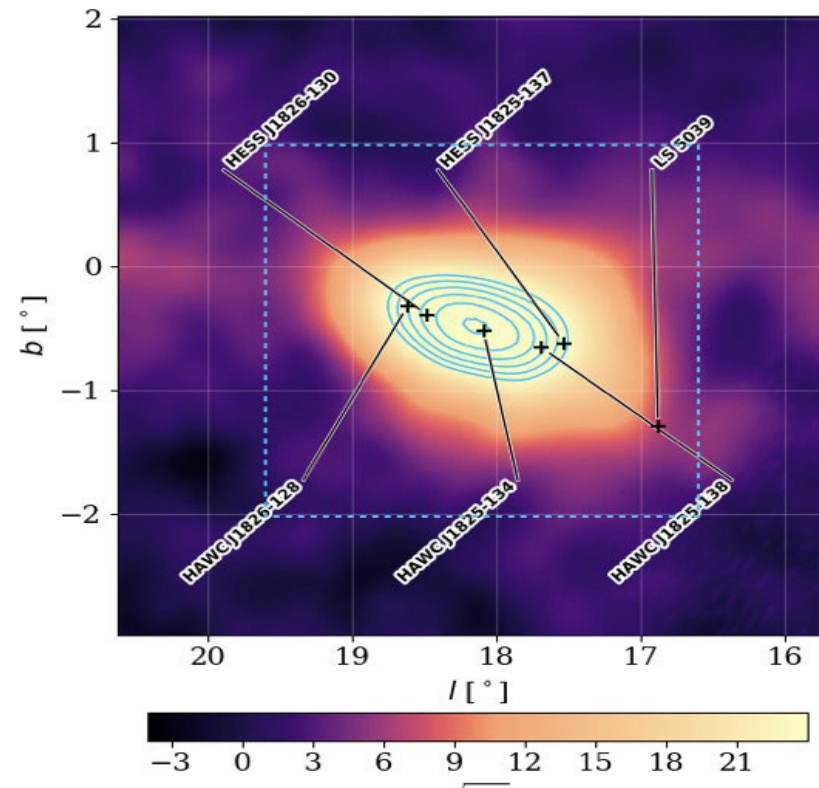


Pushing to even higher energies ($E_{\text{reco}} > 200 \text{ TeV}$)

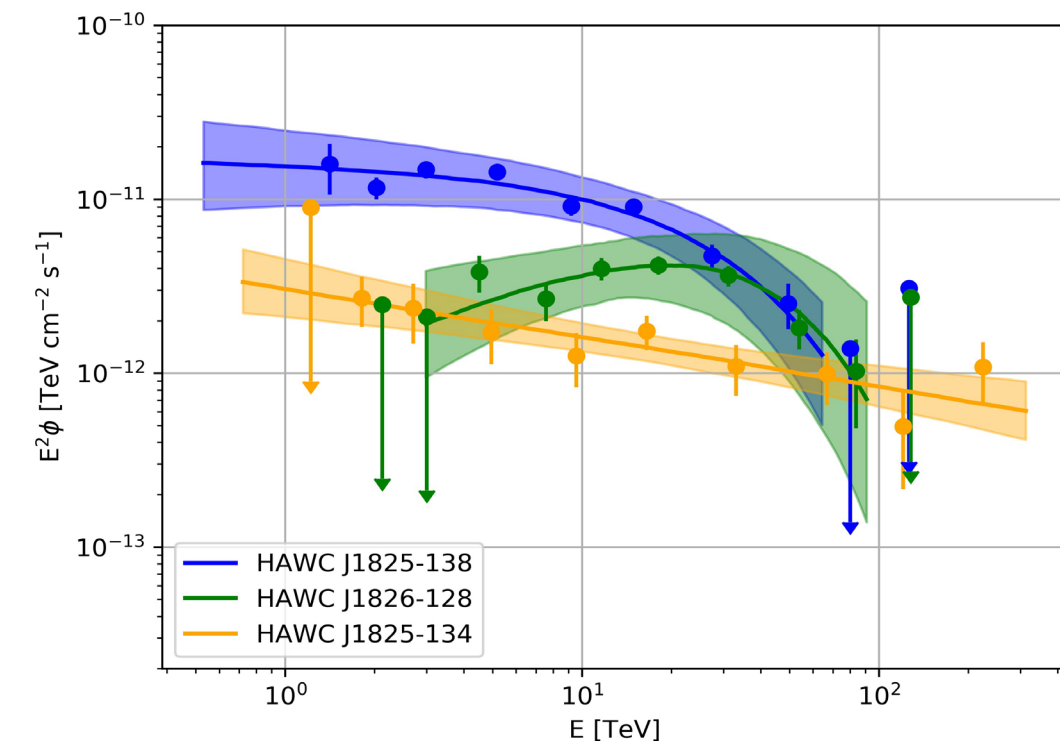
[Evidence of 200 TeV photons from HAWC j1825-134](#)

HAWC Collaboration: A. Albert et al. 2021, [ApJL 907 \(2021\), L30](#).

- Source coincident with Giant Molecular Cloud
- Pevatron?



J1825-138 Significance map



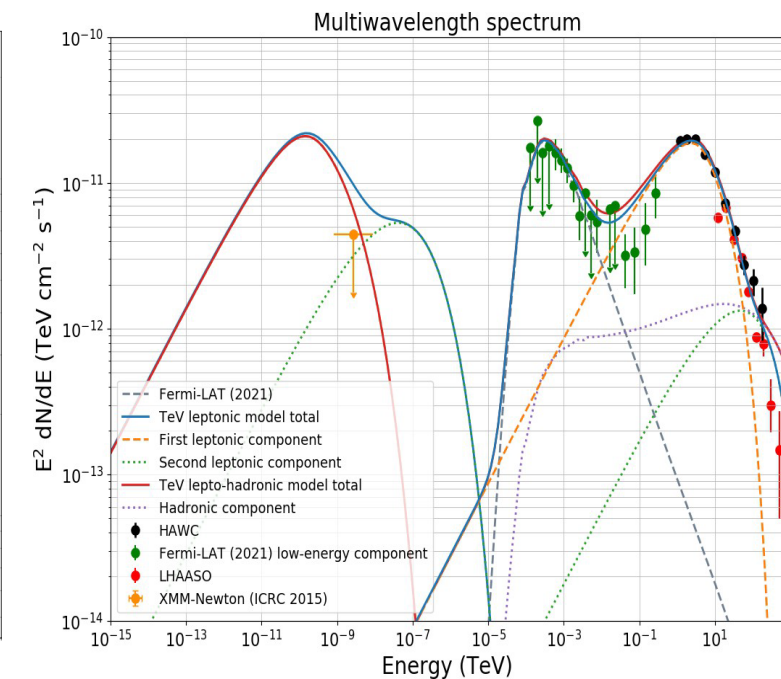
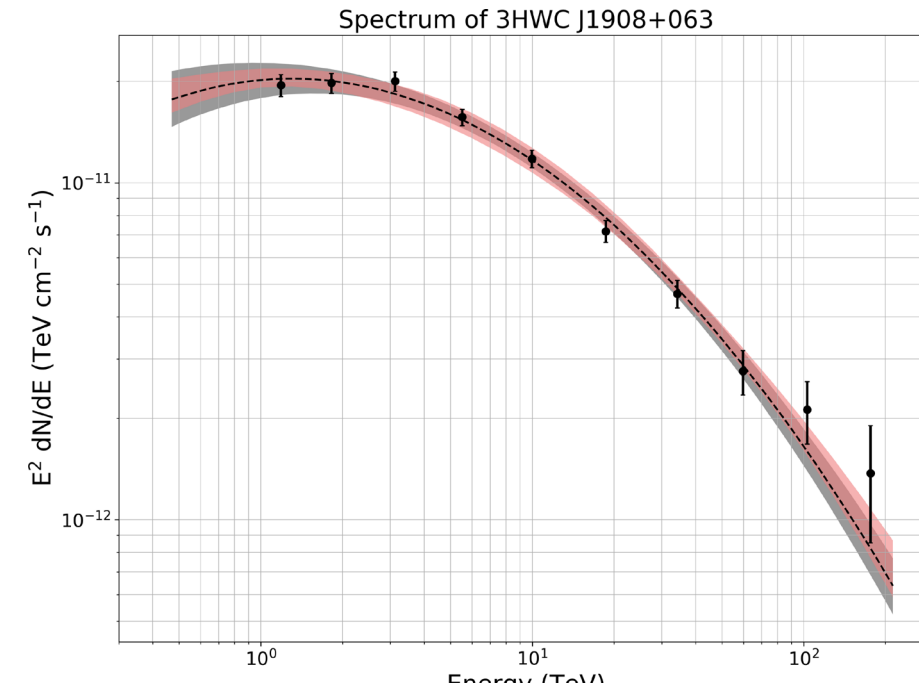
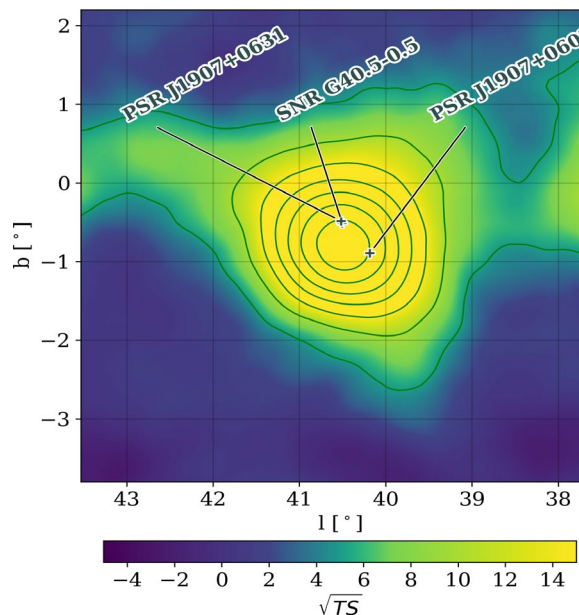
J1825-138 Spectral Energy Distribution

Pevatron Cosmic Ray Accelerators?

[HAWC Study of the Ultra-High-Energy Spectrum of MGRO J1908+06](#)

HAWC Collaboration: A. Albert et al. 2022, [ApJ 928 \(2022\), 116](#).

- Galactic Gamma-Ray sources may be Pevatrons – sources of cosmic rays
- Spectrum of Gamma Rays may be of hadronic origin



Spectral Energy Density
from HAWC data

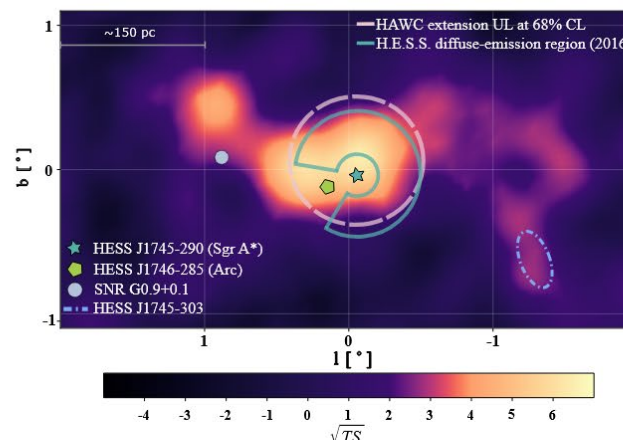
Modeling Leptonic &
Hadronic Components

Galactic Center Pevatron?

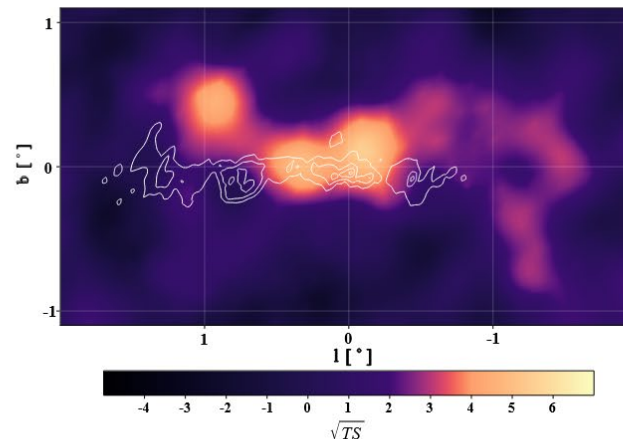
Observation of the Galactic Center PeVatron Beyond 100 TeV with HAWC

HAWC Collaboration, A. Albert *et al* 2024 *ApJL* 973 L34

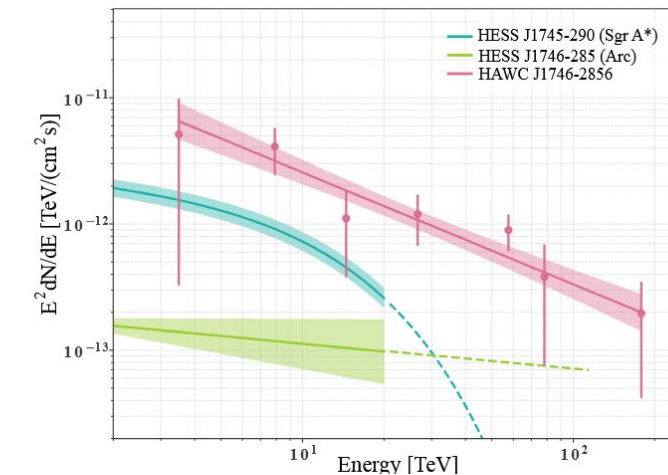
- Hot off the press. Published last week
- HAWC J1746-2856 98 events observed with energies above 100 TeV
- First detection of gamma rays above 100 TeV from the galactic center.
- 2546 days of HAWC data
- maximum significance of 6.5σ above the background
- <https://cerncourier.com/a/a-pevtron-at-the-galactic-centre/>



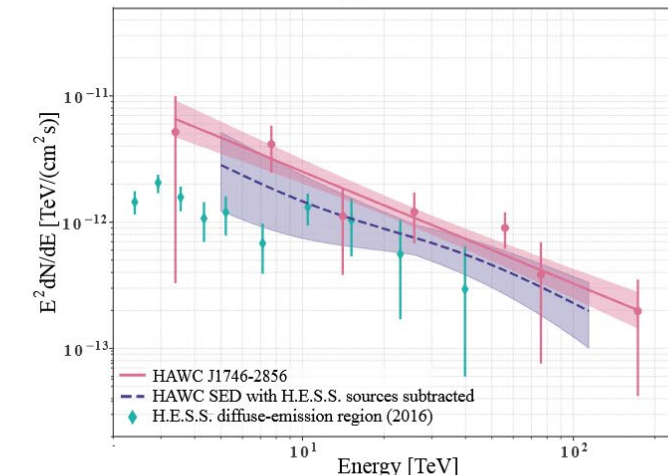
HAWC Significance map using NN



HAWC Significance map using NN with H.E.S.S. sources subtracted



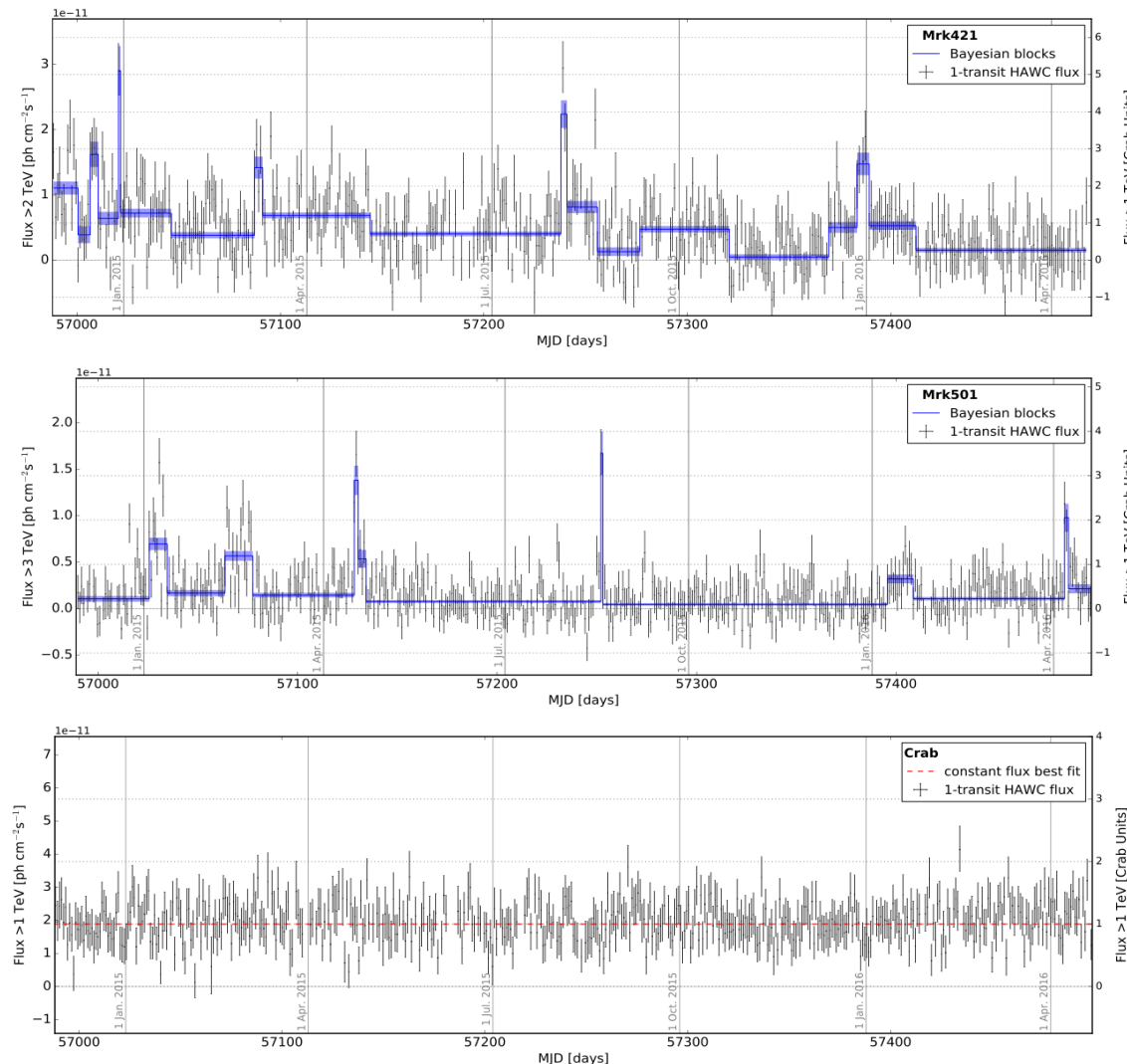
HAWC Spectral Energy Distribution



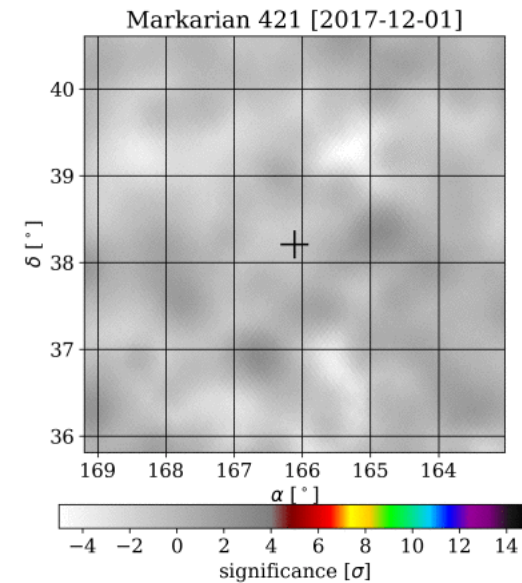
HAWC Spectral Energy Distribution with H.E.S.S. sources subtracted

Monitoring of flaring sources MKN 421, MKN 501 and Crab

Daily monitoring of TeV gamma-ray emission from Mrk 421, Mrk 501, and the Crab Nebula with HAWC
HAWC Collaboration: A.U. Abeysekara et al., [ApJ 841 \(2017\), 100](#).



- Monitoring AGN flares:
 - [ATel #8922](#), [#9137](#), [#9936](#), [#9946](#), [#11077](#), [#11194](#).
 - Many notifications under MoU.
- Monitoring few hundreds sources on multiple time scales (seconds to days).



Short GRB searches

[Constraints on the very high energy gamma-ray emission from short GRBs with HAWC](#)

HAWC Collaboration: A. Albert et al. 2022, [ApJ 936 \(2022\), 2](#).

Table 1
Short GRBs Detected in the Field of View of HAWC

GRB Name	Detection Time (UT)	R.A. J2000 (deg)	Decl. J2000 (deg)	Error Box (deg)	Zenith Angle (deg)	T_{90} (s)	R.A. (deg)	Decl. (deg)	HAWC Upper Limit [0–2 s] ($\text{erg cm}^{-2} \text{s}^{-1}$)	Significance (σ)
Fermi-GBM										
GRB 141202470	11:17:05.606	145.01	59.87	3°32'	40.83	1.34	142.89	60.7	1.603e-05	0.43
GRB 150201040	00:56:54.289	5.63	19.75	13°92'	39.53	0.51	11.28	8.13	8.420e-06	-1.82
GRB 150522944	22:38:44.068	130.86	58.58	10°47'	40.02	1.02	112.49	55.82	8.517e-06	-0.52
GRB 150705588	14:07:11.608	66.54	-6.62	12°60'	38.34	0.70	63.12	3.31	2.767e-06	0.57
GRB 150811849	20:22:13.749	186.35	-14.11	0°99'	37.77	0.64	2.512e-06	...
GRB 150906944	22:38:47.307	212.04	1.09	5°19'	23.76	0.32	209.83	5.52	1.333e-06	0.34
GRB 150923297	07:07:36.184	316.80	31.82	10°76'	50.29	0.19	327.262	38.1856	2.926e-05	-0.49
GRB 151022577	13:51:02.089	110.37	40.23	21°36'	33.64	0.32	120.27	49.19	6.415e-06	-0.86
GRB 160211119	02:50:48.276	123.20	53.43	4°97'	44.87	0.96	121.57	51.57	2.921e-05	0.02
GRB 160406503	12:04:36.798	261.80	32.26	11°80'	20.28	0.43	266.8	22.05	7.265e-07	-0.03
GRB 160820496	11:54:10.646	6.82	21.85	4°52'	40.67	0.38	2.542e-06	...
GRB 161026373	08:57:16.281	67.70	41.85	11°68'	23.16	0.11	54.67	37.98	1.968e-06	0.65
GRB 170203486	11:40:25.855	245.09	-0.51	14°06'	38.39	0.34	234.97	9.55	1.157e-05	1.85
GRB 170219002	00:03:07.123	54.84	50.07	1°41'	31.20	0.10	54.19	51.32	2.179e-06	-1.03
GRB 170403583	13:59:17.798	267.08	14.53	7°16'	35.96	0.48	1.133e-05	...
GRB 170604603	14:28:05.086	340.44	40.67	4°10'	35.12	0.32	344.3	42.56	4.005e-06	0.03
GRB 170709334	08:00:23.979	310.04	2.20	7°49'	16.73	1.86	311.76	5.563	6.360e-07	-1.65
GRB 170818137	03:17:19.979	297.22	6.35	11°54'	22.16	0.58	287.11	9.09	8.255e-07	0.18
GRB 170826369	08:51:07.514	64.34	21.07	0°86'	50.83	0.26	2.355e-04	...
GRB 171011810	19:26:27.946	177.04	26.93	15°96'	35.39	0.48	187.80	14.53	2.150e-06	-0.75
GRB 171207055	01:18:42.452	314.39	51.67	9°54'	47.33	0.18	319.53	48.74	2.935e-05	-0.49
GRB 180103090	02:09:12.118	25.40	28.01	6°97'	14.26	0.02	32.51	28.99	7.235e-07	0.59
GRB 180128881	21:09:19.457	323.18	-13.55	9°22'	40.56	1.79	314.86	-11.37	6.350e-05	1.14
GRB 181222841	20:11:37.438	311.15	22.86	1°60'	14.03	0.576	311.68	22.63	4.935e-07	-0.782
GRB 190226515	12:21:45.676	224.43	-8.61	5°11'	33.71	0.192	221.914	-12.88	3.397e-06	-1.083
GRB 190630257	06:09:58.319	306.98	-1.33	7°65'	39.07	0.224	312.63	-0.36	1.231e-05	-0.824
GRB 190724031	00:43:56.792	170.35	15.15	13°62'	42.66	0.08	166.99	5.44	6.350e-05	-0.177
GRB 190905985	23:38:28.489	234.48	3.12	3°62'	17.49	0.704	232.32	0.36	7.925e-07	-1.577
GRB 191031891	21:23:31.128	283.27	47.64	0°05'	32.94	0.256	1.138e-06	...
GRB 191117637	15:17:38.361	157.42	7.23	13°07'	32.21	1.28	152.56	-3.97	3.697e-05	-0.105
GRB 200221162	03:52:58.711	157.10	33.14	5°04'	43.20	1.728	153.69	35.74	1.605e-05	-0.4236
GRB 200224416	09:58:44.567	187.02	-19.55	12°52'	42.85	0.064	187.28	-13.06	8.470e-06	-0.865
GRB 200423579	13:54:11.373	325.02	66.78	11°20'	47.88	0.032	312.924	57.27	9.970e-06	-1.635
GRB 200514380	09:07:37.124	238.32	37.22	13°12'	34.52	1.664	242.86	34.16	3.245e-06	-1.077
Swift-BAT										
GRB 141205A	08:05:17	92.86	37.88	0°03'	19.36	1.1	4.829e-07	...
GRB 150423A	06:28:04	221.58	12.28	0°0004'	12.63	0.22	2.163e-07	...
GRB 150710A	00:28:02	194.47	14.32	0°0008'	5.40	0.15	4.630e-07	...
GRB 160714A	02:19:15	234.49	63.81	0°045'	44.88	0.35	2.041e-05	...
GRB 170112A	02:02:00	15.23	-17.23	0°042'	46.34	0.06	4.66e-05	...
Fermi-LAT										
GRB 170206A	10:51:57.696	212.79	14.48	0°85'	11.10	1.168	4.736e-07	...
GRB 180225417	10:00:54.175	180.98	-9.49	7°47'	39.01	0.896	178.44	-13.19	3.710e-05	1.111
GRB 180402406	09:44:59.367	251.90	-14.96	0°05'	36.16	0.448	2.470e-06	...
GRB 180511364	08:43:35.786	250.42	-8.18	15°07'	29.67	0.128	26.68	247.96	2.156e-06	-0.769
GRB 180511437	10:29:52.606	257.78	9.07	10°16'	31.91	1.984	260.16	14.15	2.745e-06	0.378
GRB 180617872	20:55:23.463	106.89	24.87	8°24'	15.45	1.920	106.50	25.74	1.052e-06	0.868
GRB 180626392	09:23:50.648	285.06	44.82	8°21'	37.59	0.960	294.37	46.65	4.691e-06	0.575
GRB 180803590	14:09:49.734	71.63	57.65	17°37'	38.84	0.384	68.736	56.7804	8.505e-06	-1.83

- HAWC searches for GRBs.
- EBL, High Energy Threshold & Bad Luck...

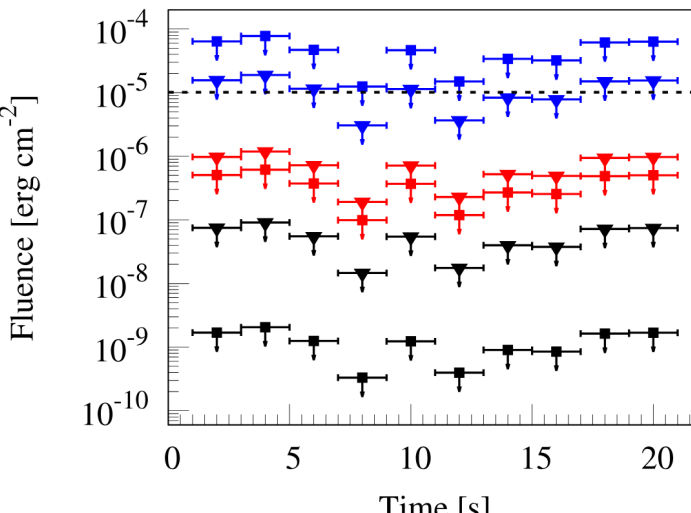
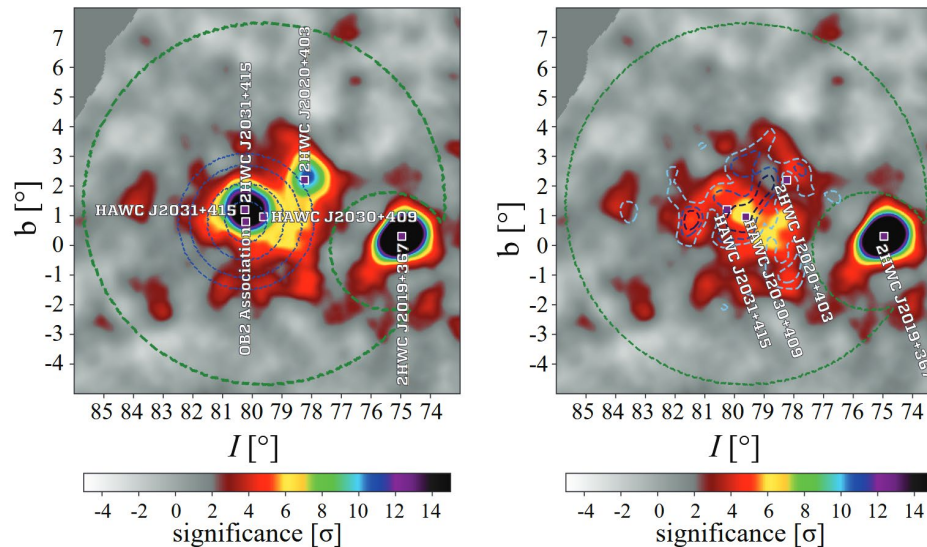


Figure 3. HAWC upper limits of the fluence extracted in the energy range 80–800 GeV for the GRB 170206A for different spectral indices and redshifts. The limits are calculated for spectral indices of -0.7 (triangles) and -2.2 (squares) and for redshifts of 0 (black), 0.3 (red), and 1 (blue). The dashed black line is the average flux measured by Fermi-LAT during the prompt emission.

Origin of Galactic Cosmic Rays?

[Hawc observations of the acceleration of very-high-energy cosmic rays in the cygnus cocoon](#)

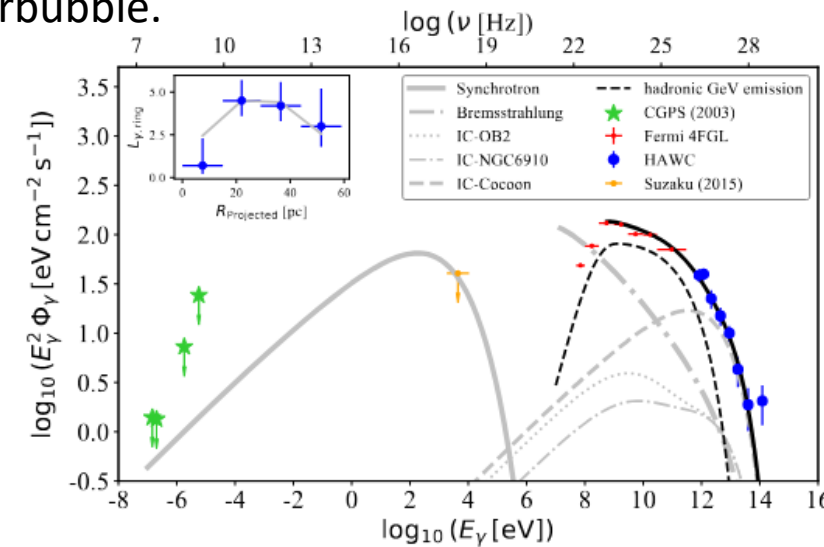
HAWC Collaboration: A. Albert et al. 2021, [Nature Astron \(2021\)](#).



Significance map of the Cocoon region before (left) and after (right) subtraction of the known sources at the region.

- Observations of 1-100 TeV γ rays coming from the ‘Cygnus Cocoon’
- These γ rays are likely produced by 10-1000 TeV freshly accelerated CRs originating from the enclosed star forming region Cygnus OB2

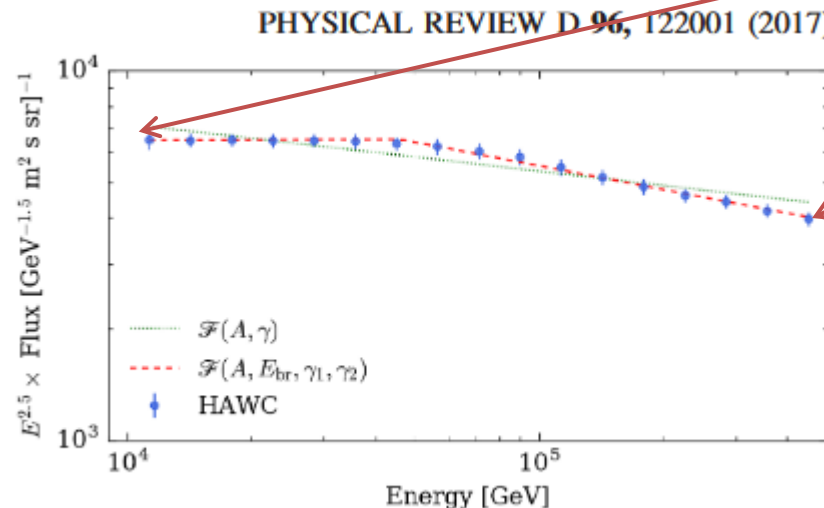
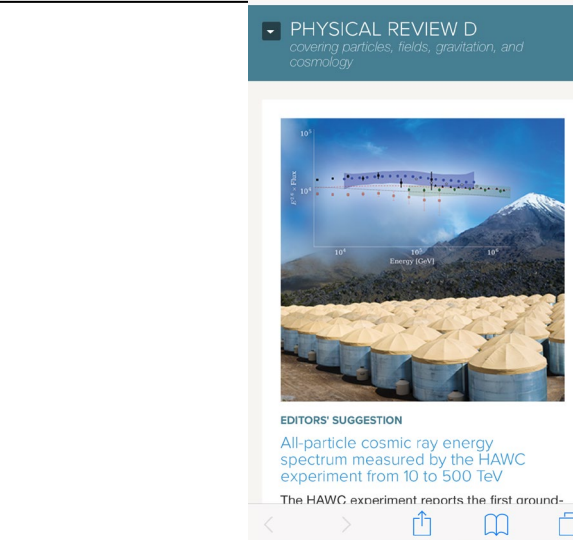
- The measured flux is likely originated by hadronic interactions.
- The spectral shape and the emission profile of the Cocoon changes from GeV to TeV energies, which reveals the transport of cosmic particles and historical activity in the superbubble.



Leptonic modelling at the Cocoon region. Multi-wavelength observations of the Cygnus Cocoon constrain the Synchrotron and Bremsstrahlung radiation of relativistic electrons. The light grey curves correspond to a “minimum leptonic model”, where only γ -rays above 1 TeV are explained by electron emission. Observations between 0.1–100 GeV are explained by hadronic interaction (black dashed curve). The red points are the GeV flux points by Fermi-LAT and the blue circles are the HAWC flux points. The sum of the emission above ~ 0.3 GeV is indicated by the black solid curve. I

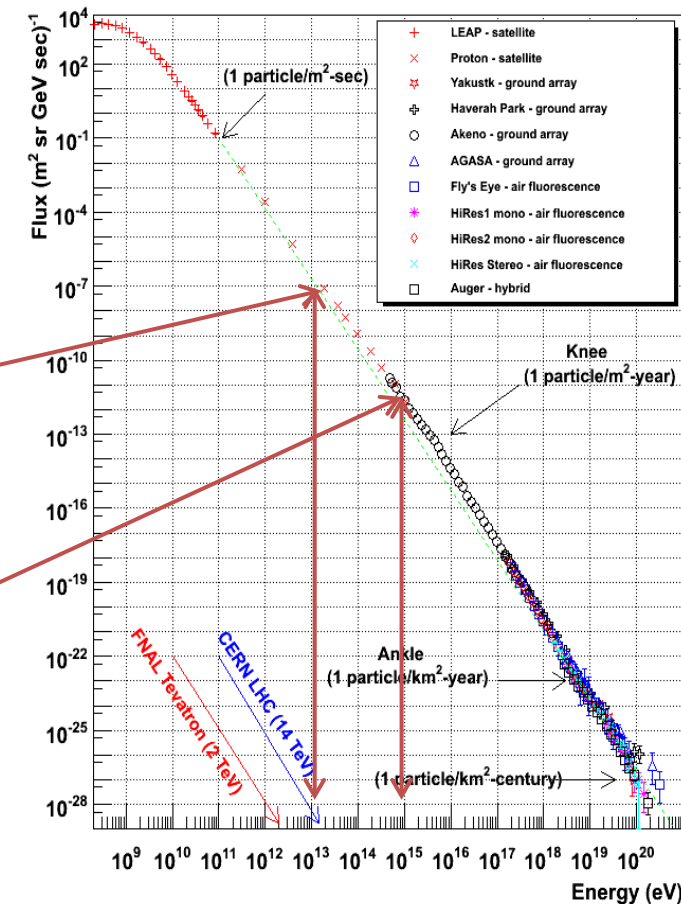
Cosmic Ray Studies – All-particle Energy Spectrum

[All-particle cosmic ray energy spectrum measured by the HAWC experiment from 10 to 500 TeV](#) HAWC Collaboration: R. Alfaro et al., [Phys. Rev. D 96 \(2017\), 122001](#)



<https://journals.aps.org/prd/abstract/10.1103/PhysRevD.96.122001>

Cosmic Ray Spectra of Various Experiments



Where do high-energy cosmic ray originate?

Cosmic Ray Spectrum of Protons Plus Helium

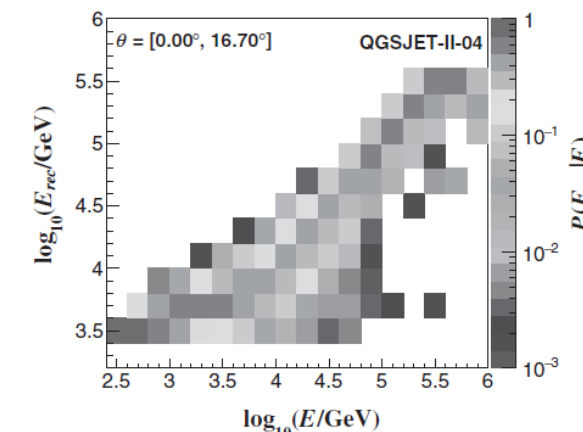
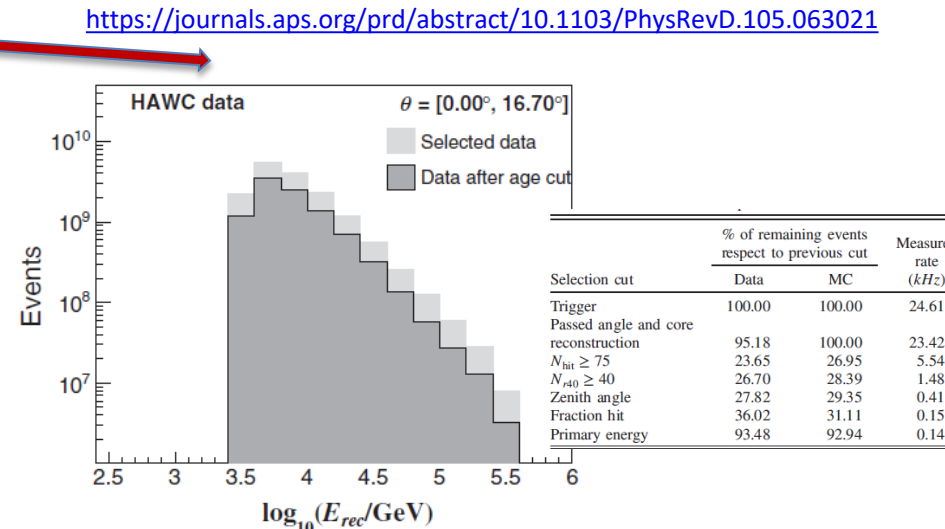
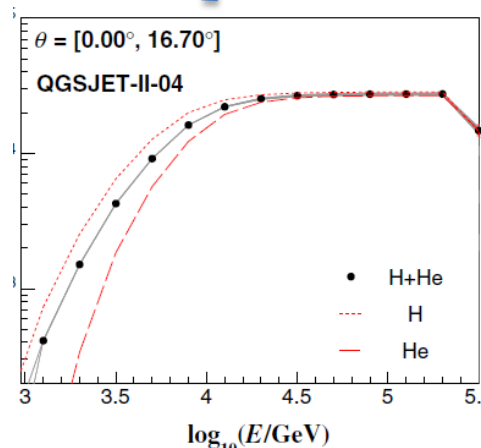
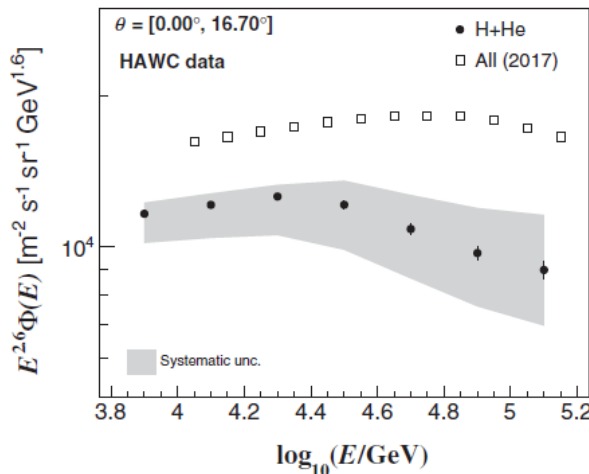
[Cosmic ray spectrum of protons plus helium nuclei between 6 and 158 TeV from HAWC data](https://journals.aps.org/prd/abstract/10.1103/PhysRevD.105.063021) HAWC Collaboration: A. Albert et al. 2022, [PRD 105 \(2022\), 063021](https://journals.aps.org/prd/abstract/10.1103/PhysRevD.105.063021)

$$\Phi(E) = \frac{N(E)}{\Delta E \Delta t A_{\text{eff}}(E) \Delta \Omega}$$

- $\Phi(E)$: Energy Spectrum: Intensity as a function of Energy
- $N(E)$: Number of selected events in energy bin with mean energy E . Sum = 7.2×10^{11} EAS events
- ΔE : width of energy bin with mean energy E
- Δt : exposure time = 3.74 years
- $\Delta \Omega$: solid angle = 1.14 sr
- $A_{\text{eff}}(E)$: Effective Area as a function of Energy

Cosmic ray spectrum of protons plus helium nuclei between 6 and 158 TeV from HAWC data

A. Albert et al.
Phys. Rev. D **105**, 063021 – Published 25 March 2022



Cosmic Ray Spectrum of Protons Plus Helium: Shower Age to inform composition

In HAWC, the lateral age of EAS is obtained event by event from a χ^2 fit with a modified Nishimura-Kamata-Greisen function,

$$f(r) = A \left(\frac{r}{r_0} \right)^{s-3} \left(1 + \frac{r}{r_0} \right)^{s-4.5}, \quad (1)$$

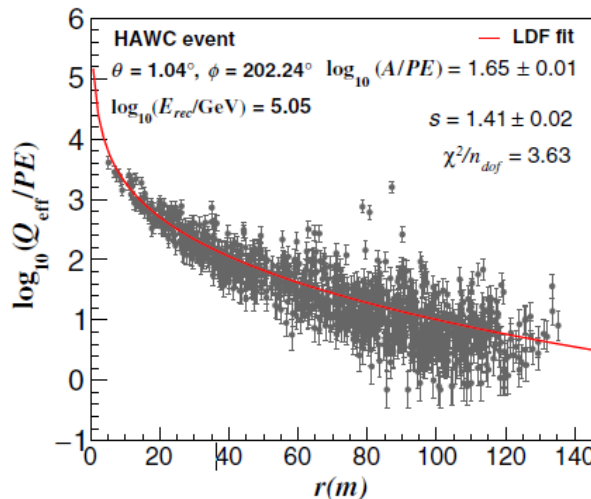


FIG. 1. The lateral effective charge distribution of an EAS event measured with HAWC on June 2, 2019. The estimated energy, zenith angle, and azimuth are $\log_{10}(E_{\text{rec}}/\text{GeV}) = 5.05$, $\theta = 1.04^\circ$, and $\phi = 202.24^\circ$, respectively. The gray dots represent the measured Q_{eff} per PMT in PE (photoelectron) units. The vertical errors are the systematic uncertainties. The result of the fit with Eq. (1) is shown with a red line. The corresponding fit parameters are shown; the number of degrees of freedom is 1018.

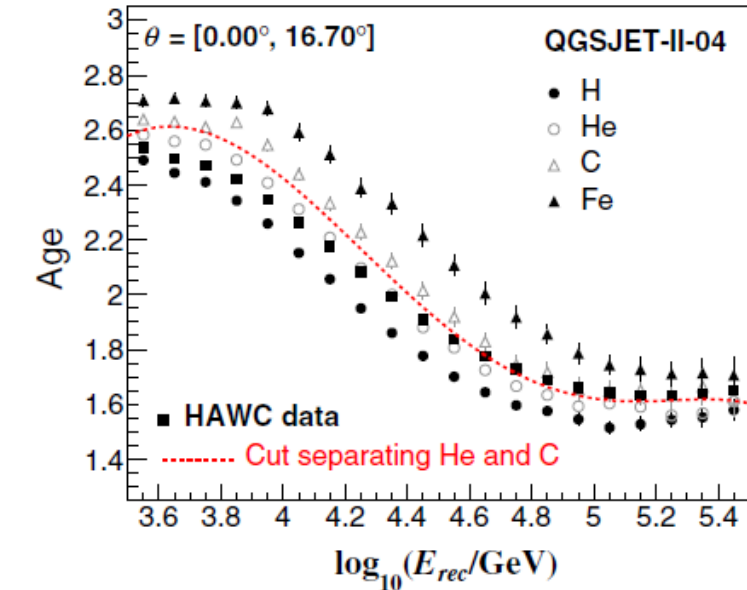
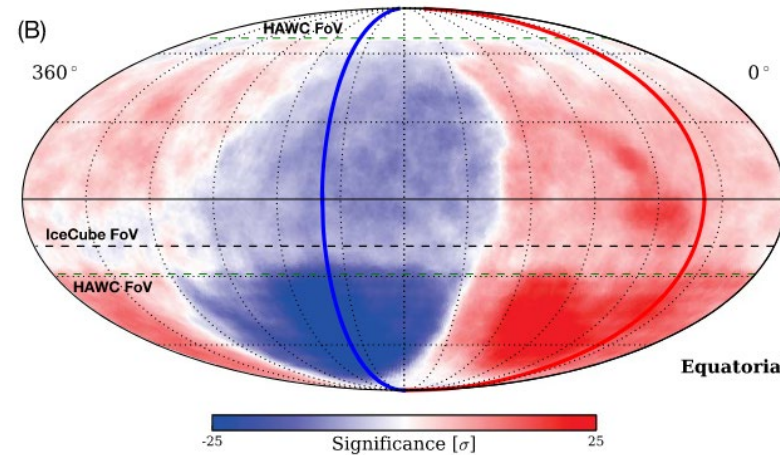
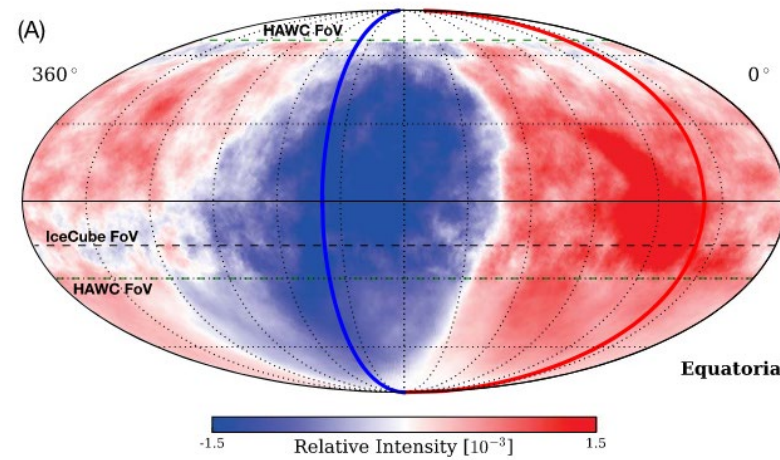


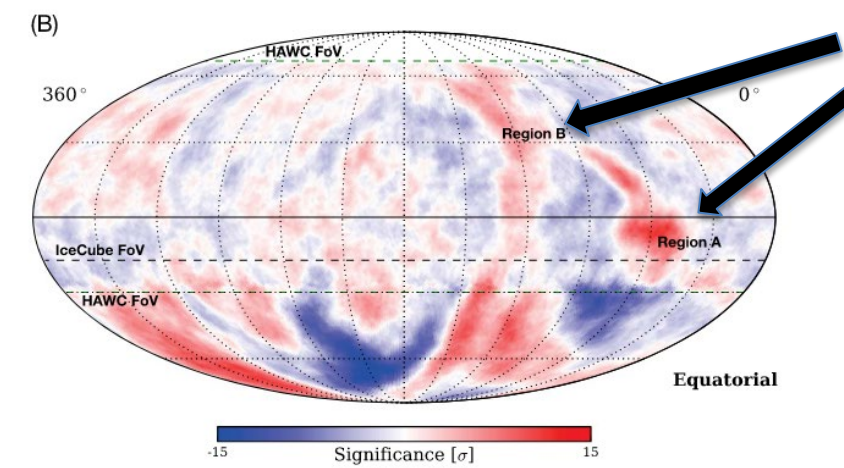
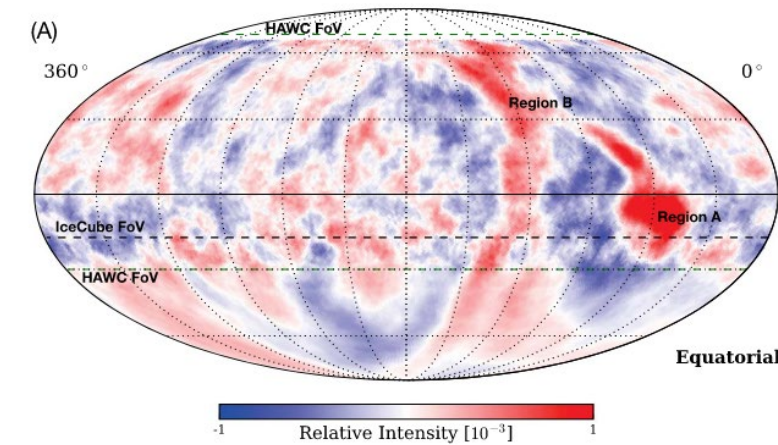
FIG. 4. Predictions of the QGSJET-II-04 model for the energy dependence of the mean lateral age in vertical air showers initiated by four cosmic ray species at HAWC. From top to bottom, the MC points correspond to Fe (solid triangles), C (hollowed triangles), He (hollowed circles), and H (solid circles) primaries, respectively. For clarity, not all the elemental nuclei simulated in this work were included in the plot. HAWC data has also been added to the figure. They are shown with black squares. The $s_{\text{He-C}}$ cut employed to extract the enriched subsample of light nuclei is plotted using a dashed line in red.

Cosmic Ray Anisotropy – All Sky (Combined HAWC & IceCube)

[All-Sky Measurement of the Anisotropy of Cosmic Rays at 10 TeV and Mapping of the Local Interstellar Magnetic Field](#) HAWC Collaboration: A.U. Abeysekara et al., and IceCube Collaboration, M.G. Aartsen et al., [ApJ871\(2019\), 096](#).



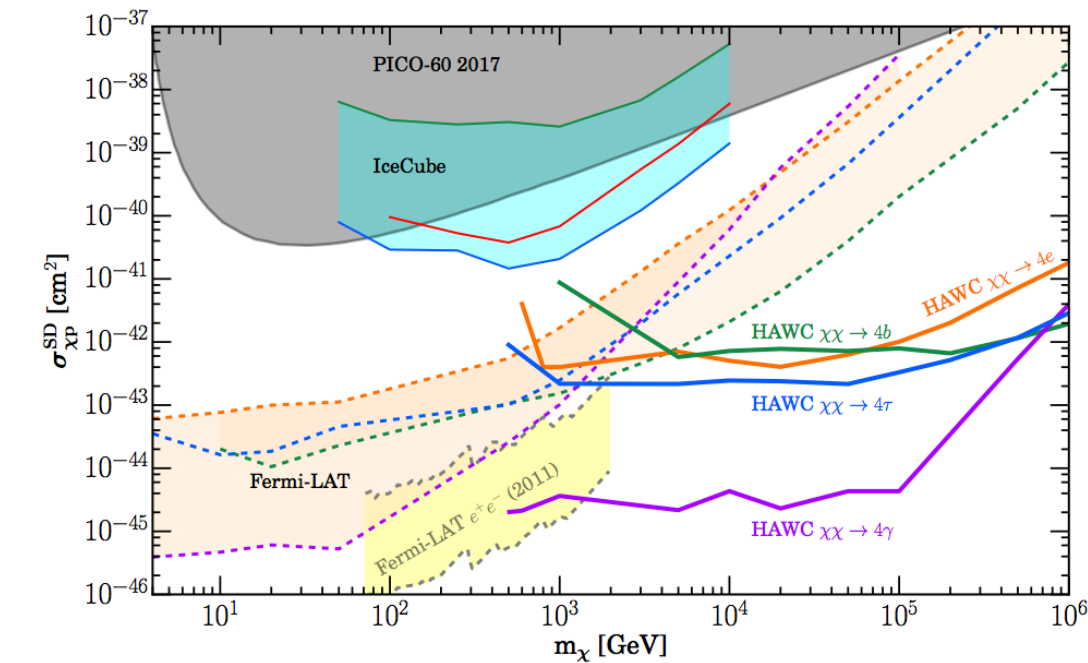
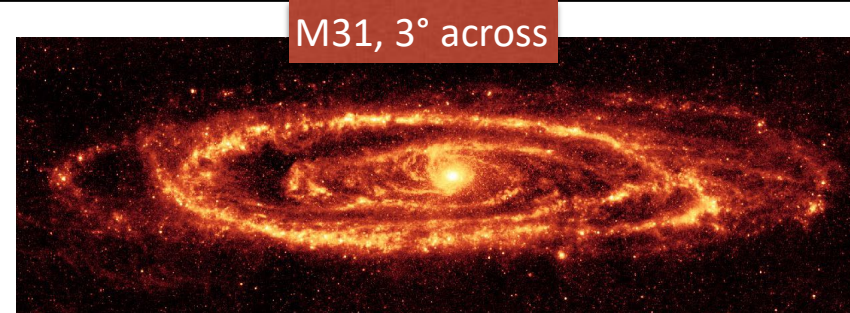
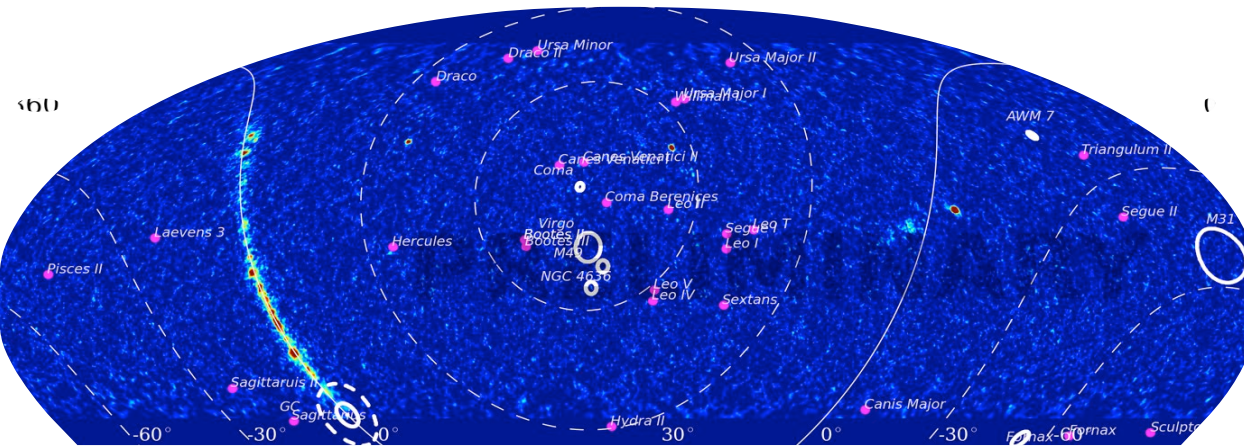
Large-Scale Anisotropy



Small-Scale Anisotropy

Dark matter searches

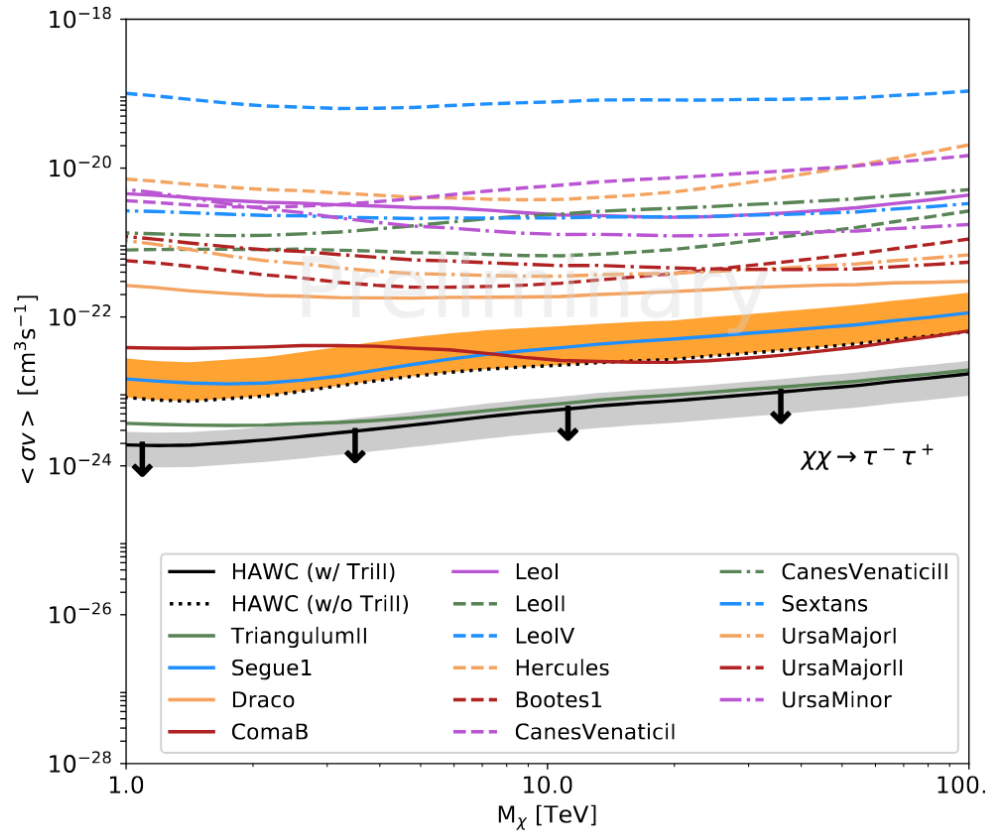
- Large sky coverage → variety of targets to look for annihilation or decay signal:
 - Dwarf Spheroidal Galaxies
 - Galactic Halo
 - Andromeda Galaxy
 - All sky search
 - Sun Virgo cluster
 - Etc.



Dark Matter Searches

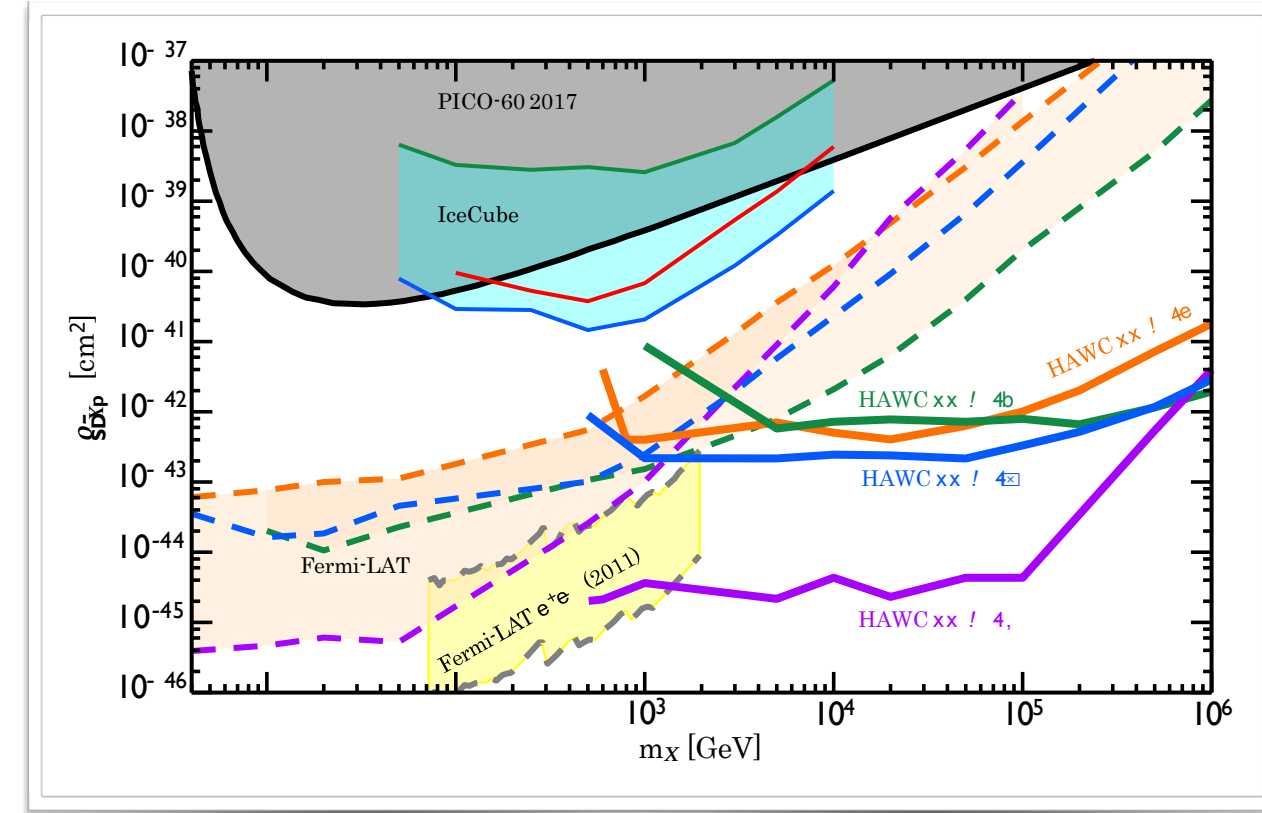
No gamma-rays from dwarf spheroidal galaxies (most sensitive limits > 30 TeV)

[Dark Matter Limits from Dwarf Spheroidal Galaxies with the HAWC Gamma-Ray Observatory](#)
HAWC Collaboration: A. Albert et al., [ApJ 853 \(2018\), 154](#).



No gamma-rays from the Sun

[Constraints on Spin-Dependent Dark Matter Scattering with Long-Lived Mediators from TeV Observations of the Sun with HAWC](#)
HAWC Collaboration: A. Albert et al., [PRD 98 \(2018\), 123012](#).



Multi-messenger Observations of a Binary Neutron Star Merger

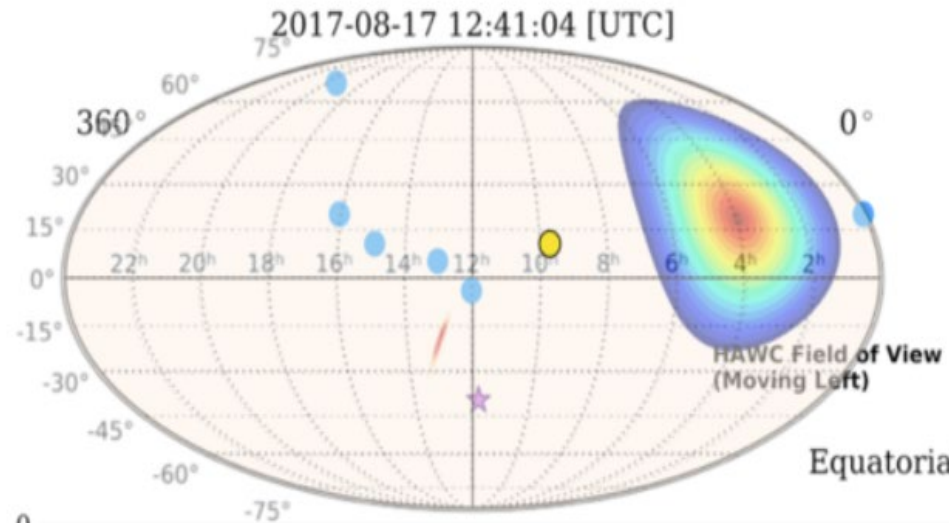
Multi-messenger Observations of a Binary Neutron Star Merger

LIGO Collaboration, Virgo Collaboration, HAWC Collaboration, etc., [ApJ 848 \(2017\), L12](#)

Multi-messenger Observations of a Binary Neutron Star Merger

LIGO Scientific Collaboration and Virgo Collaboration, Fermi GBM, INTEGRAL, IceCube Collaboration, AstroSat Cadmium Zinc Telluride Imager Team, IPN Collaboration, The Insight-Hxmt Collaboration, ANTARES Collaboration, The Swift Collaboration, AGILE Team, The IM2H Team, The Dark Energy Camera GW-EM Collaboration and the DES Collaboration, The DLT40 Collaboration, GRAVITAT: GRAVitational Wave Inaf TeAm, The Fermi Large Area Telescope Collaboration, ATCA: Australia Telescope Compact Array, ASKAP: Australian SKA Pathfinder, Las Cumbres Observatory Group, OzGrav, DWF (Deeper, Wider, Faster Program), AST3, and CAASTRO Collaborations, The VINROUGE Collaboration, MASTER Collaboration, J-GEM, GROWTH, JAGWAR, Caltech-NRAO, TTU-NRAO, and NuSTAR Collaborations, Pan-STARRS, The MAXI Team, TZAC Consortium, KU Collaboration, Nordic Optical Telescope, ePESSTO, GROND, Texas Tech University, SALT Group, TOROS: Transient Robotic Observatory of the South Collaboration, The BOOTES Collaboration, MWA: Murchison Widefield Array, The CALET Collaboration, IKI-GW Follow-up Collaboration, H.E.S.S. Collaboration, LOFAR Collaboration, LWA: Long Wavelength Array, HAWC Collaboration, The Pierre Auger Collaboration, ALMA Collaboration, Euro VLBI Team, Pi of the Sky Collaboration, The Chandra Team at McGill University, DFN: Desert Fireball Network, ATLAS, High Time Resolution Universe Survey, RIMAS and RATIR, and SKA South Africa/MeerkAT (See the end matter for the full list of authors.)

Received 2017 October 3; revised 2017 October 6; accepted 2017 October 6; published 2017 October 16



HAWC field of view at time of LIGO Virgo binary neutron star merger event GW170817. The star indicates the merger location indicated by the Fermi GBM data.

- A significant fraction of the astronomical community is an author on the LIGO Binary Neutron Star Merger paper...
- HAWC has a plethora of MOUs with many observatories to facilitate multi-wavelength (messenger) studies of astrophysical phenomenon.

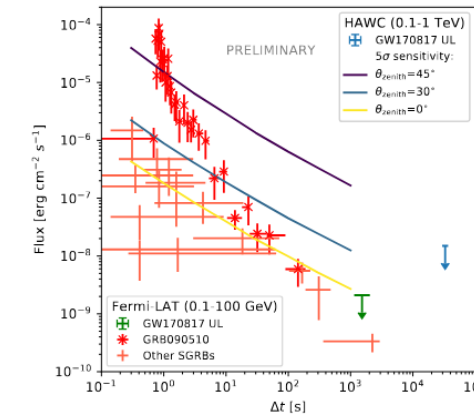


Figure 3: HAWC 95 % C.L. upper bound (blue) on GW170817 between 100 GeV and 1 TeV from $\Delta t = t - t_0 = 8.20$ hrs to $\Delta t = 10.23$ hrs where t_0 is the time of coalescence. Fermi-LAT UL between 100 MeV and 100 GeV from $\Delta t = 1153$ s to $\Delta t = 2027$ s are shown in green. For comparison we show the HAWC sensitivity (0.1–1 TeV) a function of the emission duration Δt and Fermi-LAT measurements of previously detected short GRBs (red) [23]. The Fermi-LAT measurements of GRB090510 as a function of time are highlighted.

[Search for very-high-energy gamma-ray counterparts of gravitational waves with HAWC](#)
Presented at the 36th International Cosmic Ray Conference (ICRC 2019)



STATUS AND RESULTS OF THE HIGH-ALTITUDE WATER CHERENKOV (HAWC) OBSERVATORY

THE UNIVERSITY OF UTAH
Department of
Physics & Astronomy

Multi-messenger observations of a flaring blazar coincident with high-energy neutrino IceCube-170922A

The IceCube, *Fermi*-LAT, MAGIC, AGILE, ASAS-SN, **HAWC**, H.E.S.S., INTEGRAL, Kanata, Kiso, Kapteyn, Liverpool telescope, Subaru, *Swift/NuSTAR*, VERITAS, and VLA/17B-403 teams †

Individual astrophysical sources previously detected in neutrinos are limited to the Sun and the supernova 1987A, whereas the origins of the diffuse flux of high-energy cosmic neutrinos remain unidentified. On 22 September 2017 we detected a high-energy neutrino, IceCube-170922A, with an energy of ~ 290 terra-electronvolts. Its arrival direction was consistent with the location of a known γ -ray blazar TXS 0506+056, observed to be in a flaring state. An extensive multi-wavelength campaign followed, ranging from radio frequencies to γ -rays. These observations characterize the variability and energetics of the blazar and include the first detection of TXS 0506+056 in very-high-energy γ -rays. This observation of a neutrino in spatial coincidence with a γ -ray emitting blazar during an active phase suggests that blazars may be a source of high-energy neutrinos.

No γ -ray source above 1 TeV at the location of TXS 0506+056 was found in survey data of the High Altitude Water Cherenkov (**HAWC**) γ -ray observatory (36), either close to the time of the neutrino alert, or in archival data taken since November 2014 (25).

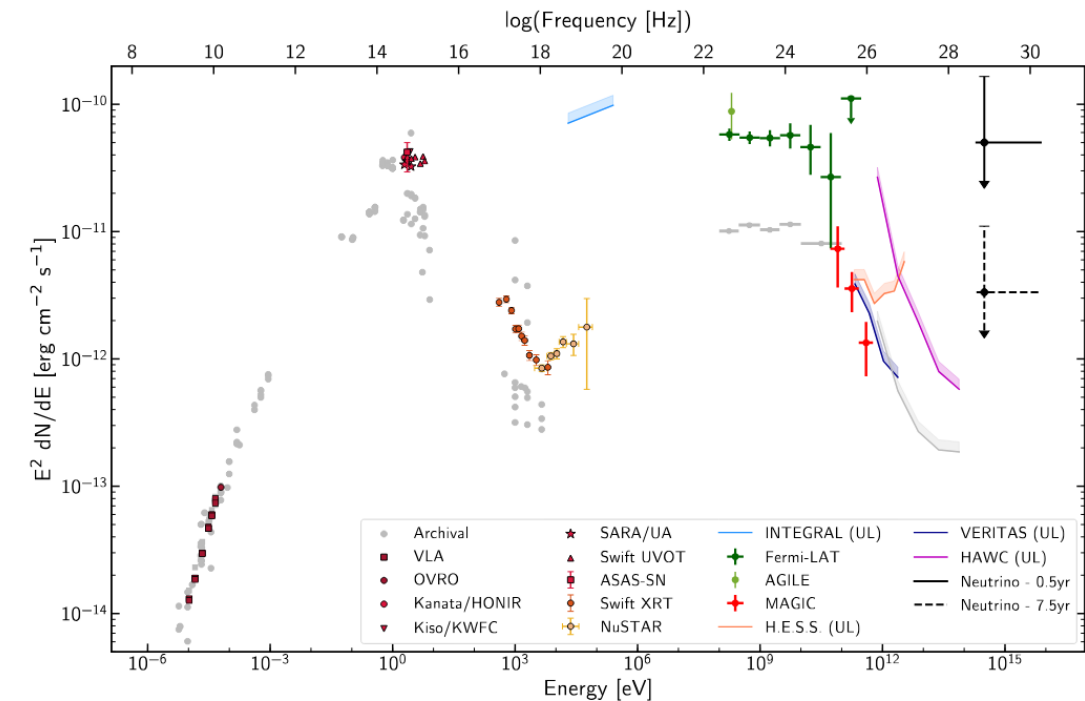


Figure 4: Broadband spectral energy distribution for the blazar TXS 0506+056. The SED

Constraints on Lorentz Invariance Violation from HAWC Observations of Gamma Rays above 100 TeV

[Constraints on Lorentz Invariance Violation from HAWC Observations of Gamma Rays above 100 TeV](#)
HAWC Collaboration: A. Albert et al., [PRL 124,021102\(2020\)](#).

Lorentz Invariance Violations (LIV)

- Higher-energy photon observation constrains the energy scale of LIV because photon decay is allowed
- Also, constrained by distant, fast transients (e.g. gamma-ray bursts, and blazar flares)

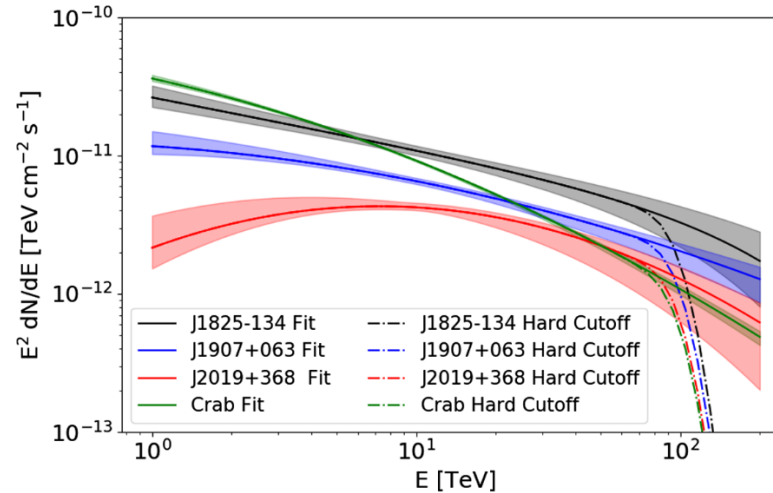


FIG. 1. Comparison of the best-fit spectra with those expected were a hard cutoff found at 100 TeV. From top to bottom at 1 TeV: the spectra for the Crab, J1825 – 134, J1907 + 063, and J2019 + 368. The bands represent statistical uncertainties of the fits

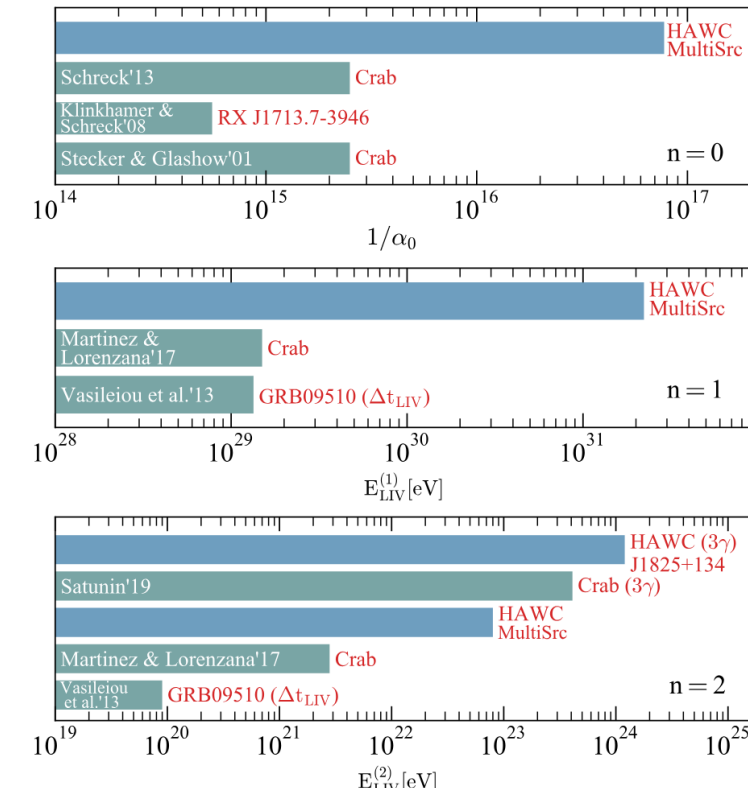


FIG. 2. HAWC 95% C.L. LIV limits for $n = 0, 1$, and 2 . We show previous strong constraints due to photon decay, as well as based on an energy-dependent time delay (Δt_{LIV}) and photon splitting (3γ). For $n = 1$, HAWC limits are orders of magnitude above E_{Pl} . ($\sim 10^{28}$ eV).

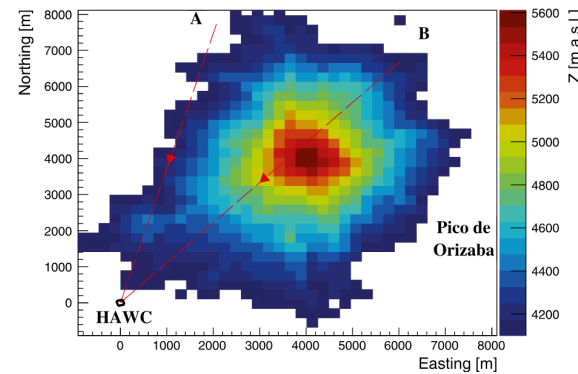


Fig. 1. Elevation map of the Pico de Orizaba volcano. The observatory footprint is shown with a black square around the origin of the coordinate system. The colour code indicates the altitude above sea level. Note that HAWC is located at ≈ 4100 m a.s.l. The arrows A and B show the approximate angular region (36° in azimuth) used in the analysis.

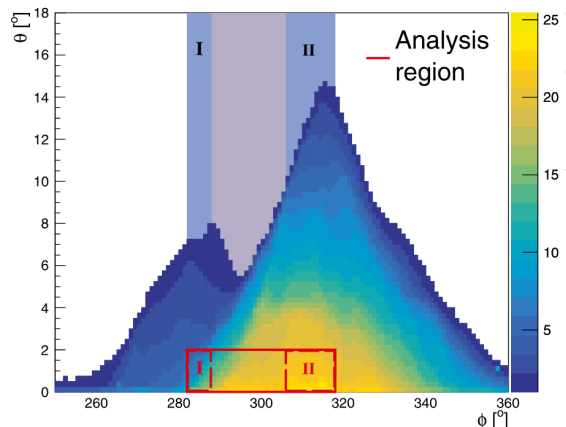


Fig. 6. Pico de Orizaba profile as seen from the centre of the HAWC main array. The shaded areas behind the mountain show the solid angles where muons propagate before being scattered towards almost horizontal directions into the three analysis regions, delimited by red lines (full region and regions I and II).

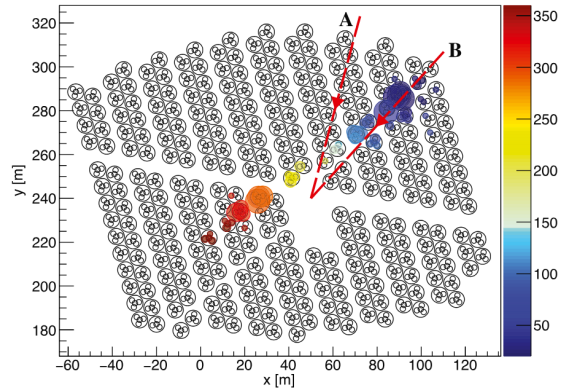


Fig. 2. Simulation of a horizontal muon passing through HAWC. The colour code indicates the PMT hit time while the size of the filled circles is proportional to the measured charge. The muon track points to the thickest region of the Pico de Orizaba volcano. The arrows show the approximate angular region used in the analysis and correspond to those shown in **Fig. 1**. The x and y axis are oriented along the Easting and Northing directions respectively.

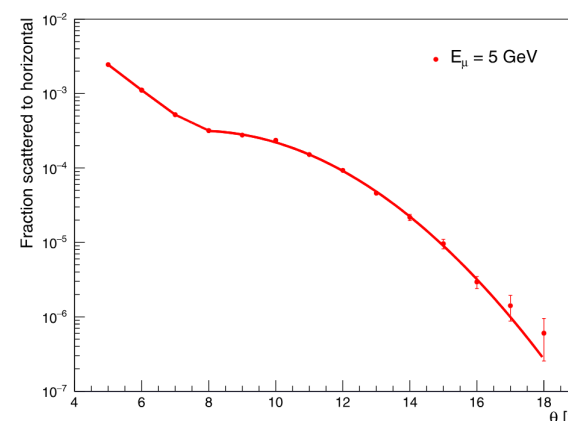


Fig. 8. Fraction of simulated 5 GeV muons that are scattered towards almost horizontal directions as a function of the elevation angle. The solid line shows the fit used in the calculations.

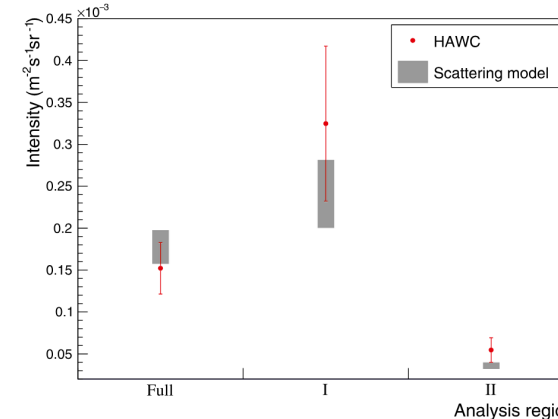


Fig. 9. Muon intensity for the analysis bins that point back to the base of the Pico de Orizaba volcano. The shaded area shows the estimation of the scattered intensity in the corresponding regions.

Scattered
Muon



Fake Muon
coming
through
Volcano

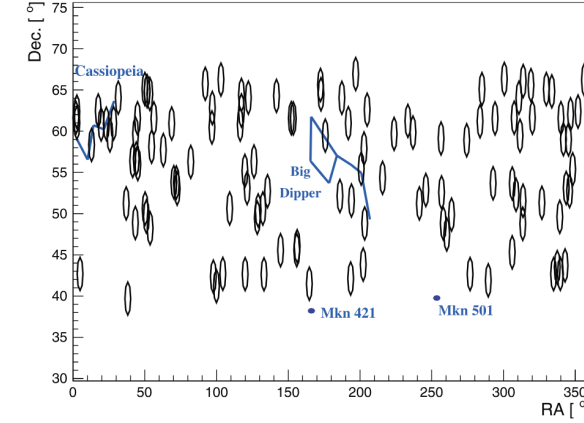


Fig. 11. Celestial coordinates for the 122 track events found in the data. The size of the circles shows the average angular resolution of the tracker. The muon signals reported on this work are dominated by those of scattered atmospheric muons, the figure illustrates the field of view accessible with our analysis. The location of the Cassiopeia and Big Dipper constellations are shown as reference, as well as the Mkn 421 and Mkn 501 AGNs.

Exploring the Coronal Magnetic Field with Galactic Cosmic Rays: The Sun Shadow Observed by HAWC

[Exploring the coronal magnetic field with galactic cosmic rays](#)
HAWC Collaboration: R. Alfaro et al. 2024, *ApJ* 966 67

The relative intensity of the cosmic rays passing through the heliosphere is related to solar magnetic fields.

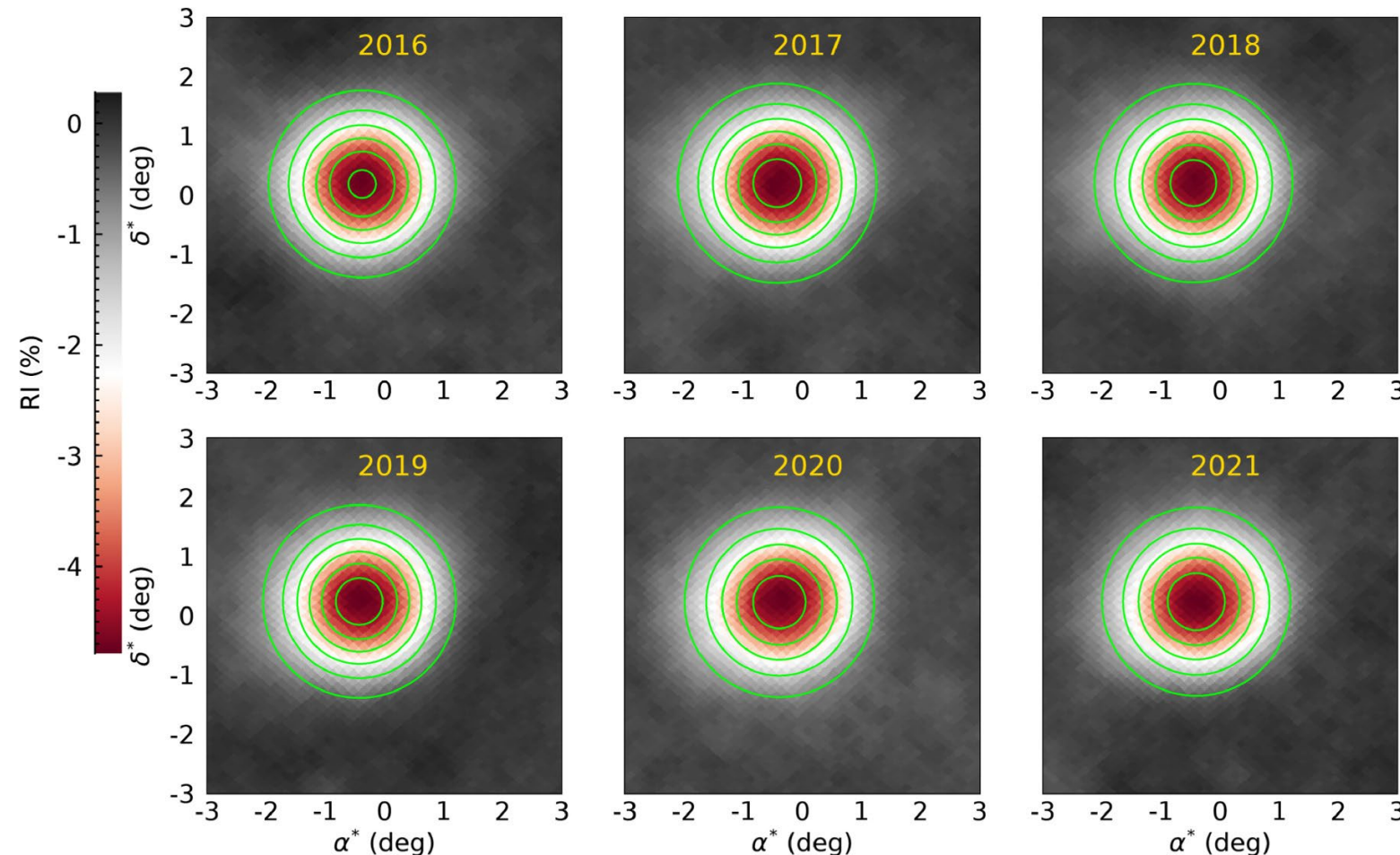


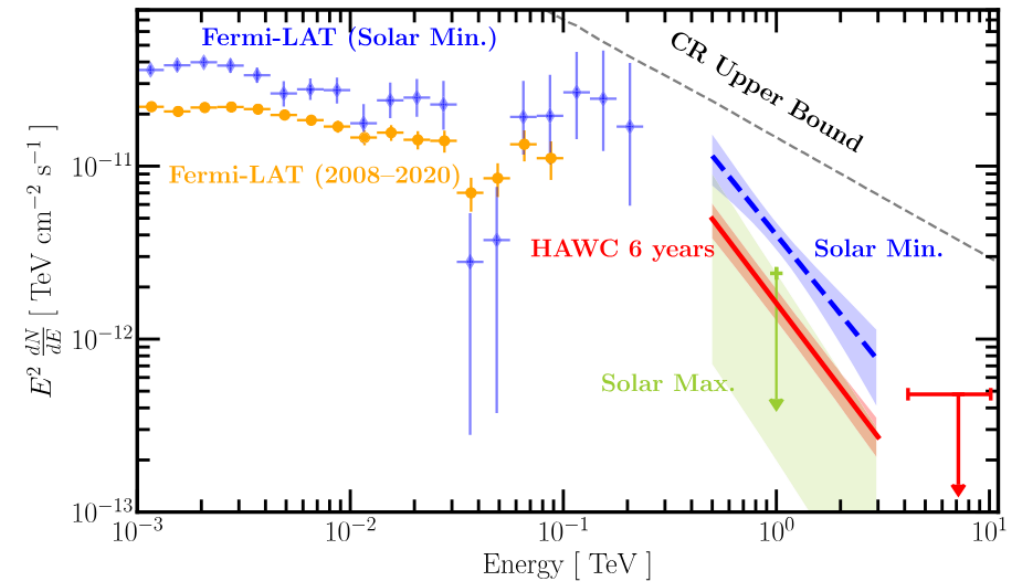
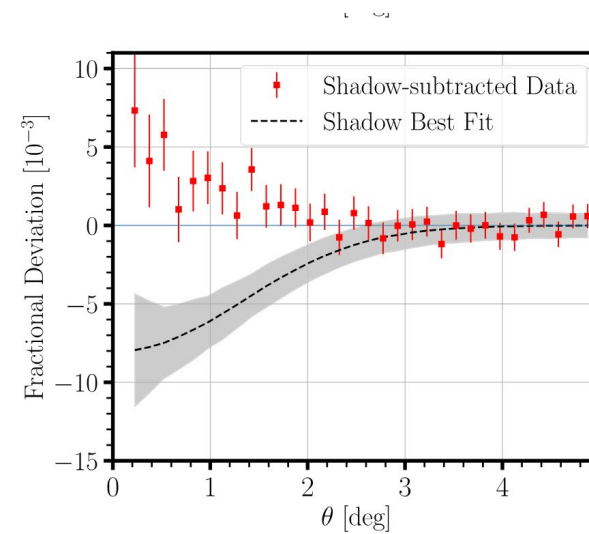
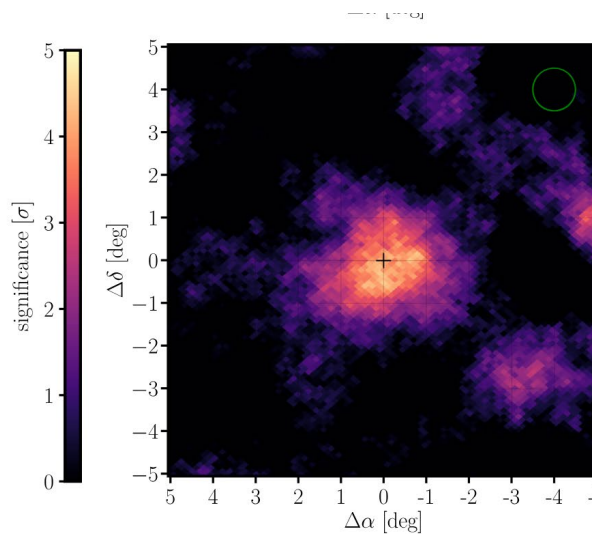
Figure 1. Relative Intensity maps (in percentage as marked by the color scale) of the GCR flux arriving from the Sun direction and integrated over 1 yr duration periods for the years 2016–2021 as marked in each panel. The contours mark the 15%, 30%, 45%, 60%, 75%, and 90% levels of the maximum significance ($\sim 59\sigma$) reached during the 2020 year. In all frames, the outer contour corresponds to 15%, and the subsequent internal contours correspond to an addition of 15% to each one up to 90%.

- TeV Gamma Ray flux measured at 6.3 sigma significance
- 6.1 years exposure
- The 0.5–2.6 TeV spectrum is well fit by

$$dN/dE = A(E/1\text{ TeV})^{-\gamma}$$

$$A = (1.6 \pm 0.3) \times 10^{-12} \text{ TeV}^{-1} \text{ cm}^{-2} \text{ s}^{-1} \quad \gamma = 3.62 \pm 0.14.$$

- Flux anti-correlated with solar activity.
- Seemingly due to hadronic Galactic cosmic rays



Spectrum of the solar disk

The HAWC Collaboration



USA:

Pennsylvania State University
University of Maryland
Los Alamos National Laboratory
University of Wisconsin
University of Utah
Univ. of California, Irvine
University of New Hampshire
University of New Mexico
Michigan Technological University
NASA/Goddard Space Flight Center
Georgia Institute of Technology
Colorado State University
Michigan State University
University of Rochester
University of California Santa Cruz

Europe:

Max Planck Institute KernPhysik Heidelberg
Krakow Nuclear Institute, Poland
INFN Padova, Italy

Mexico:

Instituto Nacional de Astrofísica, Óptica y Electrónica (INAOE)
Universidad Nacional Autónoma de México (UNAM)
Instituto de Física
Instituto de Astronomía
Instituto de Geofísica
Instituto de Ciencias Nucleares
Universidad Politécnica de Pachuca
Benemérita Universidad Autónoma de Puebla
Universidad Autónoma de Chiapas
Universidad Autónoma del Estado de Hidalgo
Universidad de Guadalajara
Universidad Michoacana de San Nicolás de Hidalgo
Centro de Investigación y de Estudios Avanzados
Instituto Politécnico Nacional
Centro de Investigación en Computación - IPN

Central America:

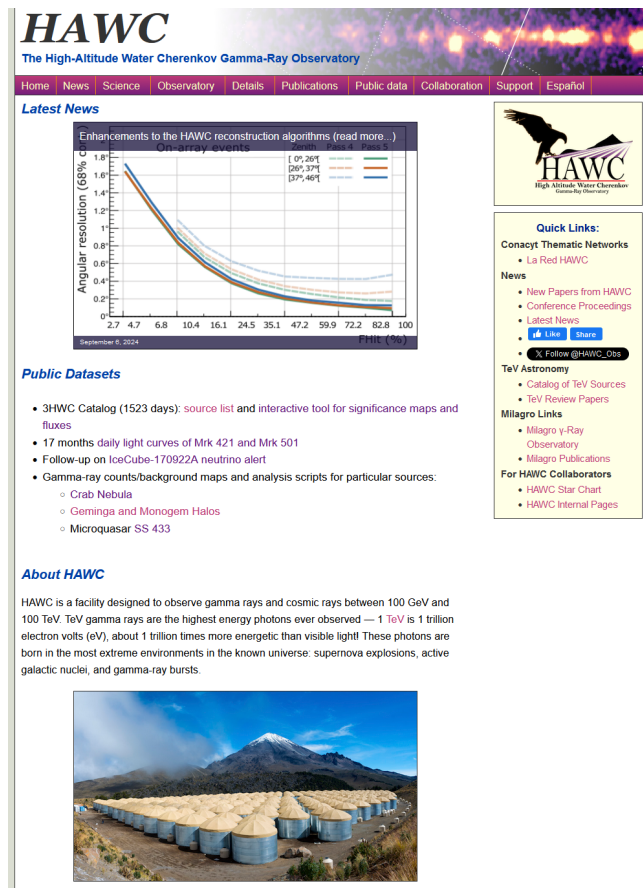
University of Costa Rica



STATUS AND RESULTS OF THE HIGH-ALTITUDE WATER CHERENKOV (HAWC) OBSERVATORY

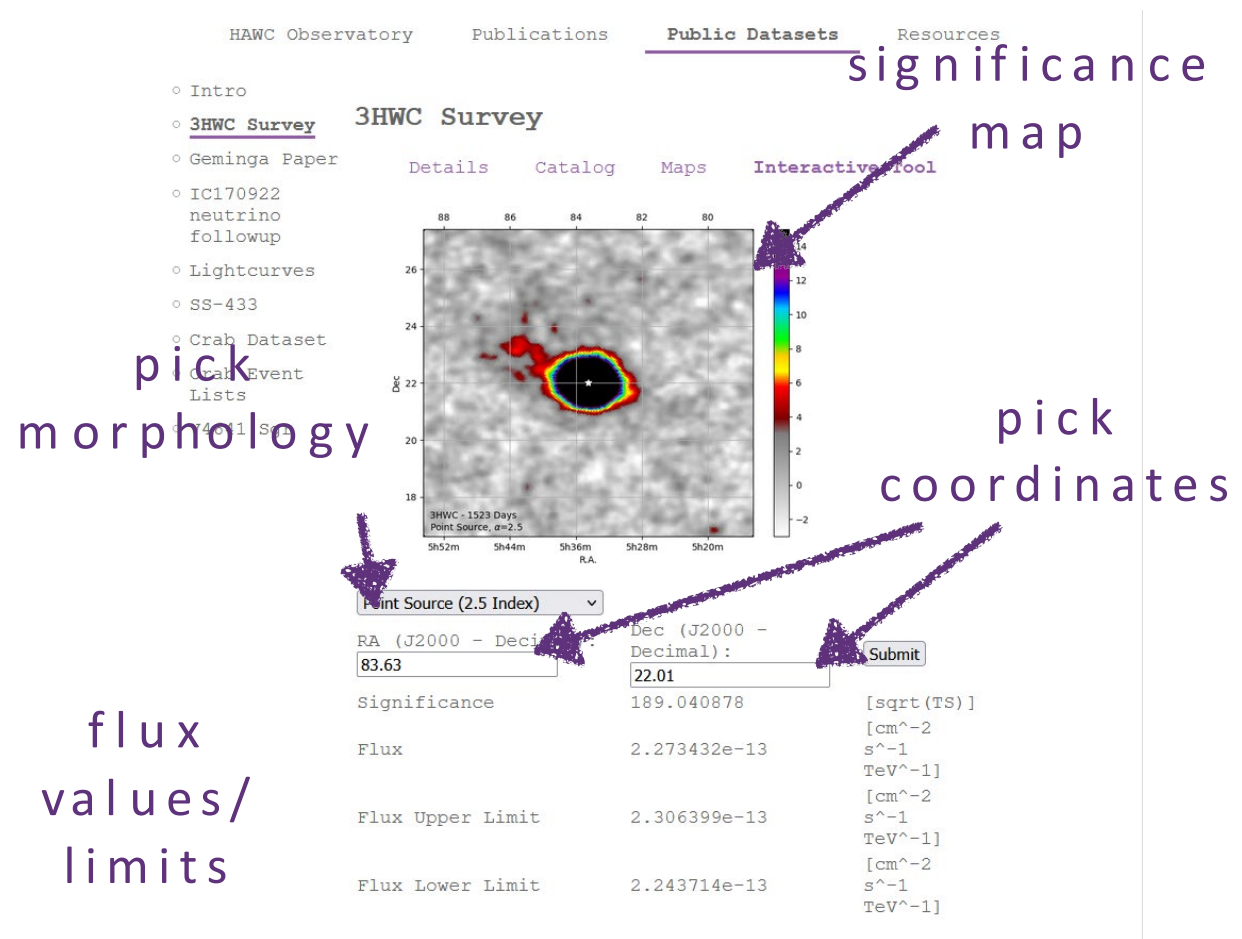
HAWC public website and Data Access

Public Website (<https://www.hawc-observatory.org/>)



For a (nearly) complete list of publications including Theses)
See <https://www.hawc-observatory.org/publications/>

Public Data access (data.hawc-observatory.org)



STATUS AND RESULTS OF THE HIGH-ALTITUDE WATER CHERENKOV (HAWC) OBSERVATORY

HAWC Summary/Outlook

HAWC has produced many Results

- As of Sept 19, 2024
- At least [55 published journal articles](#)
- 3 articles accepted but not yet in print
- 5 articles in journal review

HAWC continues producing Results

- As of Sept 19, 2024
- 11 articles in collaboration review
- 7 paper drafts in preparation

Near Future

- Outrigger Array Repair → Higher Energies
- Improved Reconstruction Techniques → Lower Energies
- Support Multi-messenger observations
- Continue various analyses

Transition to SWGO

- Ramp-down HAWC operations
- Possibly re-use PMTs in SWGO-A
- See [talk by Ulisses Barres](#) (Wed at 9 AM)



Drone Overflight of HAWC observatory



STATUS AND RESULTS OF THE HIGH-ALTITUDE WATER CHERENKOV (HAWC) OBSERVATORY

THE UNIVERSITY OF UTAH
Department of
Physics & Astronomy

HAWC Publications

<https://www.hawc-observatory.org/publications/>



STATUS AND RESULTS OF THE HIGH-ALTITUDE WATER CHERENKOV (HAWC) OBSERVATORY

Outlook - Papers in Collaboration or Journal Review or Accepted but not yet published

Paper Title	Status
Ultra High Energy Gamma-ray Bubble around Microquasar V4641 Sgr	(accepted by Nature)
Precise measurements of TeV Halos around Geminga and Monogem pulsars with HAWC	(accepted by ApJ)
Ubiquitous TeV halos around isolated middle-aged pulsars	(In Collaboration Review)
Multiwavelength Investigation of MGRO J1908+06 emission	(accepted by ApJ) arXiv
Search for joint multimessenger signals from potential Galactic PeVatrons with HAWC and IceCube	(In Journal Review) arXiv
Understanding the Emission and Morphology of the Unidentified Gamma-Ray Source TeV J2032+4130	(In Journal Review) arXiv
Exploring Molecular Clouds in the Vicinity of SNR G106.3+2.7 and How they Relate to HAWC's Very-High-Energy Gamma-Ray Emission	(accepted by A&A) arXiv
Spectral study of very high energy gamma rays from SS 433 with HAWC	(In Journal Review)
Observation of the Galactic Center PeVatron Beyond 100 TeV with HAWC	(In Journal Review) arXiv
An Absence of TeV halos around Millisecond Pulsars	(In Collaboration Review)
A measurement of the all-particle energy spectrum of cosmic rays from 10^{13} to 10^{15} eV using HAWC	(In Journal Review) arXiv
TeV Radio Galaxies	(In Collaboration Review)
HAWC, VERITAS and XMM Newton follow-up observations of LHAASO J2108+5157	(In Collaboration Review)
A measurement of the intensity spectrum of cosmic rays from $1e13$ to $1e15$ eV using HAWC	(In Collaboration Review)
TeV halo search	(In Collaboration Review)
An Abscence of TeV Halos around MSPs	(In Collaboration Review)
LS5039	(In Collaboration Review)
Sensitivity of HAWC to the Crab-like pulsars, above 300 GeV	(In Collaboration Review)
Limits on Diffuse Dark Matter with HAWC	(In Collaboration Review)
Glory Duck Multi-Experiment Dark Matter Search	(In Collaboration Review)

Outlook - Papers in Preparation

4HWC Catalog	First draft in preparation
VHE emission as possible interaction of the kilonova with the reverse shock	First draft in preparation
Model Background Paper	First draft in preparation
Fermi Bubble Paper 2	First draft in preparation
41 Month GRB Paper	1st draft complete. Editorial board not yet formed.
Outriggers	First draft in preparation
GRBs alike GRB 170817A as GW counterparts	working technical note

TeV Gamma-Ray Sky – Galactic Results (all published)

Galactic

[Observation of the Galactic Center PeVatron Beyond 100 TeV with HAWC](#)
HAWC Collaboration, A. Albert et al [2024 ApJL 973 L34](#)

[Galactic Gamma-Ray Diffuse Emission at TeV Energies with HAWC Data](#)
HAWC Collaboration: R. Alfaro et al. 2024, [ApJ 961 \(2024\), 104](#).

[HAWC Study of the Very-high-energy \$\gamma\$ -Ray Spectrum of HAWC J1844–034](#)
HAWC Collaboration: A. Albert et al. 2023, [ApJ 954 \(2023\), 205](#).

[HAWC Detection of a TeV Halo Candidate Surrounding a Radio-quiet Pulsar](#)
HAWC Collaboration: A. Albert et al. 2023, [ApJL 944 \(2023\), L29](#).

[Detailed Analysis of the TeV Gamma-Ray Sources 3HWC J1928+178, 3HWC J1930+188, and the New Source HAWC J1932+192](#)
HAWC Collaboration: A. Albert et al. 2023, [ApJ 942 \(2023\), 96](#).

[Gamma-Ray Emission from Classical Nova V392 Per: Measurements from Fermi and HAWC](#)
HAWC Collaboration: A. Albert et al. 2022, [ApJ 940 \(2022\), 141](#).

[HAWC Study of the Ultra-High-Energy Spectrum of MGRO J1908+06](#)
HAWC Collaboration: A. Albert et al. 2022, [ApJ 928 \(2022\), 116](#).

[TeV Emission of Galactic Plane Sources with HAWC and H.E.S.S.](#)
H.E.S.S. and HAWC Collaborations 2021, [ApJ 917 \(2021\), 6](#).

[HAWC Search for High-mass Microquasars](#)
HAWC Collaboration: A. Albert et al. 2021, [ApJL 912 \(2021\), L4](#).

[Spectrum and Morphology of the Very-High-Energy Source HAWC J2019+368](#)
HAWC Collaboration: A. Albert et al. 2021, [ApJ 911 \(2021\), 143](#).

[Hawc observations of the acceleration of very-high-energy cosmic rays in the cygnus cocoon](#)
HAWC Collaboration: A. Albert et al. 2021, [Nature Astron \(2021\)](#).

[Evidence that Ultra-high-energy Gamma Rays Are a Universal Feature near Powerful Pulsars](#)
HAWC Collaboration: A. Albert et al. 2021, [ApJL 911 \(2021\), L27](#).

[Evidence of 200 TeV photons from HAWC j1825-134](#)
HAWC Collaboration: A. Albert et al. 2021, [ApJL 907 \(2021\), L30](#).

Galactic

[3hwc: The third HAWC catalog of very-high-energy gamma-ray sources](#)
HAWC Collaboration: A. Albert et al. 2020, [ApJ 905 \(2020\), 76](#).

[HAWC and Fermi-LAT Detection of Extended Emission from the Unidentified Source 2HWC J2006+341](#)
HAWC Collaboration: A. Albert et al. 2020, [ApJL 903 \(2020\), L14](#).

[HAWC J2227+610 and Its Association with G106.3+2.7, a New Potential Galactic PeVatron](#)
HAWC Collaboration: A. Albert et al. 2020, [ApJL 896 \(2020\), L29](#).

[Multiple Galactic Sources with Emission Above 56 TeV Detected by HAWC](#)
HAWC Collaboration: A.U. Abeysekara et al., [PRL 124,021102\(2020\)](#).

[Measurement of the Crab Nebula Spectrum past 100 TeV with HAWC](#)
HAWC Collaboration: A.U. Abeysekara et al., [ApJ881\(2019\), 134](#).

[Very high energy particle acceleration powered by the jets of the microquasar SS 433](#)
HAWC Collaboration: A.U. Abeysekara et al., [Nature 562 \(2018\), 82-85](#).

[VERITAS and Fermi-LAT Observations of TeV Gamma-Ray Sources Discovered by HAWC in the 2HWC Catalog](#)
VERITAS Collaboration: A.U. Abeysekara et al.; Fermi-LAT Collaboration: S. Abdollahi et al.; HAWC Collaboration: R. Alfaro et al., [ApJ 866 \(2018\), 24](#).

[Extended gamma-ray sources around pulsars constrain the origin of the positron flux at Earth](#)
HAWC Collaboration: A.U. Abeysekara et al., [Science 6365 \(2017\), 911-914](#).

[The 2HWC HAWC Observatory Gamma-Ray Catalog](#)
HAWC Collaboration: A.U. Abeysekara et al., [ApJ 843 \(2017\), 40](#).

[Observation of the Crab Nebula with the HAWC Gamma-Ray Observatory](#)
HAWC Collaboration: A.U. Abeysekara et al., [ApJ 843 \(2017\), 39](#).

[Search for Very High Energy Gamma Rays from the Northern Fermi Bubble Region with HAWC](#)
HAWC Collaboration: A.U. Abeysekara et al., [ApJ 842 \(2017\), 85](#).

[Search for TeV Emission from Point-like Sources in the Galactic Plane with a Partial Configuration of the HAWC Observatory](#)
HAWC Collaboration: A.U. Abeysekara et al., [Astrophys. J. 817 \(2016\), 3](#).



TeV Gamma-Ray Sky – Extra-Galactic (all published results)

Extra-Galactic

[Probing the extragalactic mid-infrared background with HAWC](#)

HAWC Collaboration: A. Albert et al. 2022, [ApJ 933 \(2022\), 223..](#)

[Long-term spectra of the blazars Mrk 421 and Mrk 501 at TeV energies seen by HAWC](#)

HAWC Collaboration: A. Albert et al. 2022, [ApJ 929 \(2022\), 125.](#)

[A survey of active galaxies at TeV photon energies with the HAWC gamma-ray observatory](#)

HAWC Collaboration: A. Albert et al. 2021, [ApJ 907 \(2021\), 67.](#)

[Constraints on the Emission of Gamma-Rays from M31 with HAWC](#)

HAWC Collaboration: A. Albert et al. 2020, [ApJ 893 \(2020\), 16.](#)

[Constraints on the very high energy gamma-ray emission from short GRBs with HAWC](#)

HAWC Collaboration: A. Albert et al. 2022, [ApJ 936 \(2022\), 2.](#)

[The HAWC real-time flare monitor for rapid detection of transient events](#)

HAWC Collaboration: A.U. Abeysekara et al., [ApJ 843 \(2017\), 116.](#)

[Search for very-high-energy emission from Gamma-ray Bursts using the first 18 months of data from the HAWC Gamma-ray Observatory](#)

HAWC Collaboration: R. Alfaro et al., [ApJ 843 \(2017\), 88.](#)

[Daily monitoring of TeV gamma-ray emission from Mrk 421, Mrk 501, and the Crab Nebula with HAWC](#)

HAWC Collaboration: A.U. Abeysekara et al., [ApJ 841 \(2017\), 100.](#)

[On the Sensitivity of the HAWC Observatory to Gamma-Ray Bursts](#)

HAWC Collaboration: A. U. Abeysekara et al., [Astropart. Phys. 35 \(2012\) 641-650.](#)



Cosmic Ray Studies– (all published results)

Cosmic Ray Studies

[High Altitude characterization of the Hunga Pressure Wave with Cosmic Rays by the HAWC Observatory](#)

HAWC Collaboration: R. Alfaro et al. 2024, [Advances in Space Research 73 \(2024\), 1.](#)

[Cosmic ray spectrum of protons plus helium nuclei between 6 and 158 TeV from HAWC data](#)

HAWC Collaboration: A. Albert et al. 2022, [PRD 105 \(2022\), 063021](#)

[Probing the Sea of Cosmic Rays by Measuring Gamma-Ray Emission from Passive Giant Molecular Clouds with HAWC](#)

HAWC Collaboration: A. Albert et al. 2021, [ApJ 914 \(2021\), 106.](#)

[Hawc observations of the acceleration of very-high-energy cosmic rays in the cygnus cocoon](#)

HAWC Collaboration: A. Albert et al. 2021, [Nature Astron \(2021\).](#)

[All-Sky Measurement of the Anisotropy of Cosmic Rays at 10 TeV and Mapping of the Local Interstellar Magnetic Field](#)

HAWC Collaboration: A.U. Abeysekara et al., and IceCube

Collaboration, M.G. Aartsen et al., [ApJ871\(2019\), 096.](#)

[Constraining the p/p Ratio in TeV Cosmic Rays with Observations of the Moon Shadow by HAWC](#)

HAWC Collaboration: A.U. Abeysekara et al., [Phys. Rev. D 97, 102005 \(2018\).](#)

[Very high energy particle acceleration powered by the jets of the microquasar SS 433](#)

HAWC Collaboration: A.U. Abeysekara et al., [Nature 562 \(2018\), 82-85.](#)

[Observation of Anisotropy of TeV Cosmic Rays with Two Years of HAWC](#)

HAWC Collaboration: A.U. Abeysekara et al., [ApJ 865 \(2018\), 57-71.](#)

[All-particle cosmic ray energy spectrum measured by the HAWC experiment from 10 to 500 TeV](#)

HAWC Collaboration: R. Alfaro et al., [Phys. Rev. D 96 \(2017\), 122001](#)



Dark Matter Searches– (all published results)

Dark Matter Searches

Search for decaying dark matter in the Virgo cluster of galaxies with HAWC

HAWC Collaboration: A. Albert et al. 2024, [Phys. Rev. D 109 \(2024\), 043034](#).

An optimized search for dark matter in the galactic halo with HAWC

HAWC Collaboration: A. Albert et al. 2023, [JCAP 12 \(2023\), 038](#).

Searching for TeV Dark Matter in Irregular Dwarf Galaxies with HAWC Observatory

HAWC Collaboration: R. Alfaro et al. 2023, [ApJ 945 \(2023\), 25](#).

Searching for Dark Matter Sub-structure with HAWC

HAWC Collaboration: A.U. Abeysekara et al., [JCAP07 \(2019\), 22](#).

Search for Dark Matter Gamma-ray Emission from the Andromeda Galaxy with the High-Altitude Water Cherenkov Observatory

HAWC Collaboration: A.U. Albert et al., [JCAP 1806 \(2018\), 043](#).

A Search for Dark Matter in the Galactic Halo with HAWC

HAWC Collaboration: A.U. Abeysekara et al., [JCAP 02 \(2018\), 049](#).

Constraints on Spin-Dependent Dark Matter Scattering with Long-Lived Mediators from TeV Observations of the Sun with HAWC

HAWC Collaboration: A. Albert et al., [PRD 98 \(2018\), 123012](#).

Dark Matter Limits from Dwarf Spheroidal Galaxies with the HAWC Gamma-Ray Observatory

HAWC Collaboration: A. Albert et al., [ApJ 853 \(2018\), 154](#).



Multi-Messenger Studies– (all published results)

Multi-Messenger Studies

[Search for Gamma-Ray and Neutrino Coincidences Using HAWC and ANTARES Data](#)

H. A. Ayala Solares et al. 2023, [ApJ 944](#) (2023), 166.

[Multi-messenger observations of a flaring blazar coincident with high-energy neutrino](#)

[IceCube-170922A](#) The IceCube, Fermi-LAT, MAGIC, AGILE, ASAS-SN, HAWC Collaborations, etc., [Science 361](#) (2018), 146-155

[Multi-messenger Observations of a Binary Neutron Star Merger](#)

LIGO Collaboration, Virgo Collaboration, HAWC Collaboration, etc., [ApJ 848](#) (2017), L12.

[Multiwavelength follow-up of a rare IceCube neutrino multiplet](#)

HAWC, IceCube, Fermi-LAT Collaboration: M.G. Aartsen et al., [A&A 607](#) (2017), A115.



“Exotica” Studies– (all published results)

Exotica

Characterization of the background for a neutrino search with the HAWC observatory

HAWC Collaboration: A. Albert et al. 2022, [Astroparticle Physics 137 \(2022\), 102670.](#)

Constraining the local burst rate density of primordial black holes with HAWC

HAWC Collaboration: A. Albert et al. 2020, [JCAP 04 \(2020\), 26.](#)

Constraints on Lorentz Invariance Violation from HAWC Observations of Gamma Rays above 100 TeV

HAWC Collaboration: A. Albert et al., [PRL 124,021102\(2020\).](#)



Solar Physics Studies– (all published results)

Solar Physics

[Exploring the coronal magnetic field with galactic cosmic rays](#)

HAWC Collaboration: R. Alfaro et al. 2024, [ApJ 966 67](#)

[Discovery of Gamma Rays from the Quiescent Sun with HAWC](#)

HAWC Collaboration: A. Albert et al. 2023, [Phys. Rev. Lett. 131 \(2023\), 051201](#).

[HAWC as a Ground-Based Space-Weather Observatory](#)

HAWC Collaboration: C. Alvarez et al. 2021, [Solar Physics 296 \(2021\), 89](#)

[Interplanetary magnetic flux rope observed at ground level by HAWC](#)

HAWC Collaboration: A. Albert et al. 2020, [ApJ 905 \(2020\), 73](#).

[First HAWC Observations of the Sun Constrain Steady TeV Gamma-Ray Emission](#)

HAWC Collaboration: A. Albert et al., [PRD 98 \(2018\), 123011](#).



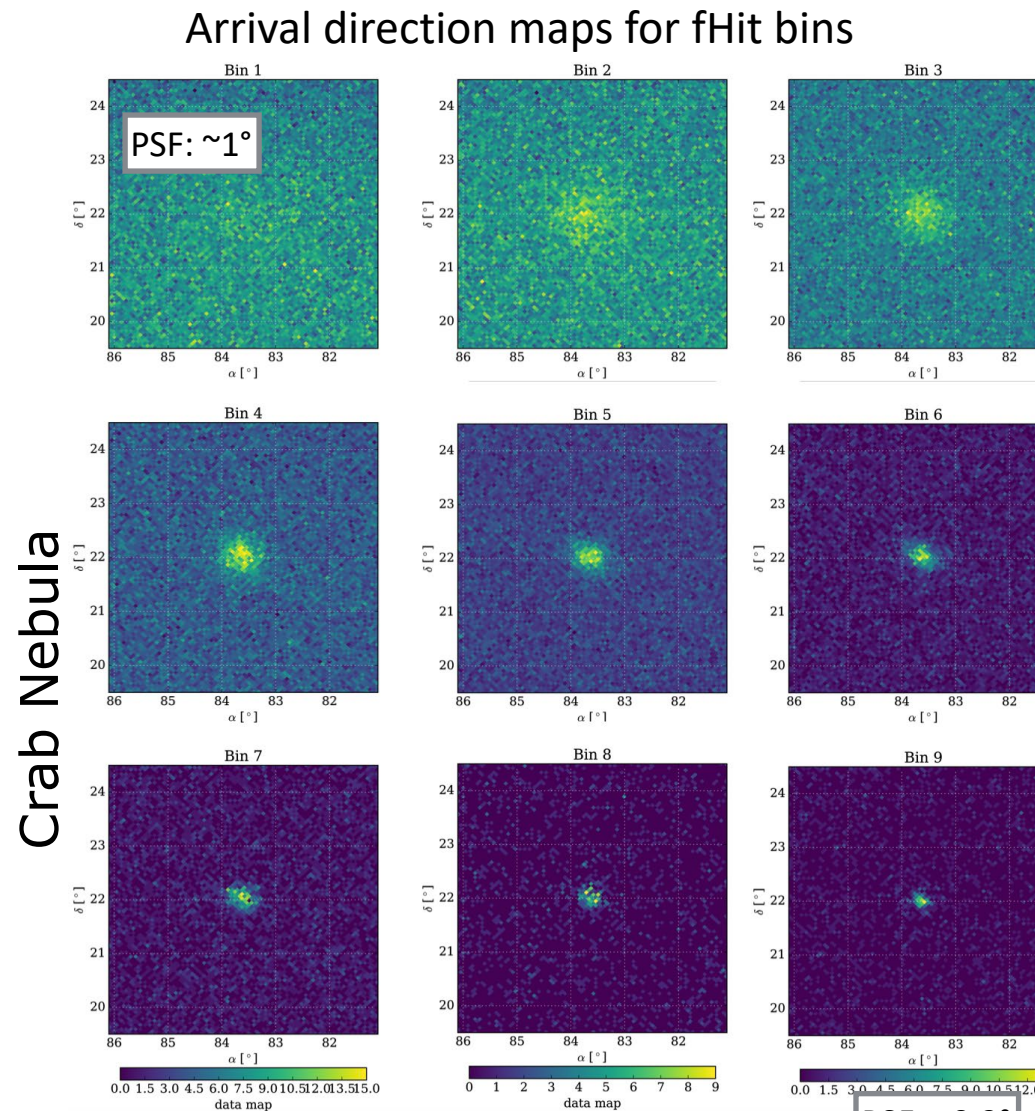
Backup Slides



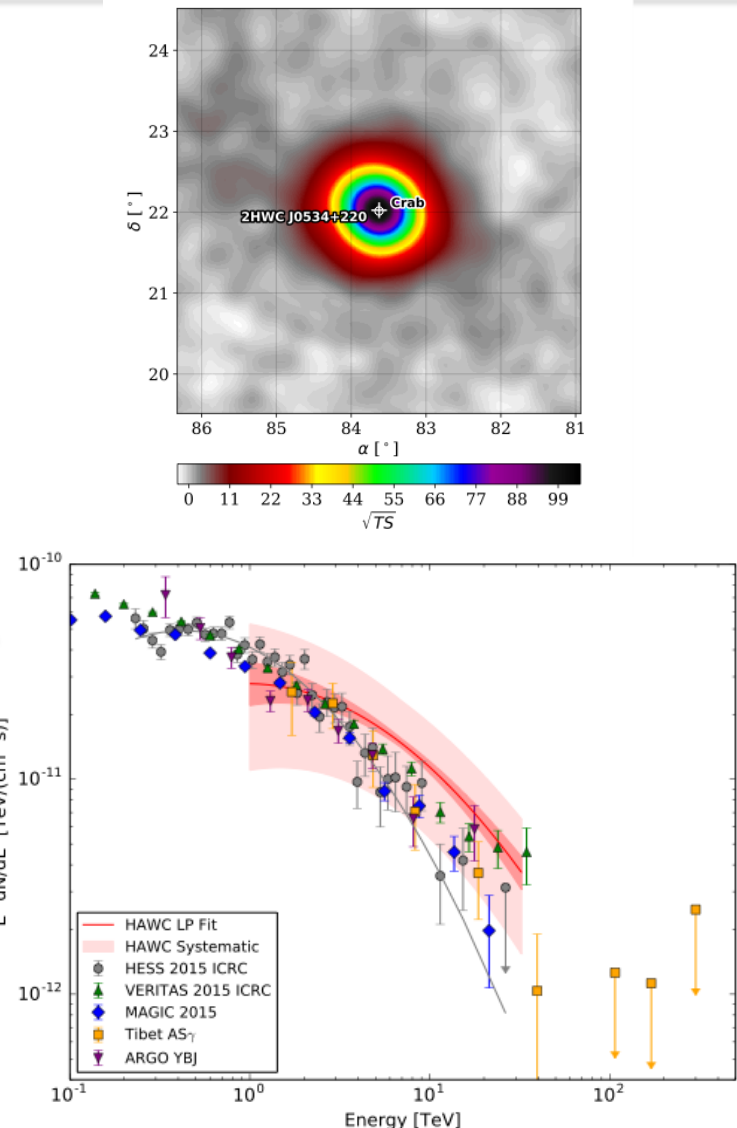
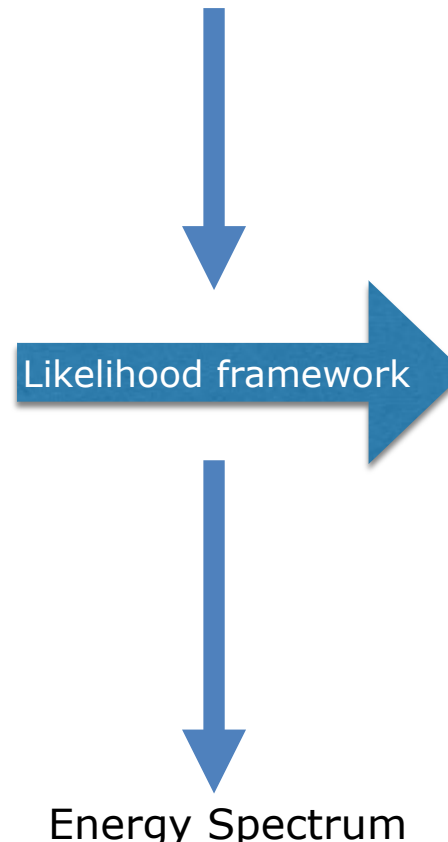
STATUS AND RESULTS OF THE HIGH-ALTITUDE WATER CHERENKOV (HAWC) OBSERVATORY



Source search and Energy Spectrum Determination – Crab Nebula



Detector response
&
Source model



HAWC Observatory –Science Goals

■ TeV Gamma Ray Sky

- Galactic Sources
 - Supernova Remnants
 - Pulsar Wind Nebula
 - Extended Sources
 - High Energy (>50TeV)
 - ...
- Extra-galactic sources
 - Active Galactic Nuclei, Blazars
 - Gamma-Ray Burst searches
 - ...
- Monitoring of Transient/Variable Sources

■ Cosmic Ray Studies (1 TeV-1 PeV)

- Anisotropies of Arrival Directions
- All-particle Energy Spectrum
- Composition Studies
- Sources of Galactic Cosmic Rays
- ...

■ Multi-messenger Astrophysics

- TeV Gamma and Neutrino Coincidence
- TeV Gamma and Gravitational Wave Coincidence
- Multiwavelength (Fermi,Swift,...)
- ...

■ Searches and Exotica

- Searches for Dark Matter
- Search for Lorentz Invariance
- Primordial Black Hole Burst Searches
- Neutrino searches
- ...

■ Solar Physics

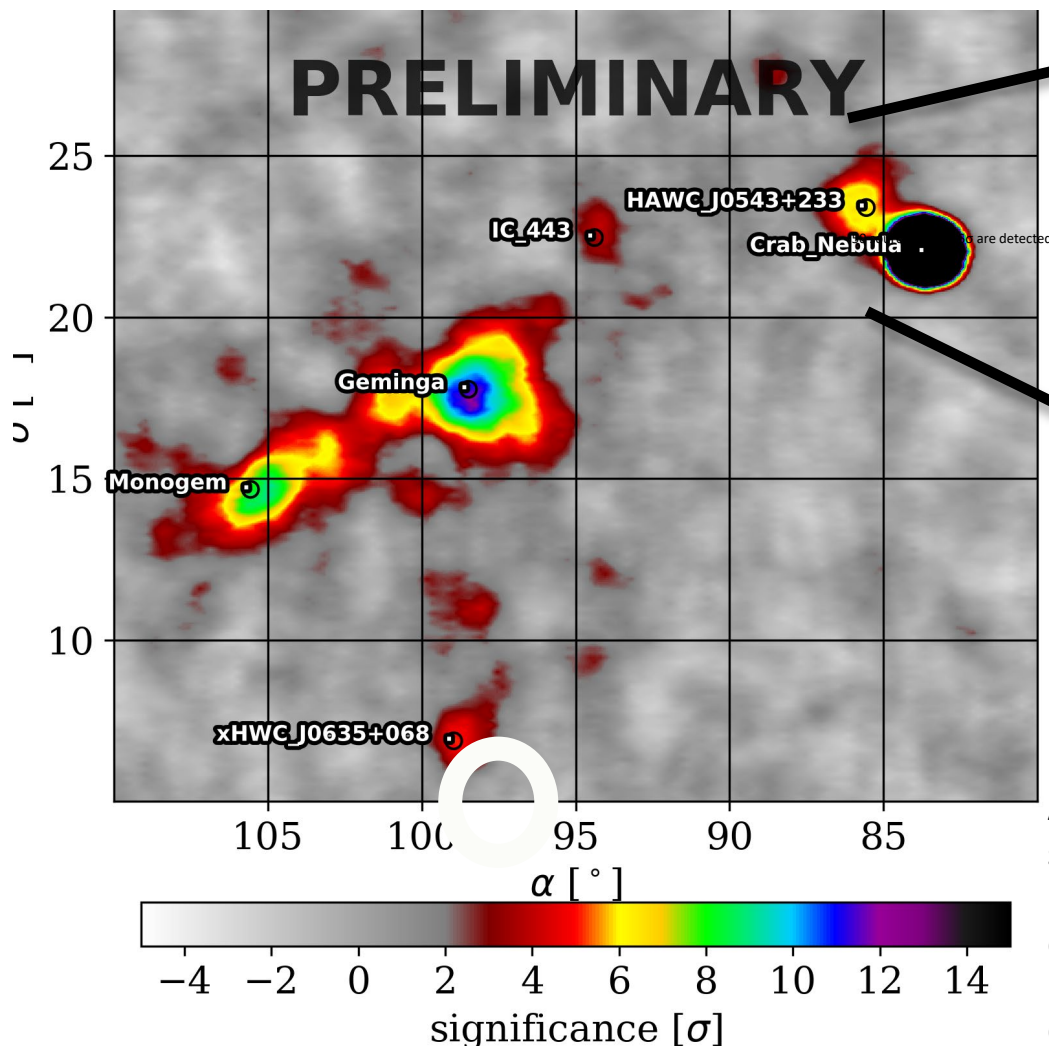
- Coronal Magnetic Fields
- TeV Gamma-ray Emission
- Magnetic Flux loops/Forbush Decrease
- ...



TeV halos : New discoveries – some hiding in plain sight!

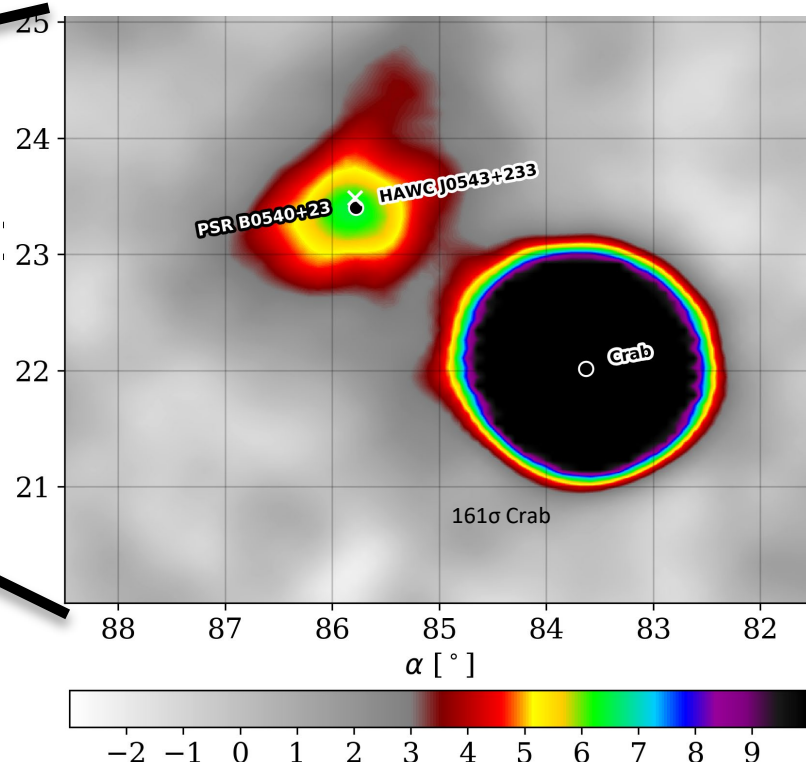
HAWC detection of TeV emission near PSR B0540+23

Colas Riviere (University of Maryland), Henrike Fleischhack (Michigan Technological University), Andres Sandoval (Universidad Nacional Autonoma de Mexico) on behalf of the HAWC Collaboration (ATel #10941 on 9 Nov 2017; 23:11 UT).



Another middle age PWN
similar to Geminga and B0656+14
 $E = 4.1 \times 10^{34}$ erg s $^{-1}$,
 $d = 1.56$ kpc, $\tau = 253$ kyr

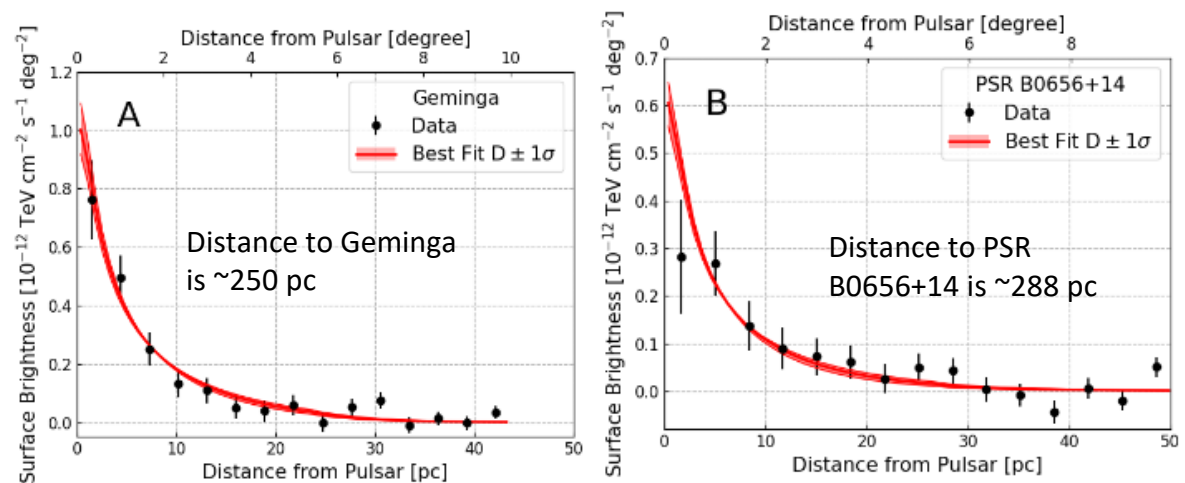
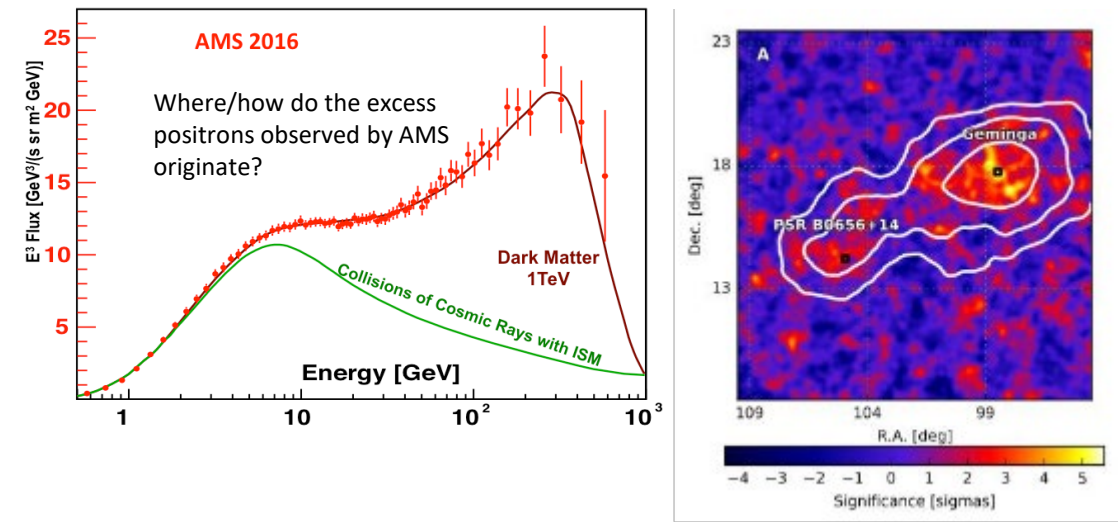
Can test if all are Geminga-like



- More discoveries:
 - HAWC J0543+233 ([ATel #10941](#))
 - HAWC J0635+070 ([ATel #12013](#))
- Probe diffusion in various locations in the Galaxy and near various objects.
 - + “invisible pulsars”?
- HAWC uniquely suited to study halos.

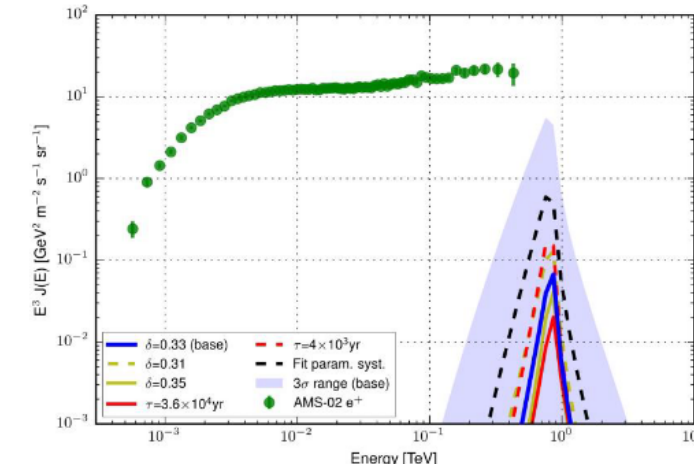
Extended gamma-ray sources around pulsars constrain the origin of the positron flux at Earth

[Extended gamma-ray sources around pulsars constrain the origin of the positron flux at Earth](#)
 HAWC Collaboration: A.U. Abeysekara et al., [Science 6365 \(2017\), 911-914.](#)



Surface brightness of the tera-electron volt gamma-ray emission. Surface brightness is shown as a function of the distance from the Geminga pulsar (A) and PSR B0656+14 (B).

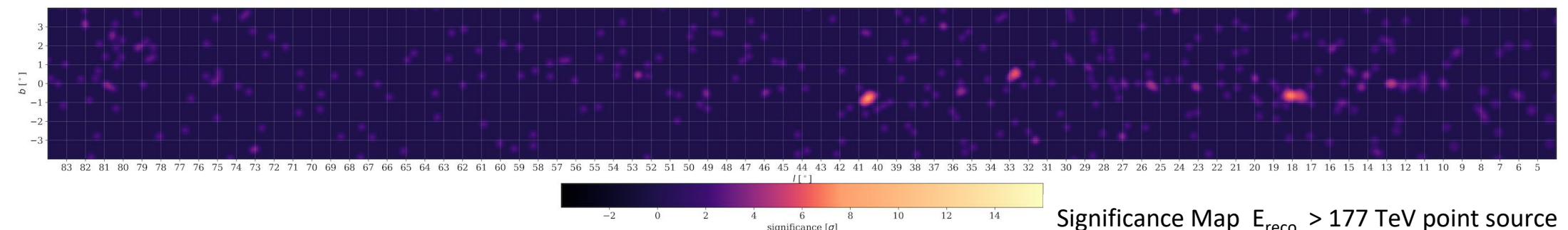
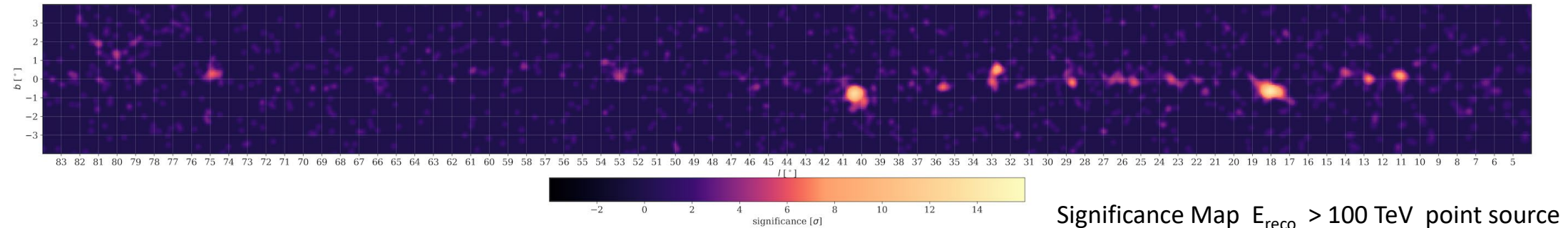
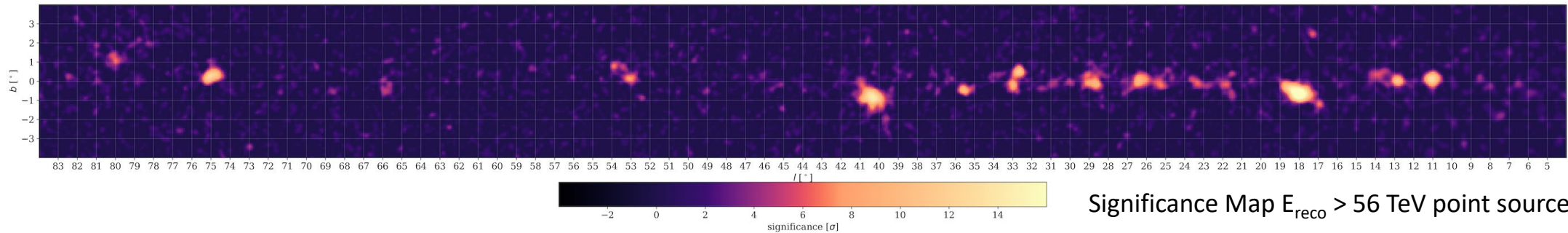
- HAWC observations prove that these sources are indeed accelerating electrons and positrons to ~ 100 TeV producing 25 TeV gamma-rays by inverse Compton scattering of CMB.
- HAWC observations measure the total energy released in electrons and positrons which is much of their measured spin down energy.
- HAWC observations of the angular extent of these TeV nebula measures the diffusion coefficient of their propagation in the interstellar medium.
- HAWC observations show that Geminga and Monogem do NOT contribute significantly to the AMS measured positron excess assuming a simple diffusion model.

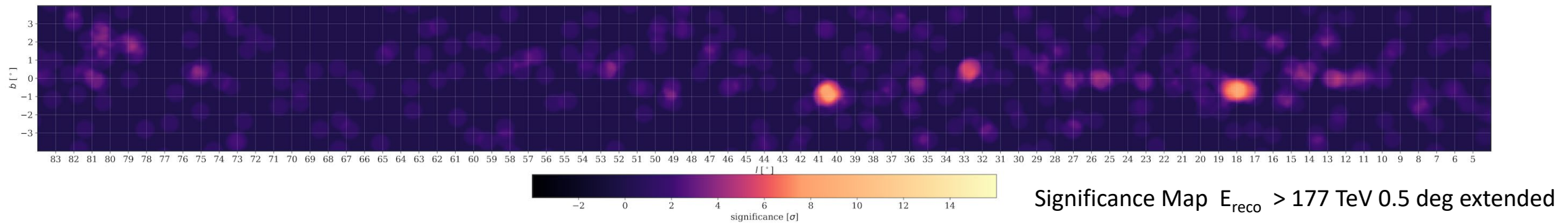
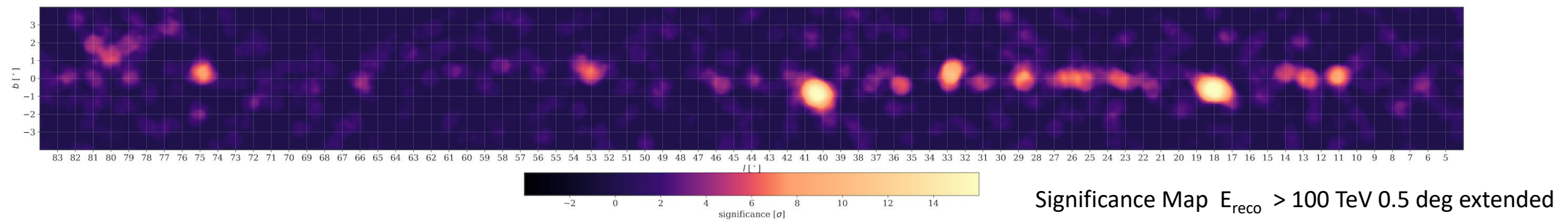
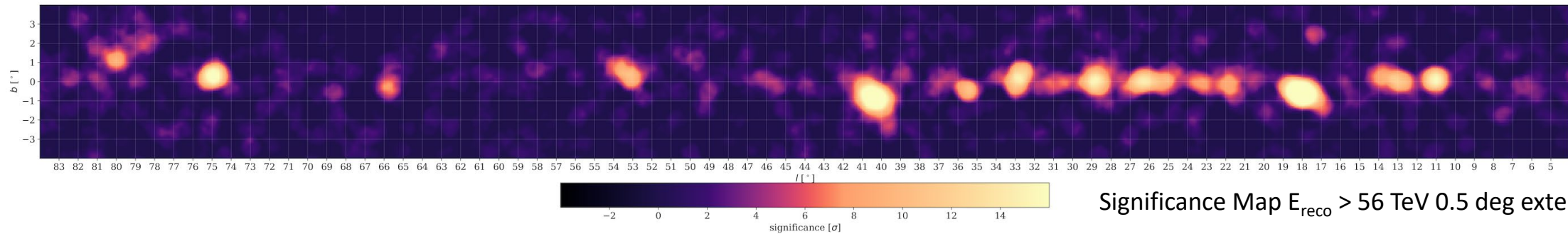


Estimated positron energy flux at Earth from Geminga (blue solid line), compared with AMS-02 experimental measurements (green dots).

Pushing to Higher Energies: ($E_{\text{reco}} > 56 \text{ TeV},$) point source hypothesis

ICRC 2023





Galactic Diffuse Emission (+unresolved sources)

[Galactic Gamma-Ray Diffuse Emission at TeV Energies with HAWC Data](#)
 HAWC Collaboration: R. Alfaro et al. 2024, [ApJ 961 \(2024\), 104](#).

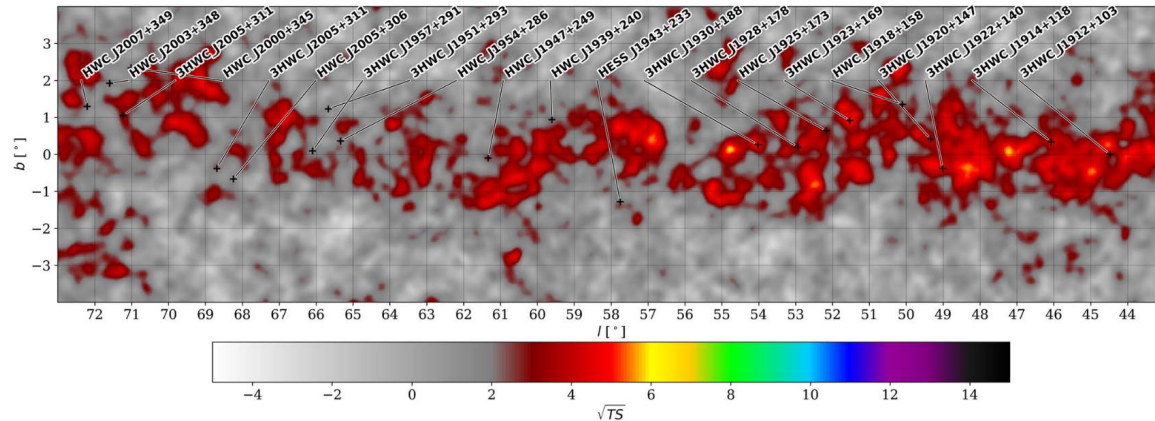


Figure 6. Significance map of the source-subtracted map, generated by subtracting the model of the source (Figure 3, top), obtained in the multisource fitting procedure, from the original map (Figure 1).

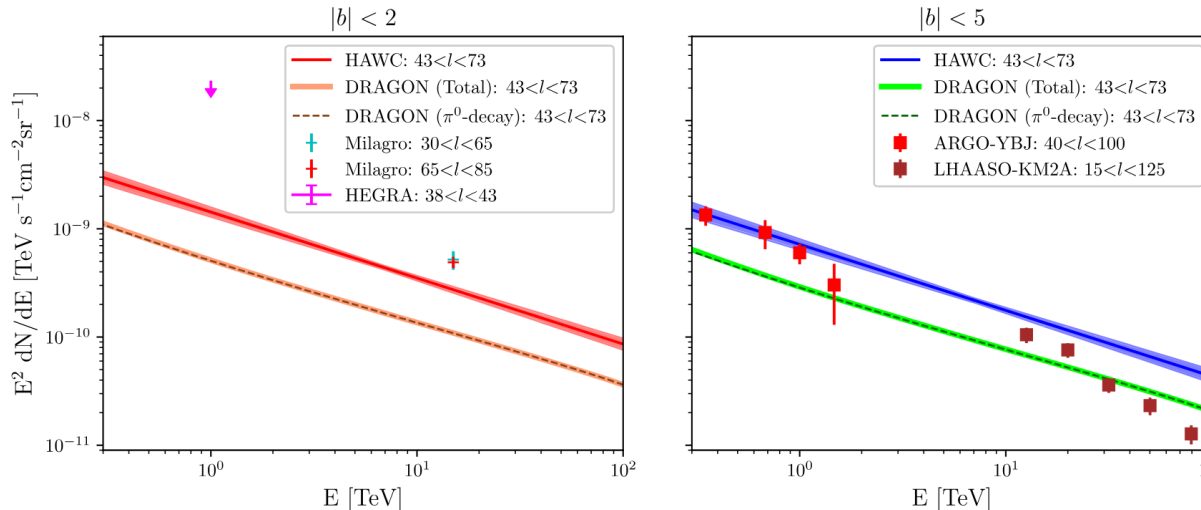


Figure 9. Spectra of the GDE measured by different experiments at different regions, and DRAGON estimations for total and π^0 -decay emission; HAWC and DRAGON within $43^\circ < l < 73^\circ$ (left panel: $|b| < 2^\circ$, and right panel: $|b| < 5^\circ$), statistical errors and the systematic errors are listed in Table 2. Milagro at 15 TeV for two regions within $|b| < 2^\circ$ (Abdo et al. 2008). An upper limit quoted by HEGRA-IACT (99% C.L.) in $|b| < 2^\circ$ (Aharonian et al. 2001). ARGO-YBJ in $40^\circ < l < 100^\circ$ (Bartoli et al. 2015), and LHAASO-KM2A in $15^\circ < l < 125^\circ$ (Cao et al. 2023), both within $|b| < 5^\circ$.

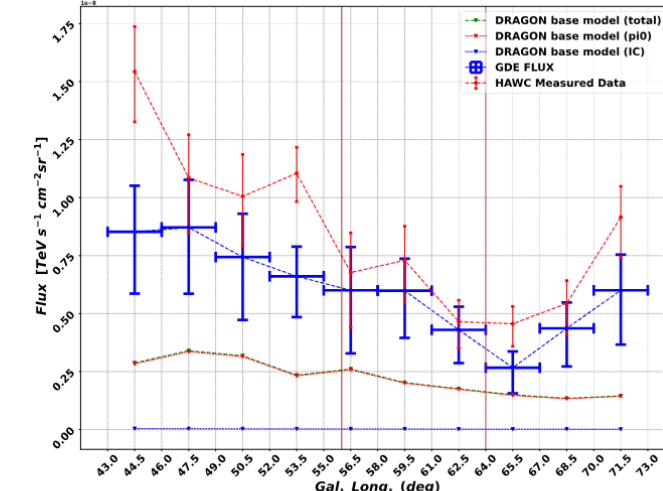


Figure 7. Longitude profiles for energy flux between 300 GeV and 100 TeV, the red line refers to the total flux ($F_{0\alpha}$), the blue line represents the GDE, as well as the prediction of diffuse emission by DRAGON for the π^0 decay and IC production mechanism. The brown lines show the border of the regions as explained in Table 2.

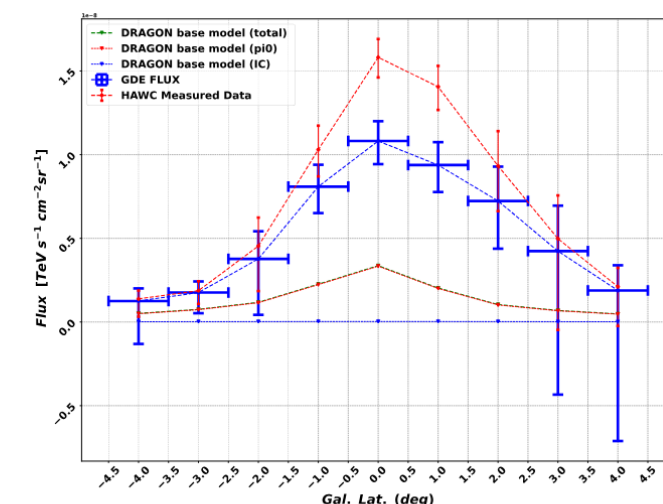


Figure 8. Latitudinal profile for the energy flux between 300 GeV and 100 TeV, red and blue lines refer to the total flux measured by HAWC and the GDE, respectively. DRAGON estimation for the π^0 decay and IC production mechanism are also presented.

Search for Very High Energy γ -rays from Fermi Bubbles

[Search for Very High Energy Gamma Rays from the Northern Fermi Bubble Region with HAWC](#)
 HAWC Collaboration: A.U. Abeysekara et al., [ApJ 842 \(2017\), 85](#).

- HAWC saw no evidence for very high energy emission from Northern Fermi Bubble using a 290 day exposure

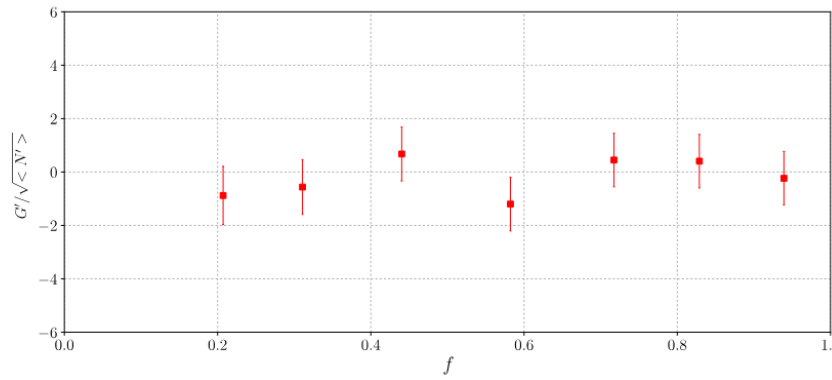
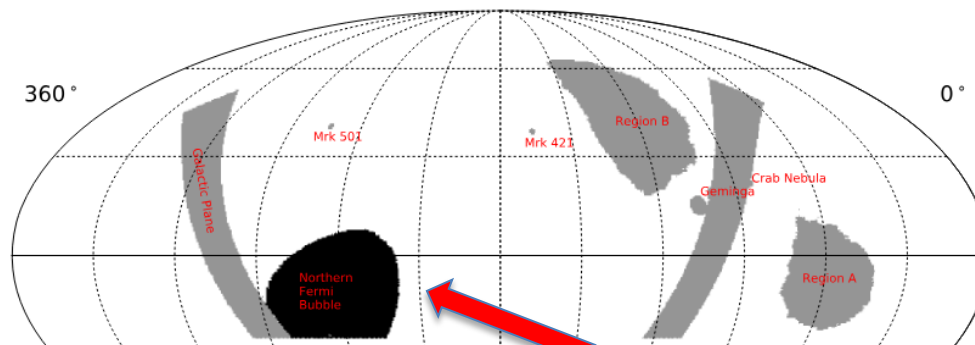
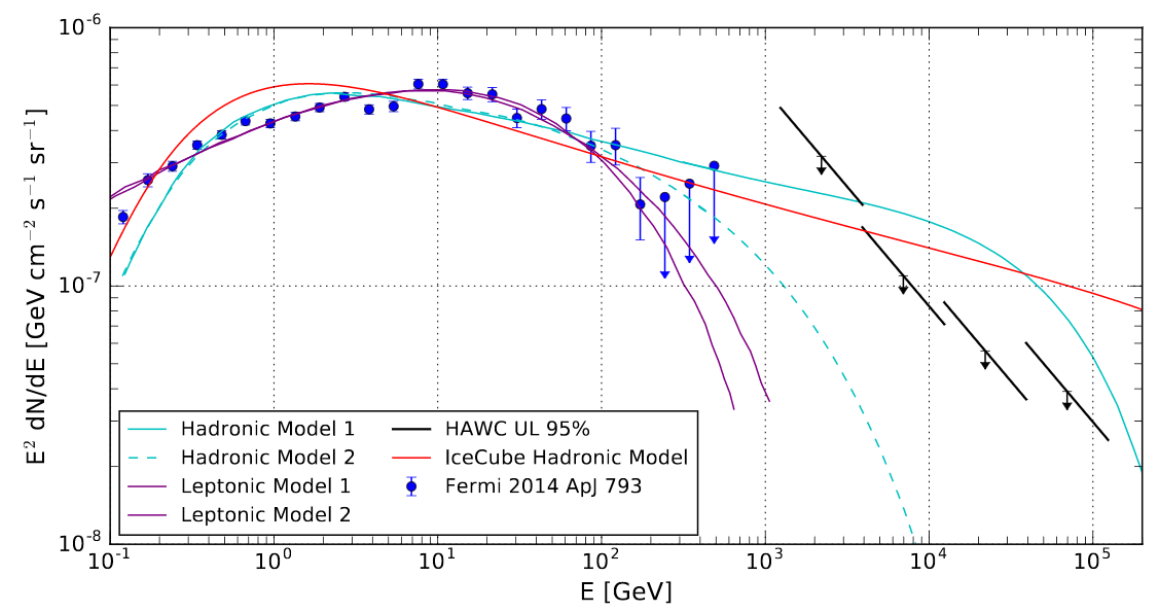
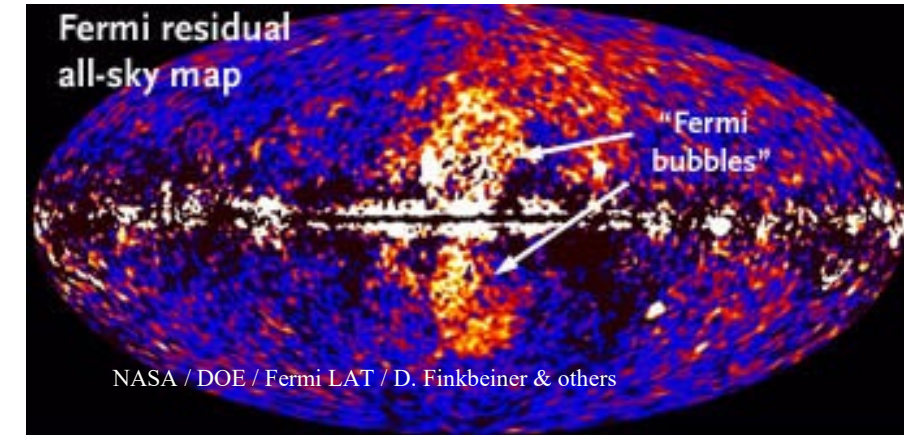


Figure 7. Event excess over the square root of the isotropic background inside the Northern *Fermi* Bubble region after applying the procedure described in Section 3.2.



HAWC upper limits together with the Fermi data and gamma-ray production

Pevatron Cosmic Ray Accelerators?

[HAWC J2227+610 and Its Association with G106.3+2.7, a New Potential Galactic PeVatron](#)

HAWC Collaboration: A. Albert et al. 2020, [ApJL 896 \(2020\), L29](#).

HAWC J2227+610 and Its Association with G106.3+2.7, a New Potential Galactic PeVatron

Abstract

We present the detection of very-high-energy gamma-ray emission above 100 TeV from HAWC J2227+610 with the High-Altitude Water Cherenkov Gamma-Ray Observatory (HAWC) observatory. Combining our observations with previously published results by the Very Energetic Radiation Imaging Telescope Array System (VERITAS), we interpret the gamma-ray emission from HAWC J2227+610 as emission from protons with a lower limit in their cutoff energy of 800 TeV. The most likely source of the protons is the associated supernova remnant G106.3+2.7, making it a good candidate for a Galactic PeVatron. However, a purely leptonic origin of the observed emission cannot be excluded at this time.

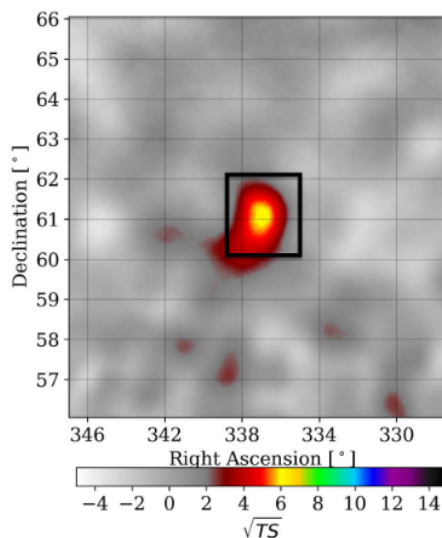


Figure 1. Left: HAWC significance map of the region, large-scale view. There are no other significant gamma-ray sources nearby that could affect the measurement. The black frame marks the size of the region shown on the right. Right: molecular hydrogen column density around HAWC J2227+610. See Appendix B for more details. The pulsar position as well as the centroids of the VERITAS and Milagro sources have been marked. The gray contours show the 1σ , 2σ , and 3σ confidence regions for the HAWC source position. The pink contours show the 1.4 GHz continuum brightness temperature from the Canadian Galactic Plane Survey (Taylor et al. 2003) in 50 logarithmically spaced steps from 1 to 100 K. Both maps have been smoothed and interpolated for display.

- Galactic Gamma-Ray sources may be PeVatrons – sources of cosmic rays
- Spectrum of Gamma Rays may be of hadronic origin
- Multimessenger observations of neutrinos from these objects may be possible with future upgrades

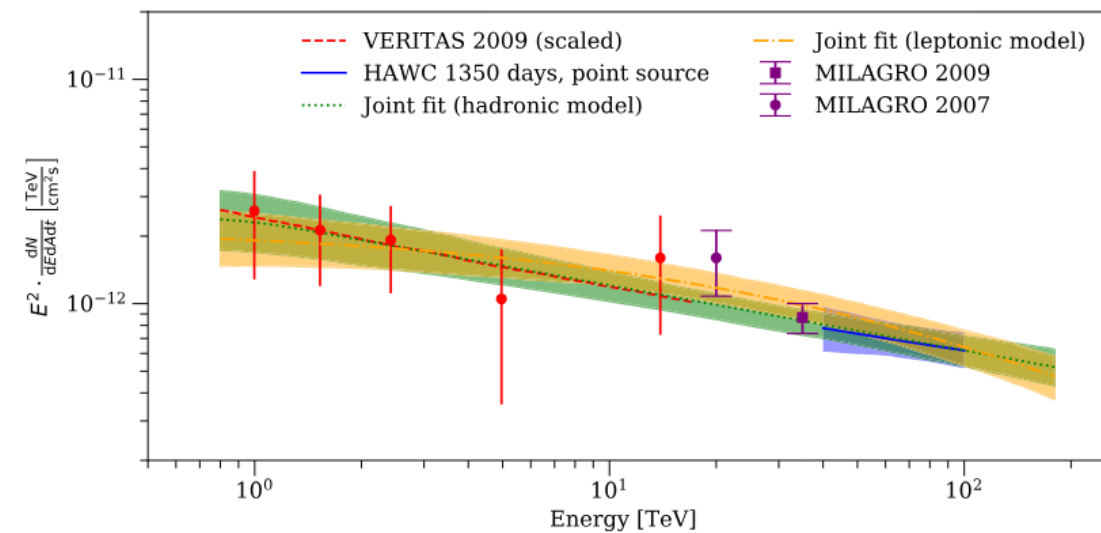


Figure 2. VHE gamma-ray energy spectrum of HAWC J2227+610, statistical uncertainties only. VERITAS data points and fit results from Acciari et al. (2009) have been scaled to account for the difference between the size of the emission region and the region over which the spectrum was extracted. Two joint fits to HAWC and VERITAS data are shown: one assuming a pion decay spectrum from a proton population following a power-law energy spectrum (hadronic model), and one assuming the gamma-ray emission is due to inverse Compton emission from electrons (leptonic model). Milagro data points from Abdo et al. (2007, 2009c) are shown for reference only.

Extragalactic Background Light

Probing the extragalactic mid-infrared background with HAWC

HAWC Collaboration: A. Albert et al. 2022, *ApJ* 933 (2022), 223..

- Indirectly set limits on the EBL by studying the effects of gamma-ray absorption in the very high energy (VHE: >100 GeV) spectra of distant blazars.

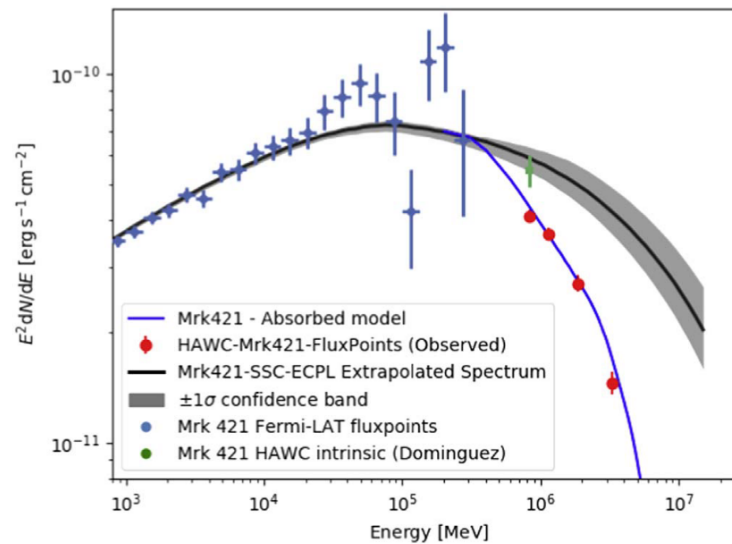


Figure 2. Extrapolated intrinsic emission spectrum for Mrk 421 (black line) along with the $\pm 1\sigma$ confidence band (statistical uncertainty only). Also shown, are the resulting absorbed spectrum (blue line) according to a random EBL model along with HAWC data, the flux points resulting from the Fermi-LAT analysis (light-blue points), and the de-absorbed HAWC flux point (green) according to the Franceschini et al. (2008) EBL model.

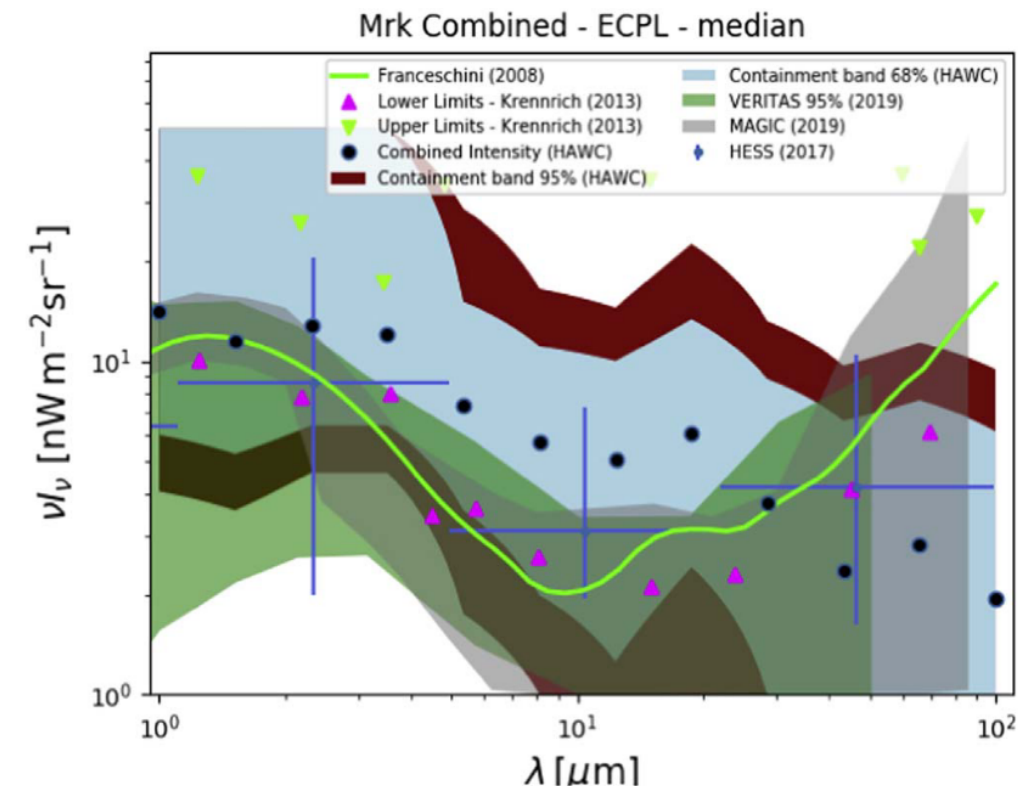
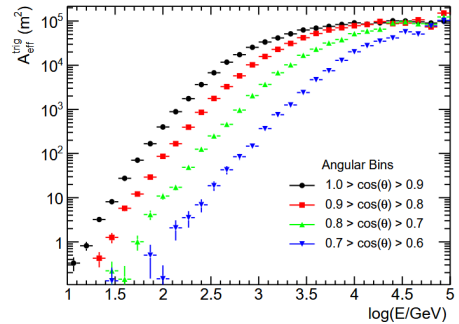


Figure 5. 95% and 68% containment bands for the EBL intensity different λ values for the combined results from Mrk 421 and Mrk 501. Red circles correspond to the combined intensities from each source's highest likelihood models (see Section 3.3). Also shown, are lower limits from galaxy counts (cyan triangles), upper limits from direct measurements (green triangles), and EBL measurements from VERITAS (Abeysekara & Archer 2019), MAGIC (Acciari & Ansoldi 2019), and H.E.S.S. (Abdalla et al. 2017).

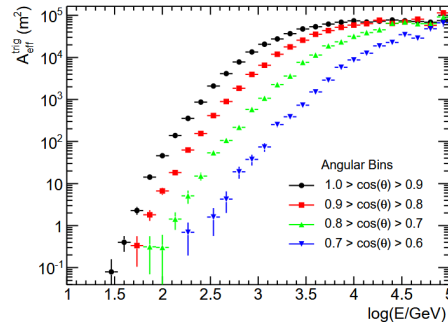
On the Sensitivity of the HAWC Observatory to Gamma-Ray Bursts

On the Sensitivity of the HAWC Observatory to Gamma-Ray Bursts

HAWC Collaboration: A. U. Abeysekara et al., [Astropart. Phys. 35 \(2012\) 641-650](#).



(a) Effective area of the HAWC for $n_{\text{Hit}} > 30$.



(b) Effective area of the HAWC for $n_{\text{Hit}} > 70$.

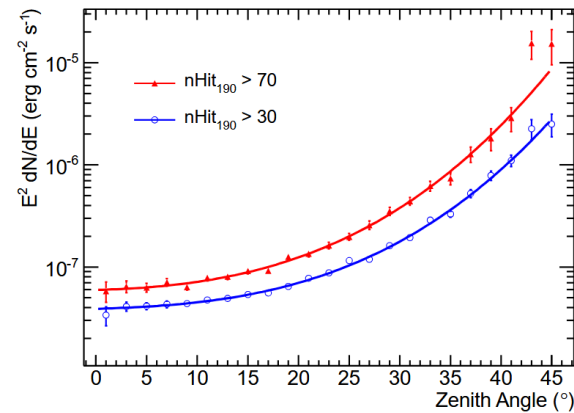


Figure 3: Sensitivity of HAWC using the main DAQ as a function of zenith angle. The sensitivity is defined as the flux detectable at 5σ significance with 50% probability. Results are given for the baseline trigger ($n_{\text{Hit}} > 70$) and a reduced threshold trigger ($n_{\text{Hit}} > 30$) for a range of zenith angles of an astrophysical source. The simulated burst has a duration of 20 s, a spectral index of -2 and a redshift of 0.5. EBL attenuation is modeled following Gilmore et al. [29].

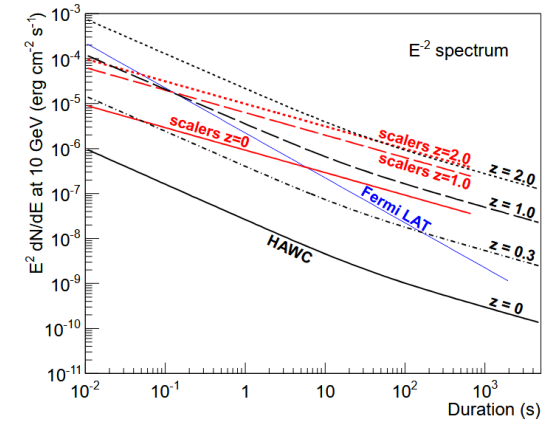
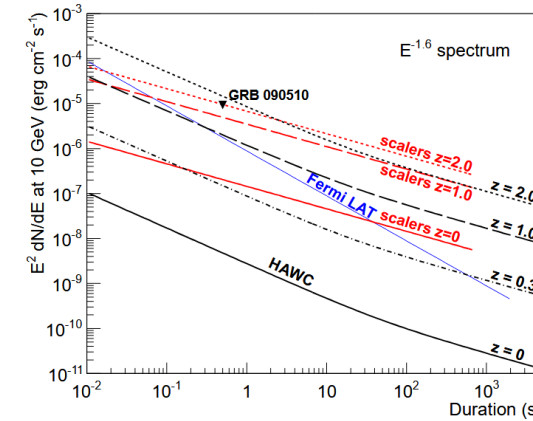


Figure 8: Sensitivity of HAWC using the main DAQ and scalers as a function of burst duration. The main DAQ uses a simple multiplicity trigger of 70 PMTs or more. The source position is set at a zenith angle of 20° . The source spectrum is $E^{-1.6}$ and $E^{-2.0}$ for the left and right plots respectively. The Gilmore model of gamma ray attenuation by EBL [29] is used to obtain the sensitivity curves for different redshifts. The lines for the scalers reflect the 5σ detection level. For the main DAQ the lines define the 5σ discovery potential. Also shown is the flux necessary for the observation of 1 photon above 10 GeV by Fermi LAT. A marker is inserted in the left plot for GRB 090510 [18].

Cosmic Ray Anisotropy – All Sky

[All-Sky Measurement of the Anisotropy of Cosmic Rays at 10 TeV and Mapping of the Local Interstellar Magnetic Field](#)

HAWC Collaboration: A.U. Abeysekara et al., and IceCube Collaboration, M.G. Aartsen et al., [ApJ871\(2019\), 096](#).

THE ASTROPHYSICAL JOURNAL, 871:96 (15pp), 2019 January 20
© 2019. The American Astronomical Society. All rights reserved.

<https://doi.org/10.3847/1538-4357/aaf5cc>



All-sky Measurement of the Anisotropy of Cosmic Rays at 10 TeV and Mapping of the Local Interstellar Magnetic Field

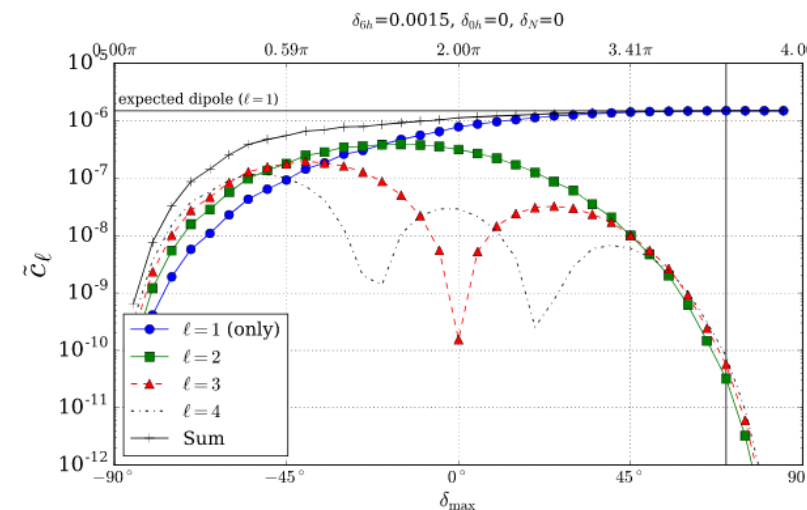


Figure 9. Angular power spectrum as a function of sky coverage for $\ell = \{1, 2, 3, 4\}$. The horizontal axis indicates the maximum decl. δ_{\max} , keeping $\delta_{\min} = -90^\circ$ for a dipole injected horizontally in direction δ_{6h} . The partial coverage of sky produces an artificial quadrupole and octupole that decrease in power with greater celestial coverage.

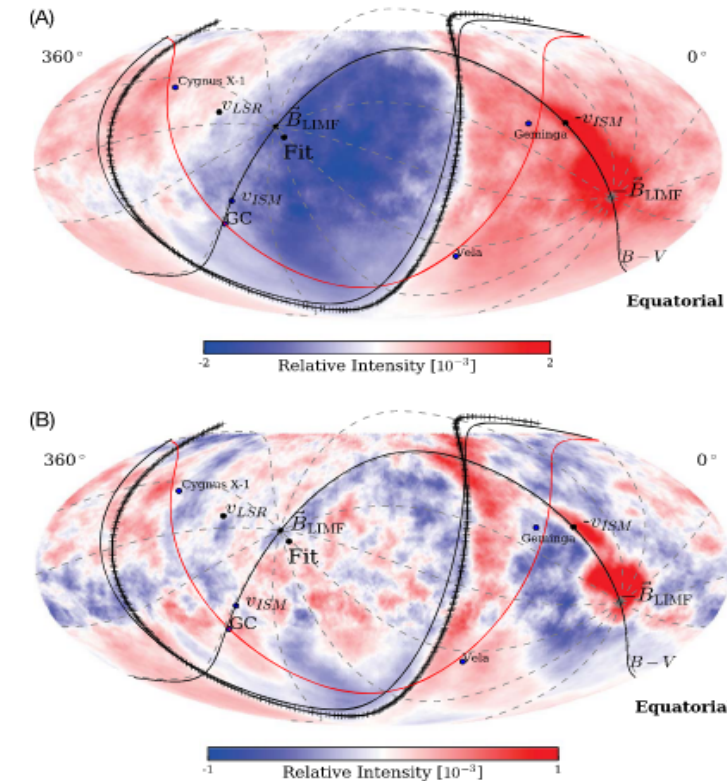
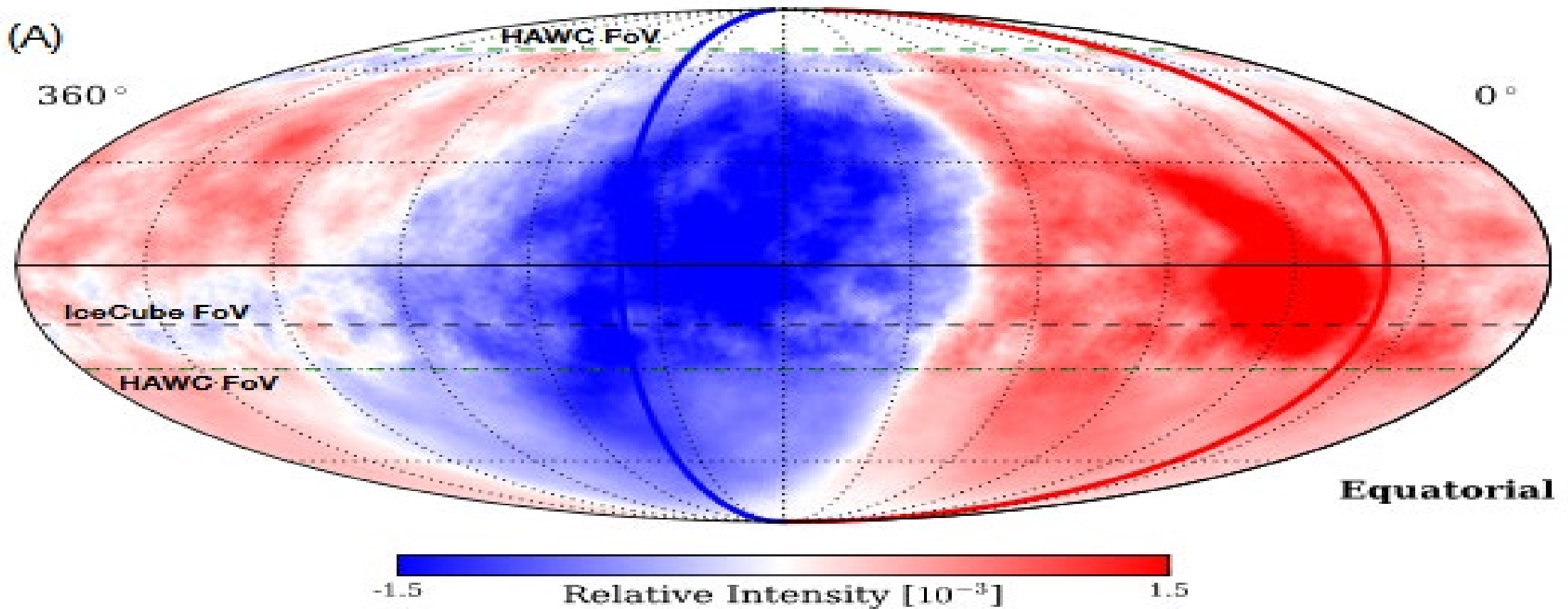


Figure 11. (A) Relative intensity of cosmic rays at 10 TeV median energy (Figures 4(A)) and (B) corresponding small-scale anisotropy (Figure 5(A)) in J2000 equatorial coordinates with color scale adjusted to emphasize features. The fit to the boundary between large-scale excess and deficit regions is shown as a black crossed curve. The magnetic equator from Zirnstein et al. (2016) is shown as a black curve, as is the plane containing the local interstellar medium magnetic field and velocity ($B-V$ plane). The Galactic plane is shown as a red curve, and two nearby supernova remnants, Geminga and Vela, are shown for reference, as is Cygnus X-1, a black hole X-ray binary known to produce high-energy γ rays (Albert et al. 2007).

HAWC/IceCube Joint Fit to the Cosmic Ray Anisotropy

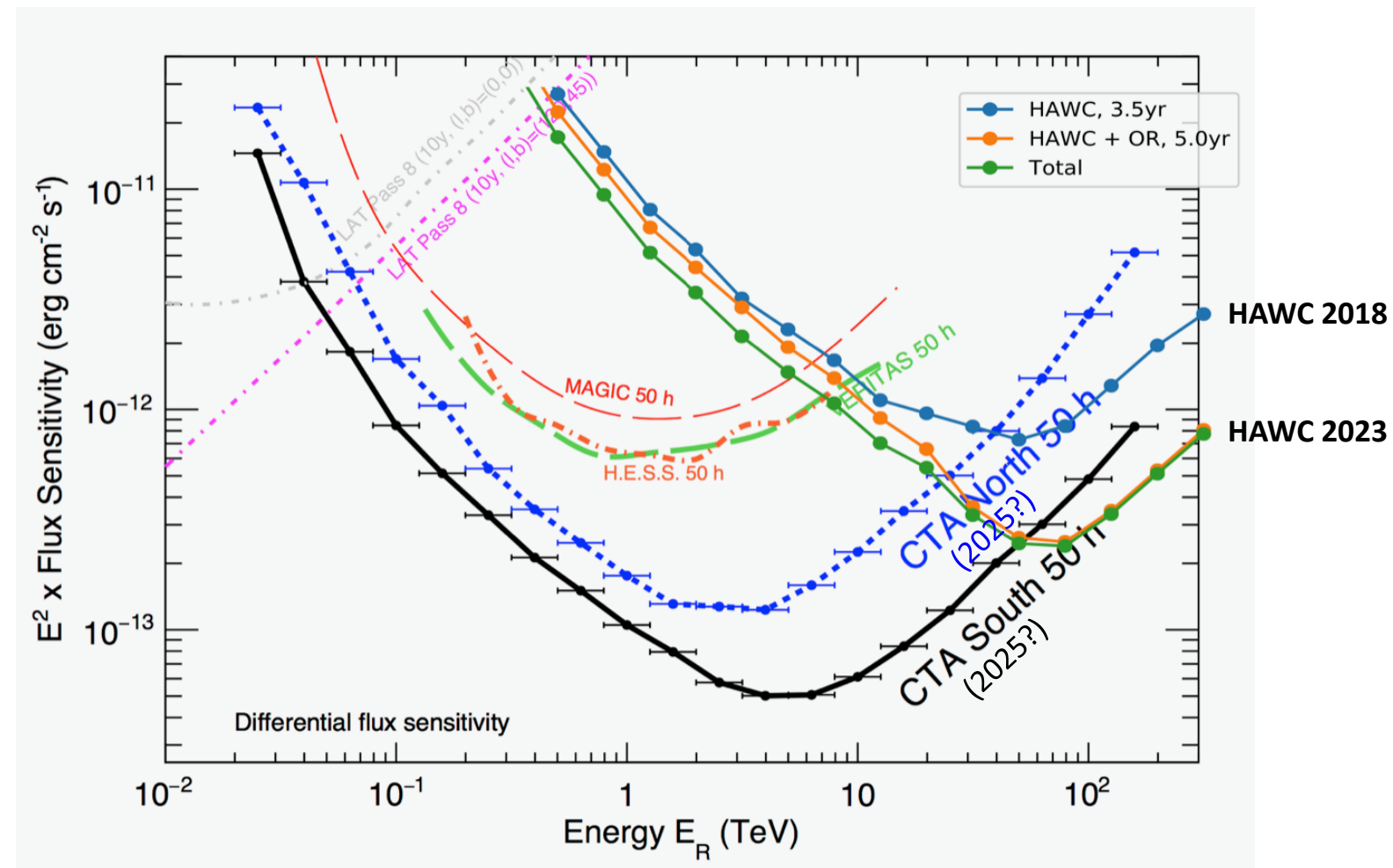


<https://arxiv.org/pdf/1812.05682.pdf>

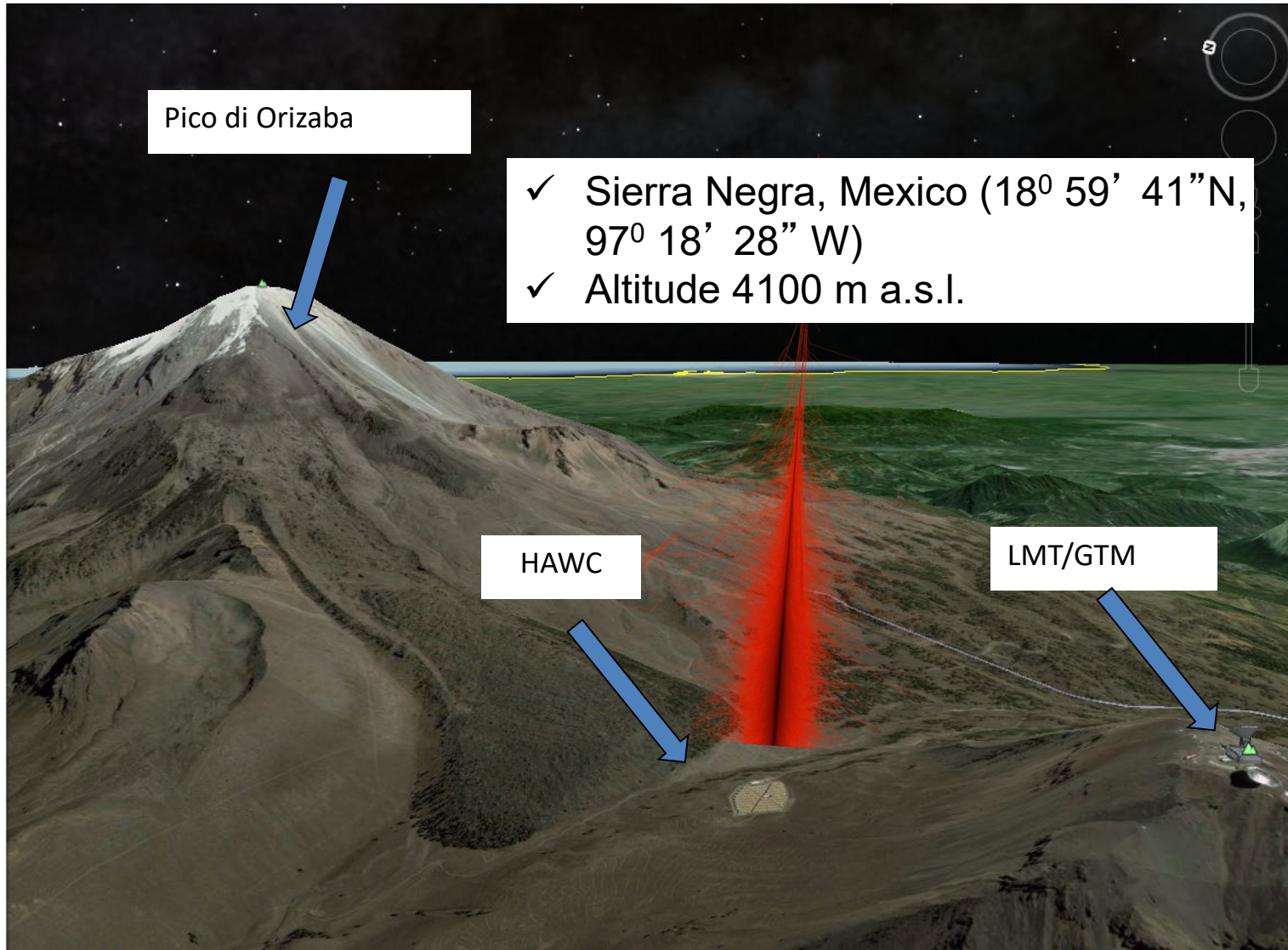
Combined HAWC/Icecube Cosmic Ray Large Scale Anisotropy Measurement

HAWC sensitivity - with outriggers

Planned improvements in HAWC reconstruction and analysis algorithms (which are about to be implemented retroactively with Pass 5) will increase sensitivity even more.

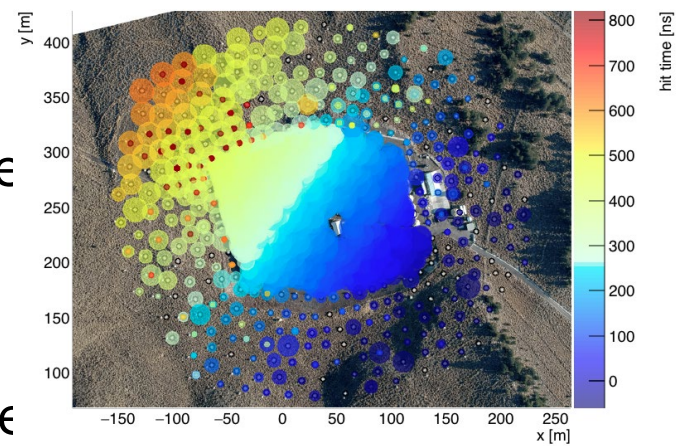


HAWC Site Location

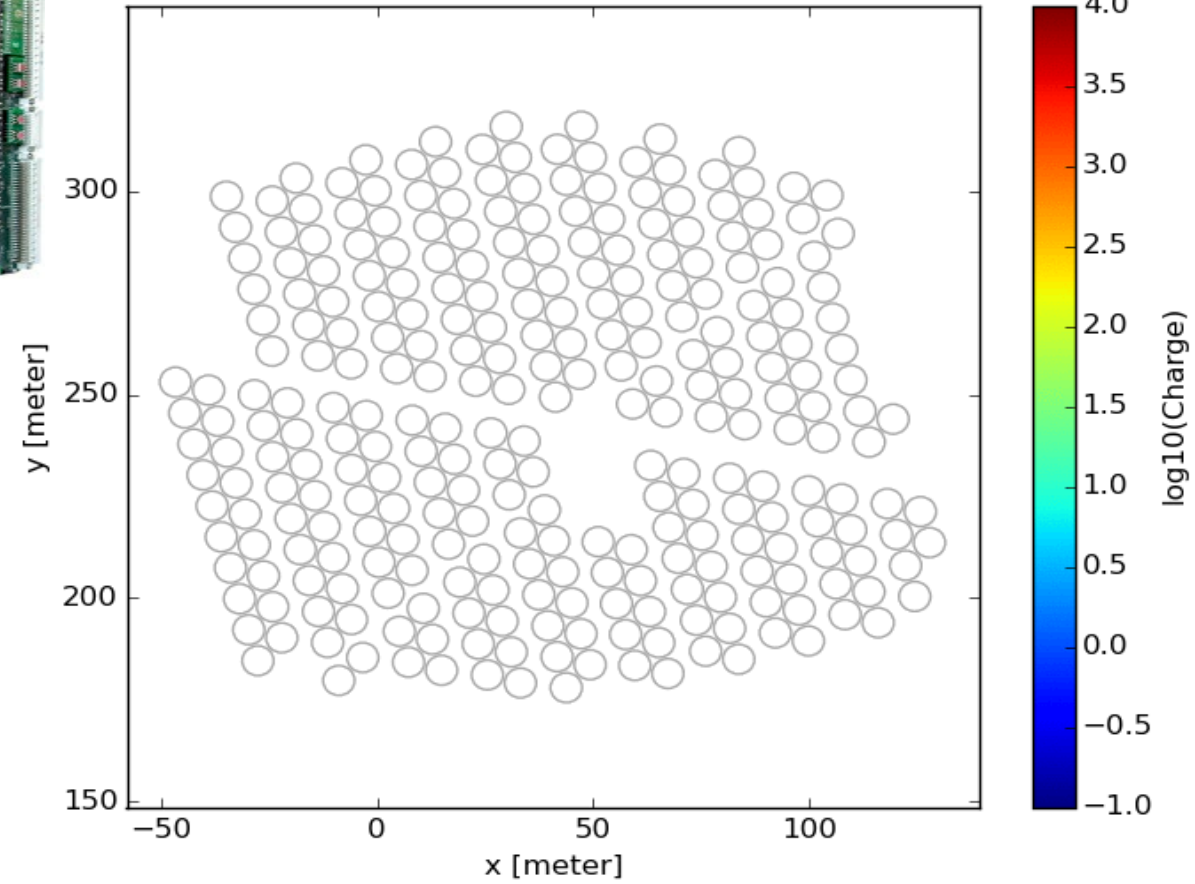
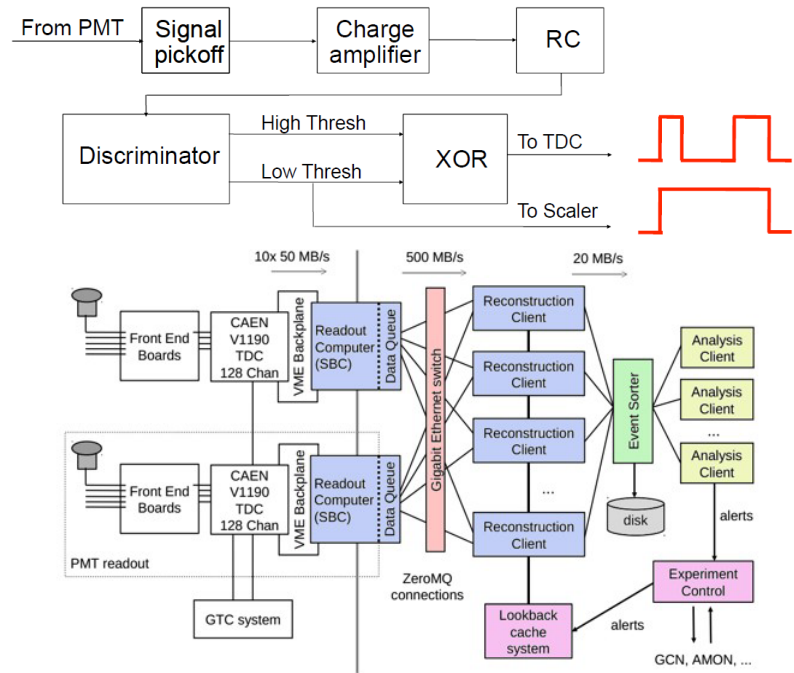
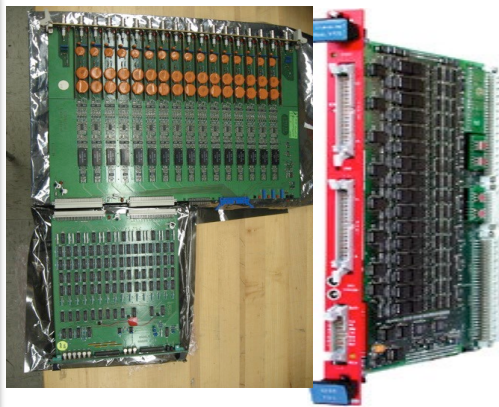
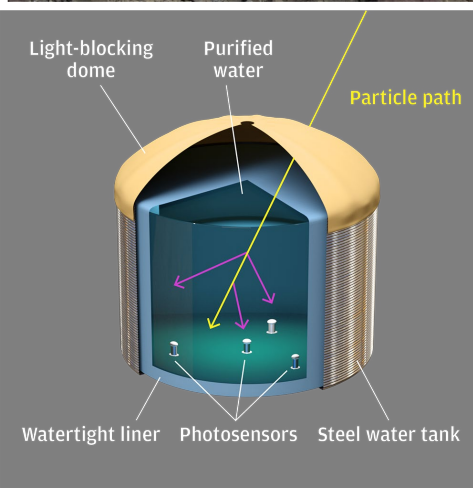


Outriggers Array: High Energy Extension

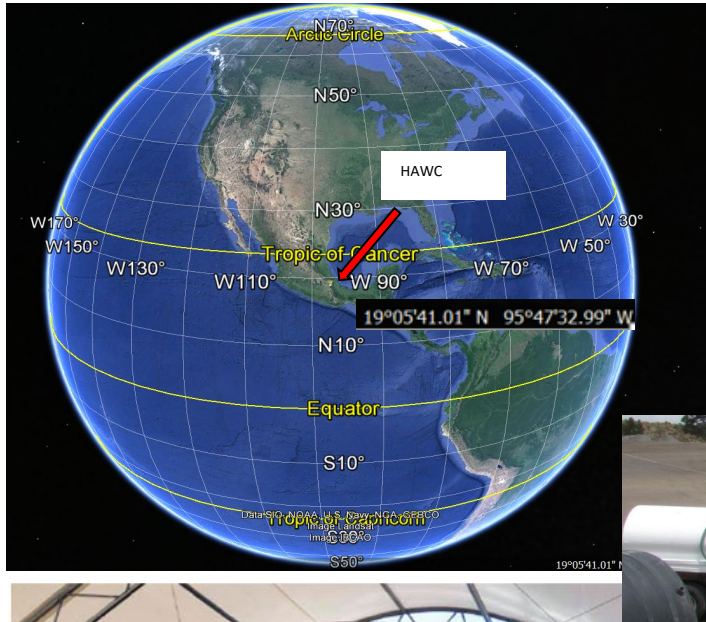
- ▶ 350 small tanks in addition to the 300 large tanks.
- ▶ Improve core localization for showers near the main array.
- ▶ x4 effective area at high energy.
- ▶ Lightning strike & fire damaged significant fraction...repairs are underway



HAWC Observatory Characteristics – Shower Reconstruction

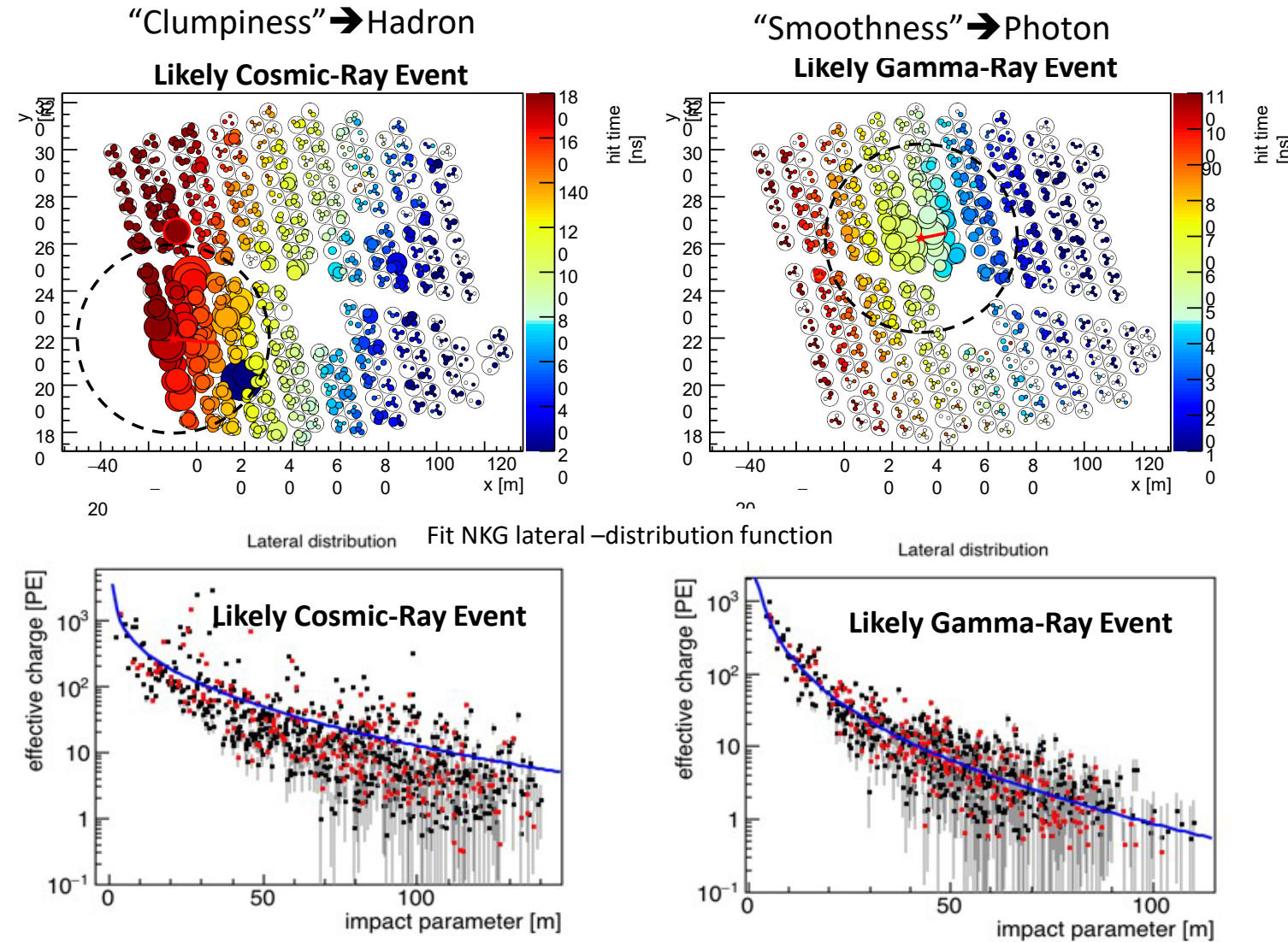


HAWC Observatory – Physical Characteristics



- WCD size -- 7.3 m dia x 4.5 m deep
 - WCD water volume -- ~200,000 L
 - Footprint of HAWC -- ~22,000 m² (~100,000 m² with outriggers)
 - Elevation - 4100 m
 - Duty cycle > 95%
 - Instantaneous field of view of 2 sr.
 - Air shower trigger rate: **25 kHz** in HAWC-300
 - Number of tanks: 300 in the main array, 345 outriggers.
 - Energy range: 300 GeV - 100 TeV (fHit), >= 1 TeV (energy estimators)
 - Angular resolution: >= 0.1 degrees
 - Declination range for sources: -26 to +64 degrees
-
-
-

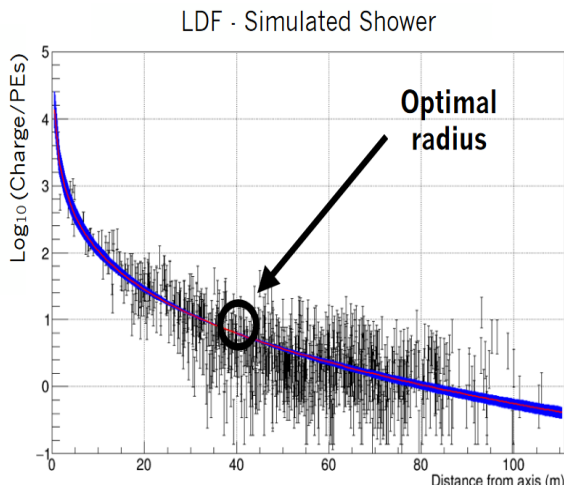
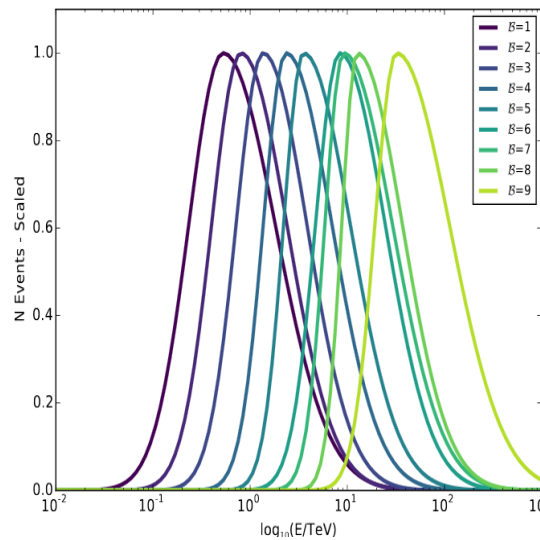
Shower Reconstruction - Photon / Hadron Separation



Shower Reconstruction - Energy

Bin	N _{chan}	Bin	E _{log} (GeV)	$\sigma_{E_{\log}}$
1	39–59		2.5	0.46
2	60–69		2.6	0.47
3	70–90		2.7	0.44
4	91–147		2.9	0.40
5	148–231		3.0	0.35
6	232–349		3.2	0.32
7	350–495		3.5	0.28
8	496–655		3.7	0.24
9	656–789		3.8	0.21
10	790–1200		4.0	0.18
11	790–1200		4.2	0.18
12	790–1200		4.6	0.07
13	790–1200		5.1	0.13
14	790–1200		5.5	0.10

Shower “size”



Ground Parameter

- Energy Estimators
- Shower “size” bin β ($f_{\text{hit}} = N_{\text{hit}} / N_{\text{tot}}$)
- Ground Parameter
- Neural Net

Neural Net

